WVT-TR-76035

APPLICATION OF FILAMENT WINDING TO CANNON AND CANNON COMPONENTS. PART III: SUMMARY REPORT

Guiliano D'Andrea
Robert Cullinan

October 1976

BENET WEAPONS LABORATORY
WATERVLIET ARSENAL
WATERVLIET, N.Y. 12189

TECHNICAL REPORT

AMCMS No. 3297.06.6681

Pron No. M1-3-23032

DISCLAIMER

The findings in this report are not to be construed as an official Department of the Army position unless so designated by other authorized documents.

The use of trade name(s) and/or manufacturer(s) in this report does not constitute an official indorsement or approval.

DISPOSITION

Destroy this report when it is no longer needed. Do not return it to the originator.

SECURITY CLASSIFICATION OF THIS PAGE *(When Date Entered)*

REPORT DOCUMENTATION PAGE

READ INSTRUCTIONS BEFORE COMPLETING FORM

1. REPORT NUMBER: WVT-TR-76035	2. GOVT ACCESSION NO.
3. RECIPIENT'S CATALOG NUMBER	
4. TITLE *(and Subtitle)*: APPLICATION OF FILAMENT WINDING TO CANNON AND CANNON COMPONENTS. PART III: SUMMARY REPORT	5. TYPE OF REPORT & PERIOD COVERED
	6. PERFORMING ORG. REPORT NUMBER
7. AUTHOR(s): Guiliano D'Andrea, Robert Cullinan	8. CONTRACT OR GRANT NUMBER(s)
9. PERFORMING ORGANIZATION NAME AND ADDRESS: Benet Weapons Laboratory, Watervliet Arsenal, Watervliet, N.Y. 12189, SARWV-RT-TP	10. PROGRAM ELEMENT, PROJECT, TASK AREA & WORK UNIT NUMBERS: AMCMS No. 3297.06.6681; Pror. No. M1-3-23032
11. CONTROLLING OFFICE NAME AND ADDRESS: U.S. Army Armament Command, Rock Island, Illinois 61201	12. REPORT DATE: October 1976
	13. NUMBER OF PAGES: 159
14. MONITORING AGENCY NAME & ADDRESS *(If different from Controlling Office)*	15. SECURITY CLASS. *(of this report)*: UNCLASSIFIED
	15a. DECLASSIFICATION/DOWNGRADING SCHEDULE

16. DISTRIBUTION STATEMENT *(of this Report)*

Approved for public release; distribution unlimited.

17. DISTRIBUTION STATEMENT *(of the abstract entered in Block 20, if different from Report)*

18. SUPPLEMENTARY NOTES

19. KEY WORDS *(Continue on reverse side if necessary and identify by block number)*

Composite Design	Gun Barrels	Rifles
Composite Materials	Recoilless Guns	Test Methods
Fatigue Tests (Mechanics)	Reinforced Plastics	Winding
Filaments	Residual Stress	Wire

20. ABSTRACT *(Continue on reverse side if necessary and identify by block number)*

The purpose of this report is to summarize WVT-7205, WVT-TR-75058 and apply the results of the previous investigations to the design, fabrication, and testing of a full size 106mm recoilless rifle.

Theoretical investigations, analysis methods, fabrication, and test results are presented and related to each other in this report. Moreover fatigue tests on composite test specimens of the 106mm tube are presented and analyzed.

DD FORM 1 JAN 73 1473 EDITION OF 1 NOV 65 IS OBSOLETE

SECURITY CLASSIFICATION OF THIS PAGE *(When Date Entered)*

FOREWORD

This is the last or summary report on work performed by the Watervliet Arsenal under MMT project: "Application of Filament Winding to Cannon and Cannon Components".

The following work has been accomplished:

1. Purchase of a filament winding machine
   Development of filament winding techniques
2. Investigation and evaluation of suitable filament winding materials
3. Determination of the feasibility of winding many composite systems
4. Design, fabrication and testing of a full scale 106mm Recoilless Rifle

Initial work has been reported in detail in two Watervliet Arsenal Technical Reports[1,2].

Another aspect of this MMT project was to establish in-house capability to fabricate cannon tubes using filament winding techniques which call for the substitution of high strength, high modulus, low density composite materials for conventional gun steel. This capability has been established, successfully demonstrated, and fully described in a third Watervliet technical report[3].

---

[1]Cullinan, R., et al. "Application of Filament Winding to Cannon and Cannon Components. Part I: Steel Filament Composites," April 1972, WVT-7205.

[2]D'Andrea, G., et al, "Application of Filament Winding to Cannon and Cannon Components. Part II: Residual Stress Analysis." October 1975, WVT-TR-75058.

[3]D'Andrea, G., et al. "Development of: Design Analyses, Manufacturing and Testing of the 81mm XM73 Fiberglass-Epoxy Recoilless Rifle" June 1974, WVT-TR-74014.

ACKNOWLEDGMENT

The authors wish to thank the following individuals for their excellent assistance, cooperation, and contributions:

Dr. J. Zweig, Lt Arnold M. Manaker, Paul J. Croteau, Philip J. Giordano, Ralph E. Peterson, and Harold S. Scheck

Special thanks to Mrs. Patricia Clinton for the preparation of the manuscript.

TABLE OF CONTENTS

TABLE OF CONTENTS (Cont)

ILLUSTRATIONS

ILLUSTRATIONS (Cont)

ILLUSTRATIONS (Cont)

TABLES

OBJECTIVE

The objective of this report is to present in a concise manner the design concepts, the fabrication technology, and testing procedures necessary to develop a composite gun tube made of a metallic liner wrapped with high-strength filaments embedded into an organic matrix. The weapon chosen for a sample problem is the 106mm Recoilless Rifle.

STATEMENT OF THE PROBLEM

Design, fabricate and test fire a lightweight composite 106mm Recoilless Rifle from the ESP*-Travel curve for the standard tube while maintaining the proper internal 106mm configuration. Obtain weight and final geometry of lightweight composite rifle and compare with the standard 106mm M40A1 R.R.

APPROACH TO THE PROBLEM

The following outline should be considered in the development of the 106mm R.R. or any other composite weapon system:

1. Material Selection
2. Theoretical Study

---

*ESP-(Elastic Strength Pressure) The pressure which produces an equivalent stress in section wall equal to the allowable stress of the gun tube material at 70°F. It is the actual pressure capacity curve of the finally designed tube.

3. Fabrication and Inspection

4. Testing

1. Material Selection

The performance of a composite tube is a direct function of the materials in the composite and how they interface with each other. In general, the mechanical properties in either the direction of the filament or transverse to the filaments will be less than the value of the filament. They also will vary with the filament type and filament volume ratio.

There are many filaments that can be used in a composite gun tube. The ultimate strength, density, specific strength, specific modulus for several candidate filaments are listed in Table 1.

If strength-to-weight ratio is the underlining factor then the magnitude of the specific strength indicates the merit of the material, with the largest value considered the best.

Values from Table 1 reflect filament properties only. When a composite material is made the strength-to-weight ratio will be substantially reduced; this is due to many factors such as filament volume ratio, effect of operating temperature, time at load, number of cycles, aging, fabrication, setup, and others.

The degree of success, then, will depend upon the ability to select materials having the desired properties. This selection can only be made if a good theoretical, fabrication, and testing background is available.

TABLE 1. PROPERTIES OF CONTINUOUS FIBROUS REINFORCEMENTS

Fiber Type	Fiber Material	Density LB/IN^3	Ten. Str PSI X 10^3	Spec Str IN. X 10^6	Elas Mod PSI X 10^6	Spec Mod IN. X 10^7
Glass	E-Glass	0.092	500	5.4	10.5	11.4
	S-Glass	0.090	650	7.2	12.6	14.0
	4H-1	0.096	730	7.6	14.5	15.1
	SiO_2	0.079	850	10.8	10.5	13.3
Polycrystal-	Al_2O_3	0.114	300	2.6	25.0	21.9
line	ZrO_2	0.175	300	1.7	50.0	28.6
	Carbon-Graphite	0.057	250	4.4	40.0	70.0
	Boron Nitride	0.069	200	2.9	13.0	18.8
Multi-Phase	Boron/Tungsten	0.095	400	4.2	55.0	57.8
	Boron/SiO_2	0.085	330	3.9	53.0	62.5
	B_4C/B/W	0.095	390	4.1	62.0	65.0
	SiC/Tungsten	0.125	300	2.4	67.0	52.0

TABLE 1. PROPERTIES OF CONTINUOUS FIBROUS REINFORCEMENTS (Cont)

Fiber Type	Fiber Material	Density LB/IN^3	Ten. Str PSI x 10^3	Spec Str IN. X 10^6	Elas Mod PSI X 10^6	Spec Mod IN. X 10^7
Metallic	Tungsten	0.697	580	0.8	59.0	8.5
	Molybdenum	0.369	320	0.9	52.0	14.1
	Rene 41	0.298	290	1.0	24.0	8.1
	Steel	0.280	600	2.1	29.0	10.3
	Beryllium	0.066	185	2.8	35.0	53.0
Organic	Kevlar 49	0.052	525	10.1	19.0	36.0

Reference 1 explains the rationale of material selection of the stainless steel wire/epoxy system for the 106mm Composite Recoilless Rifle. The most salient points for that selection are:

FILAMENT: 6 mil NS-355 Steel Wire

a) high strength - 450,000 psi

b) high modulus - 29,000,000 psi

c) availability and cost - $8.00/lb

d) ease of fabrication

e) corrosion resistance

f) high proportional limit

g) 95% composite efficiency

MATRIX: EPON 828/CIBA 906/BDMA (100/80/2). This epoxy, low viscosity anhydride hardener, and amine accelerator system was judged the best overall matrix system. This judgement, at the time, was based on a series of resin and composite tests performed early in the study.

2. Theoretical Study

The theoretical work needed to properly design composite pressure vessels is reported in detail in the following Watervliet Arsenal technical reports:

Ref (1) Cullinan, R., et al. "Application of Filament Winding to Cannon and Cannon Components, Part I: Steel Filament Composites, WVT-7205 (Apr 1972)

[1]Cullinan, R., et al "Application of Filament Winding to Cannon and Cannon Components, Part I:Steel Filament Composites" April 1972, WVT-7205

Ref (2) D'Andrea, G. et al "Application of Filament Winding to Cannon and Cannon Components. Part II: Residual Stress Analysis" WVT-TR-75058 (Oct 1975)

Ref (3) D'Andrea, G., et al "Development of Design Analysis, Manufacturing and Testing of the 81mm XM73 Fiberglas-Epoxy Recoilless Rifle" WVT-TR-74014 (June 1974)

Ref (4) Mow, C.C. "Theoretical Analysis of a Wrapped Type Gun Tube Construction" WVT-RR-5904 (1959)

Ref (5) Zweig, J.E. and Pascual, M.J. "Minimum Weight Design for Composite Tubes" WVT-6525 (1965)

Ref (6) D'Andrea, G. "Composite Cylindrical Pressure Vessels Related to Gun Tubes Part I: Theoretical Investigation" WVT-6821 (1968)

Ref (7) D'Andrea, G. "Composite Cylindrical Pressure Vessels Related to Gun Tubes Part II "Minimum Weight Design" WVT-7125 (1971)

Ref (8) Meisel, L.W. "Minimum Effective Cost Design of Composite Cylindrical Pressure Vessels Related to Gun Tubes" R-WV-T-1-7-73 (Feb 1973)

The following write-up will describe the latest input and output of computer programs used in the design of the 106mm Composite Recoilless Rifle.

a. "GUNTUC" program determines theoretically:

(1) The dimensions of a composite gun tube consisting of a liner and a jacket of dissimilar materials when subjected to

an internal pressure.

(2) The economic success of these tubes when compared with conventional tubes. The dimensions of the composite gun tube are optimized for minimum weight with the restriction that the applied stress levels in both liner and jacket do not exceed stress levels determined by a yielding criterion.

The economic success is obtained by considering the various factors which determine the tube's cost and the relationship between the tube's weight, performance and cost.

Results from "GUNTUC" for the 0.100" liner are presented in Figures 1 through 6:

Figure 1: summarizes the input needed to operate GUNTUC.

NOTE: (1) Composite density is calculated within the program and subsequently printed.

(2) With this data it is required to input the pressure-travel curve depicted in Figure 2.

Figure 2: depicts the ESP-Travel curve for the conventional 106mm M40A1 Recoilless Rifle. This curve is also used in the design of the composite 106mm R.R.

Figure 3: depicts the outside dimensions of the composite and conventional 106mm R.R. as a function of the tube length.

(a) The B-Travel curve represents the desired liner configuration. Usually the mid-portion of this curve is obtained from GUNTUC while the two ends are

```
106 MM R.R. (STEEL LINER-STEEL FILAMENT/EPOXY MATRIX JACKET)
BORE RADIUS=2.104
FILAMENT/MATRIX VOLUME RATIO=0.750
WEIGHT PENALTY FACTOR=80.000
COMPOSITE FABRICATION COST=1.000
ALL LINER FABRICATION COST=1.000
POISSON'S RATIO(LINER)=0.300
POISSON'S RATIO(FILAMENT)=0.280
POISSON'S RATIO(MATRIX)=0.300
LINER MODULUS=30000000
FILAMENT MODULUS=30000000
MATRIX MODULUS=500000
LINER DENSITY=0.2830
FILAMENT DENSITY=0.2820
MATRIX DENSITY=0.0440
COMPOSITE DENSITY=0.2225
LINER YIELD STRENGTH=160000
FILAMENT YIELD STRENGTH=450000
MATRIX YIELD STRENGTH=10000
DOLLARS PER POUND OF LINER=0.50
DOLLARS PER POUND OF FILAMENT=8.00
DOLLARS PER POUND OF MATRIX=1.50
FACTOR OF SAFETY=1.000
```

Figure 1. Input data for "GUNTUC" computer program.

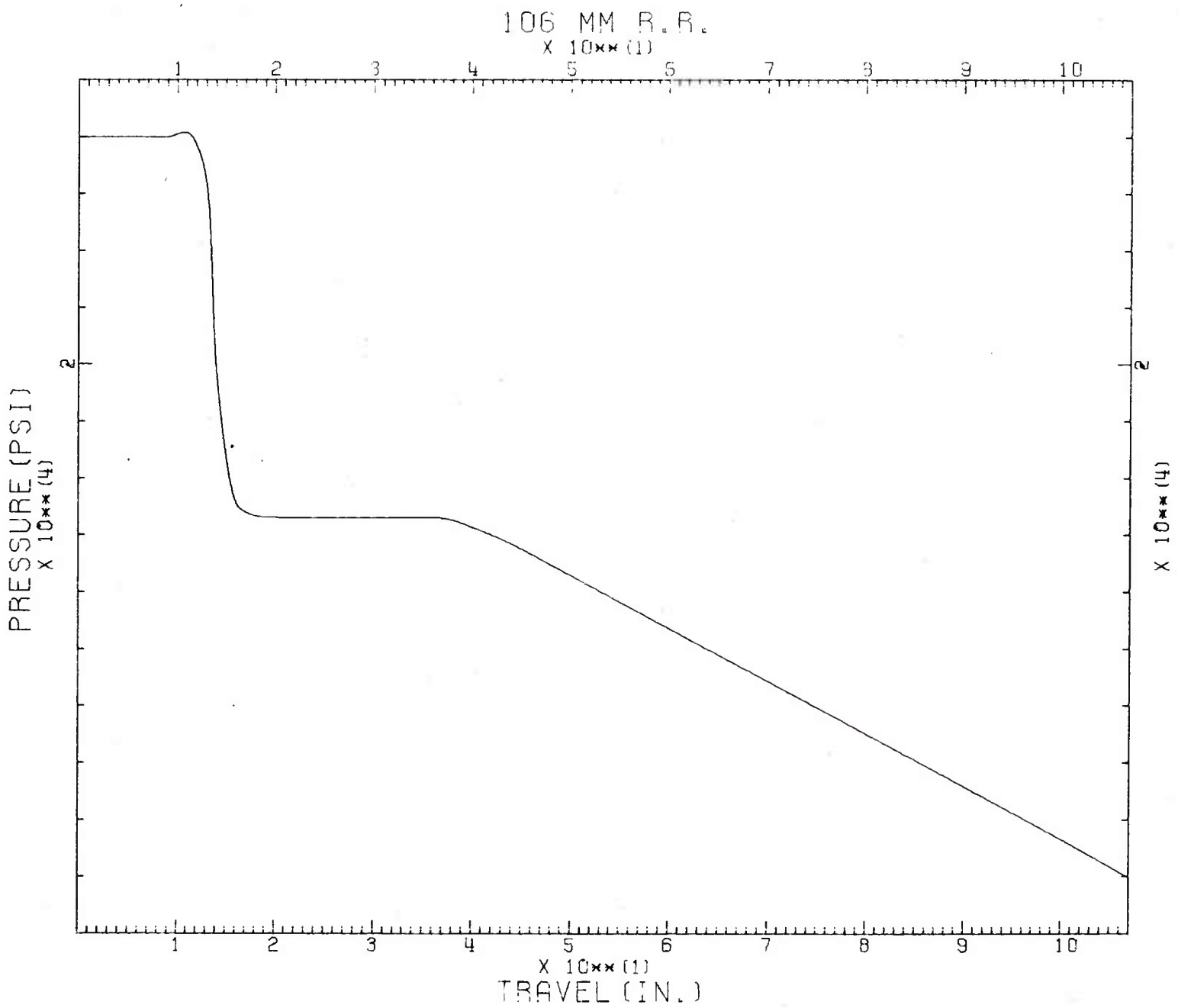

Figure 2. ESP - travel curve for conventional 106mm M40A1 recoilless rifle.

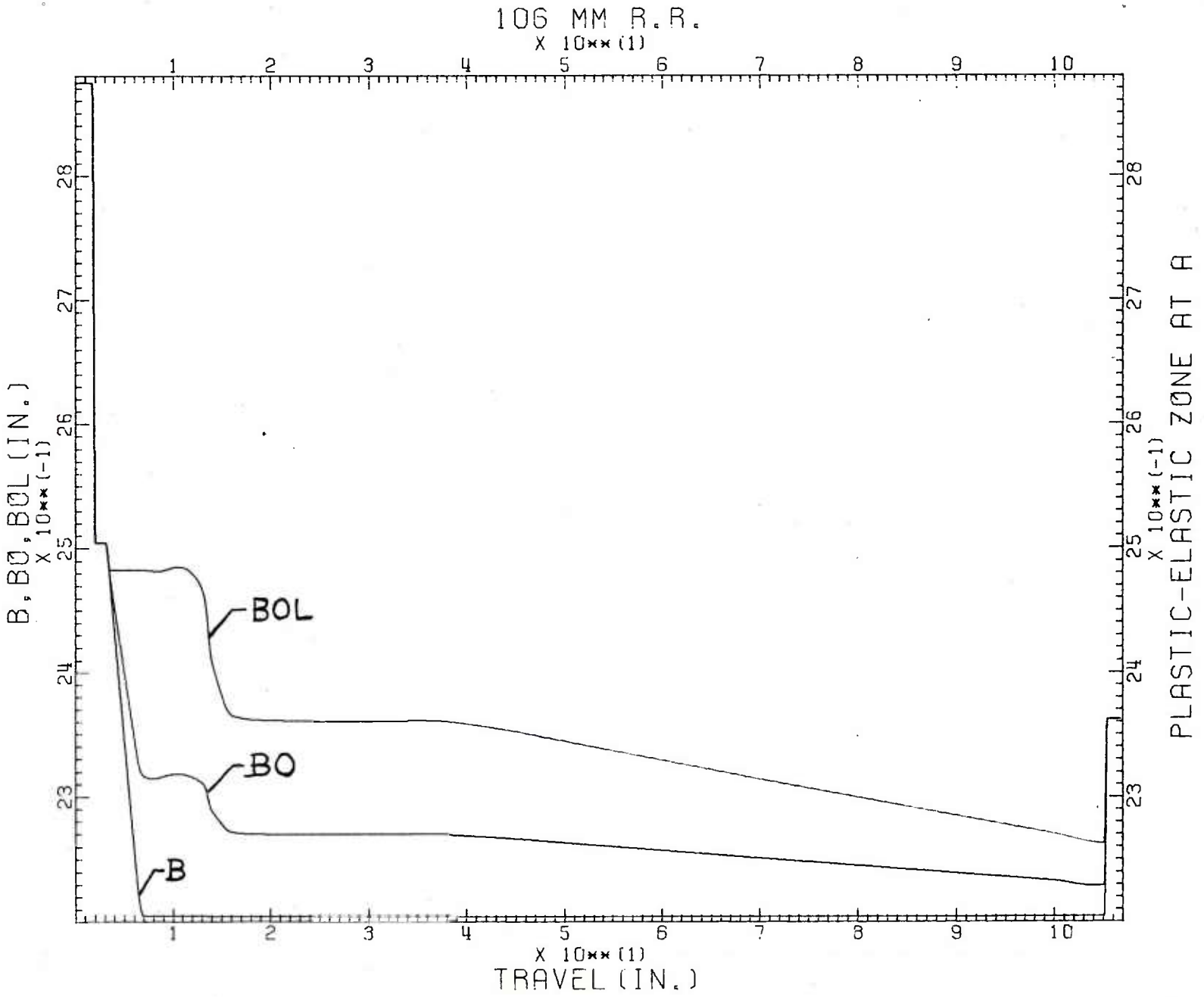

Figure 3. O.D. values of composite vs conventional 106mm gun tubes.

engineered to provide capabilities for components attachment such as the breech mechanism.

(b) The BO-Travel curve represents the theoretical outside radius of the composite tube as it varies along the tube. This variation is, of course, due to the Pressure-Travel curve (ESP).

(c) The BOL-Travel curve represents the theoretical outside radius of the tube made of gun steel designed for the same pressure-travel of Figure 2.

Figure 4: depicts the weight of the two types of gun tubes as it varies along their lengths.

NOTE: The weight calculations consider the internal radius, A, of 2.104" and the given liner outside radius B. The rifling's lands and breech attachment are not included in the analysis.

Figure 5: depicts the cumulative weight of the two gun tubes as they vary along their lengths.

Figure 6: depicts the fabrication procedure to be used in the filament winding of the steel liner shown in Figure 3.

GUNTUC's solutions are also functions of the Plastic-Elastic zone in the liner, i.e., the liner can be autofrettaged before being wound; this procedure will further decrease the weight of the composite tube. Figures 7 through 10 depict a 0.100 inch thick autofrettaged liner with the plastic-elastic zone at r = B.

In Appendix A, figures A-1 through A-10 depict the theoretical

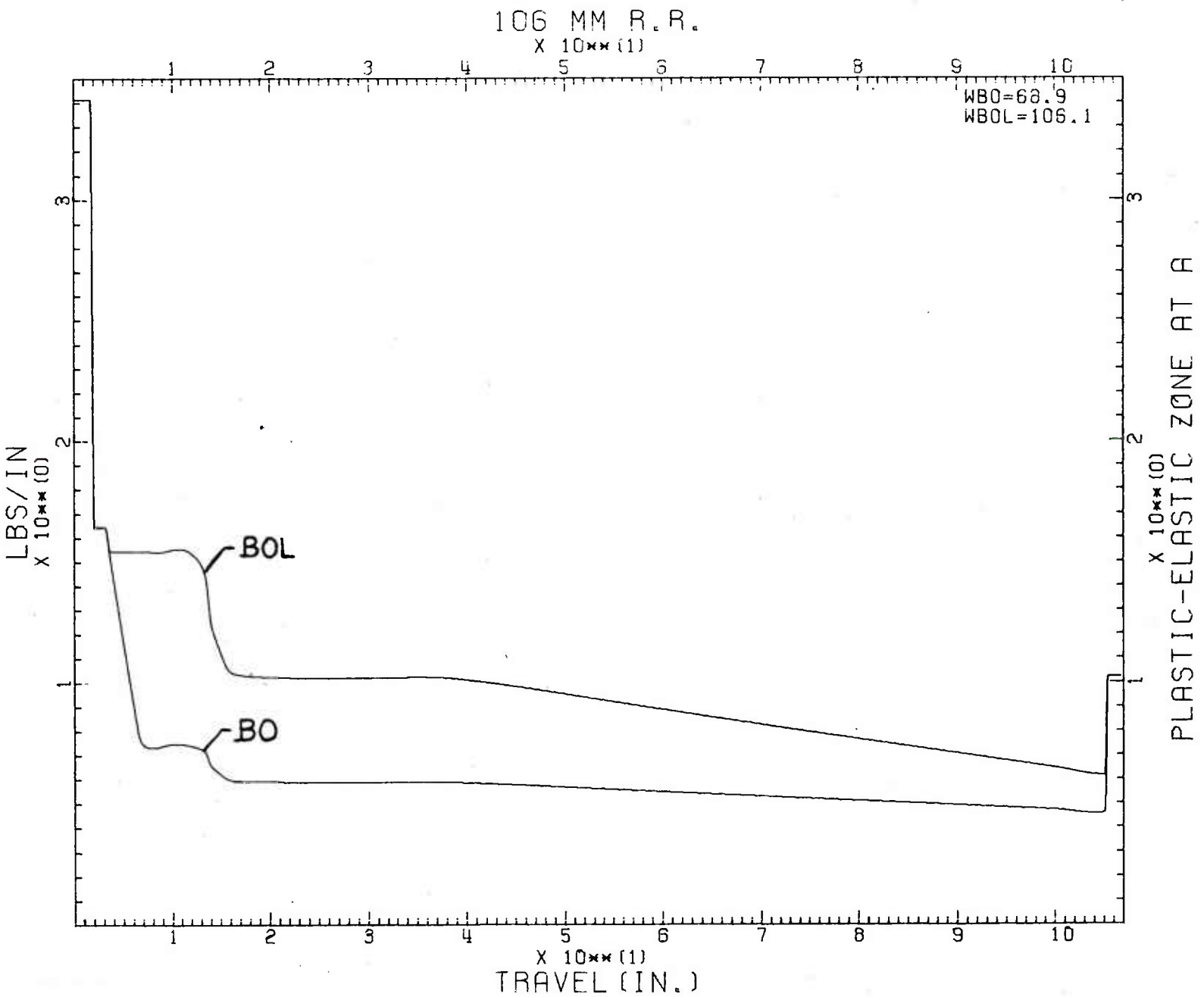

Figure 4. Weight of composite vs conventional gun tubes.

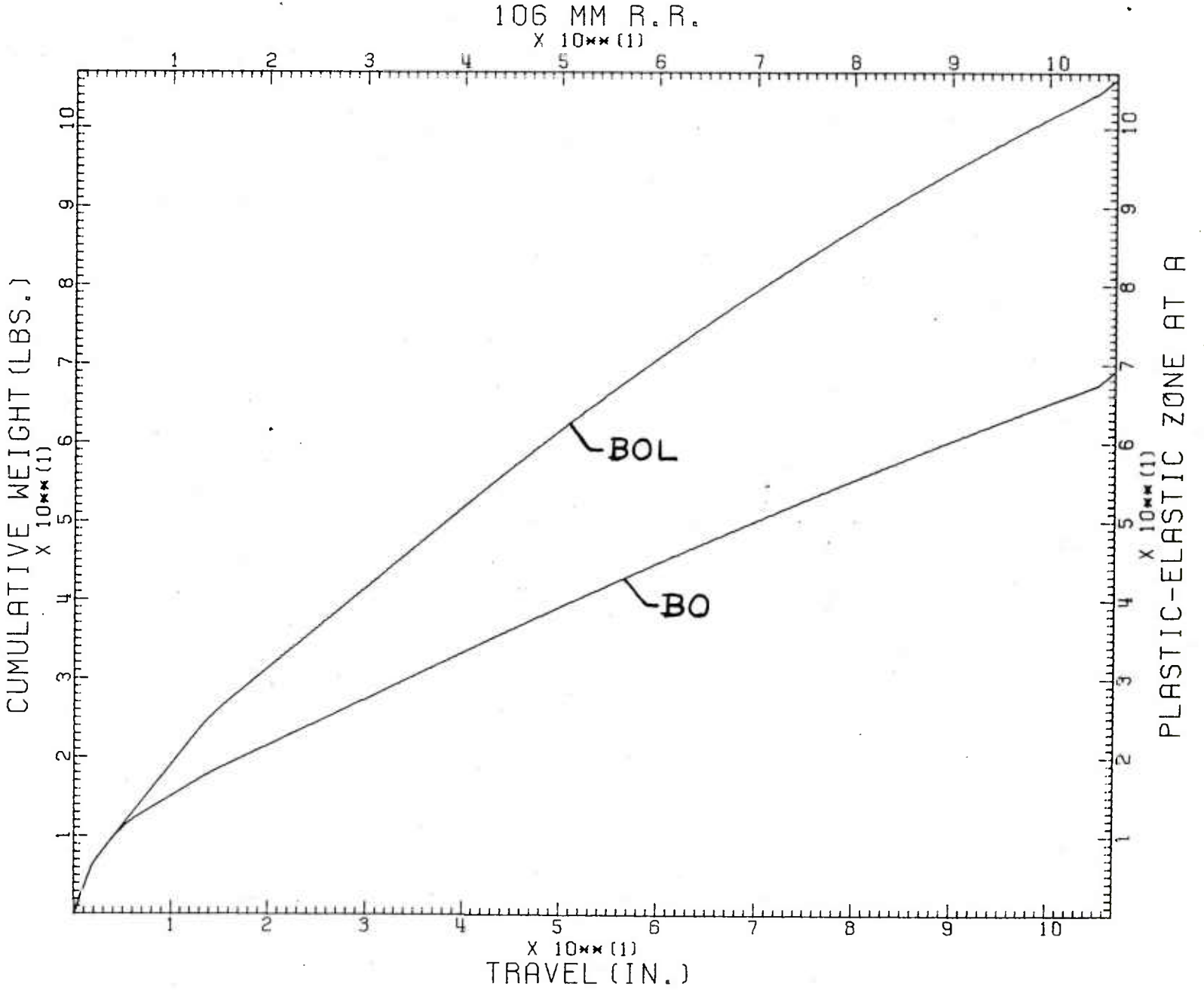

Figure 5. Cumulative weights of composite and conventional gun tubes.

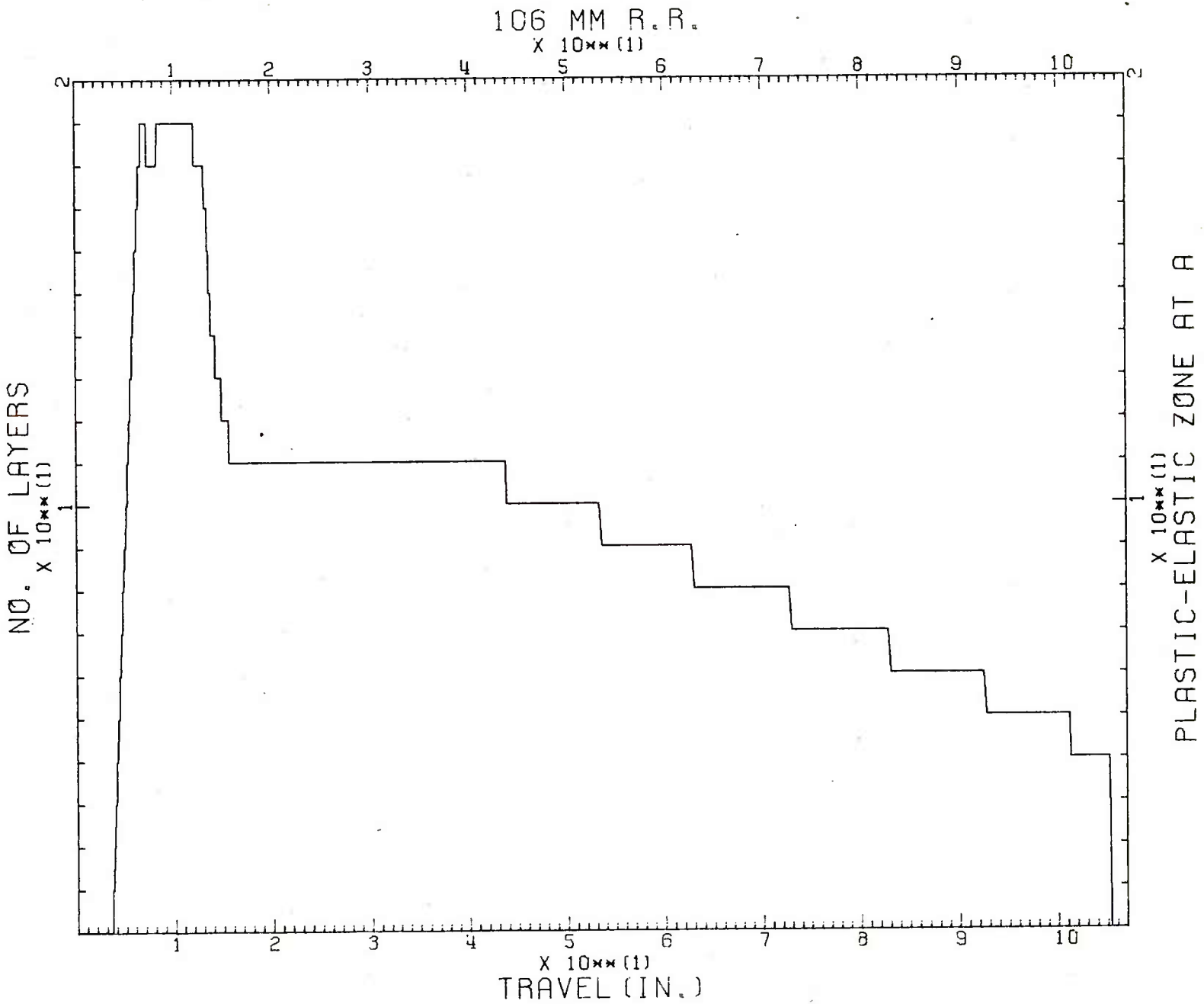

Figure 6. Fabrication pattern for winding composite tube with 0.100" liner.

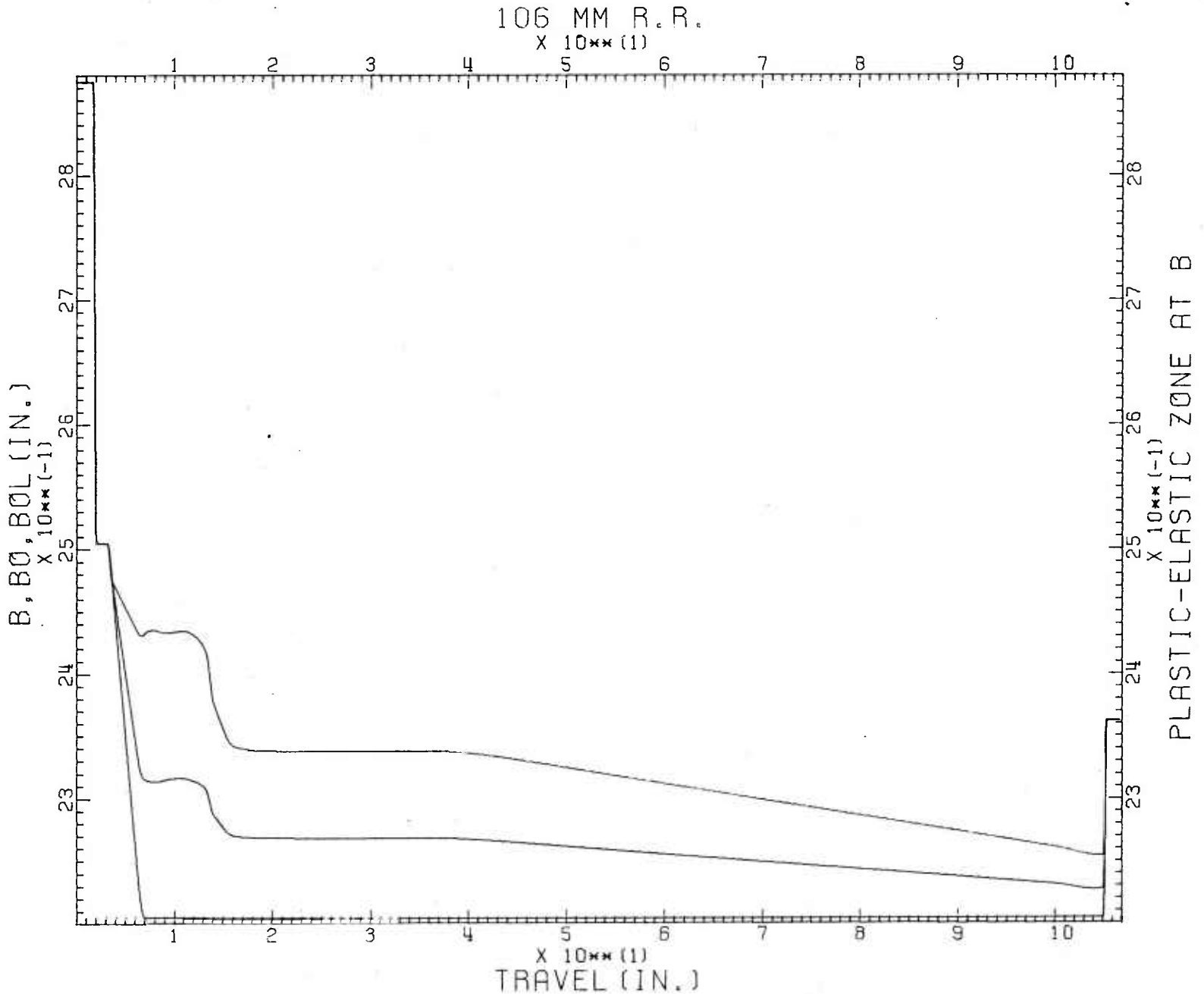

Figure 7. O.D. values of composite vs conventional tubes using autofrettaged liner.

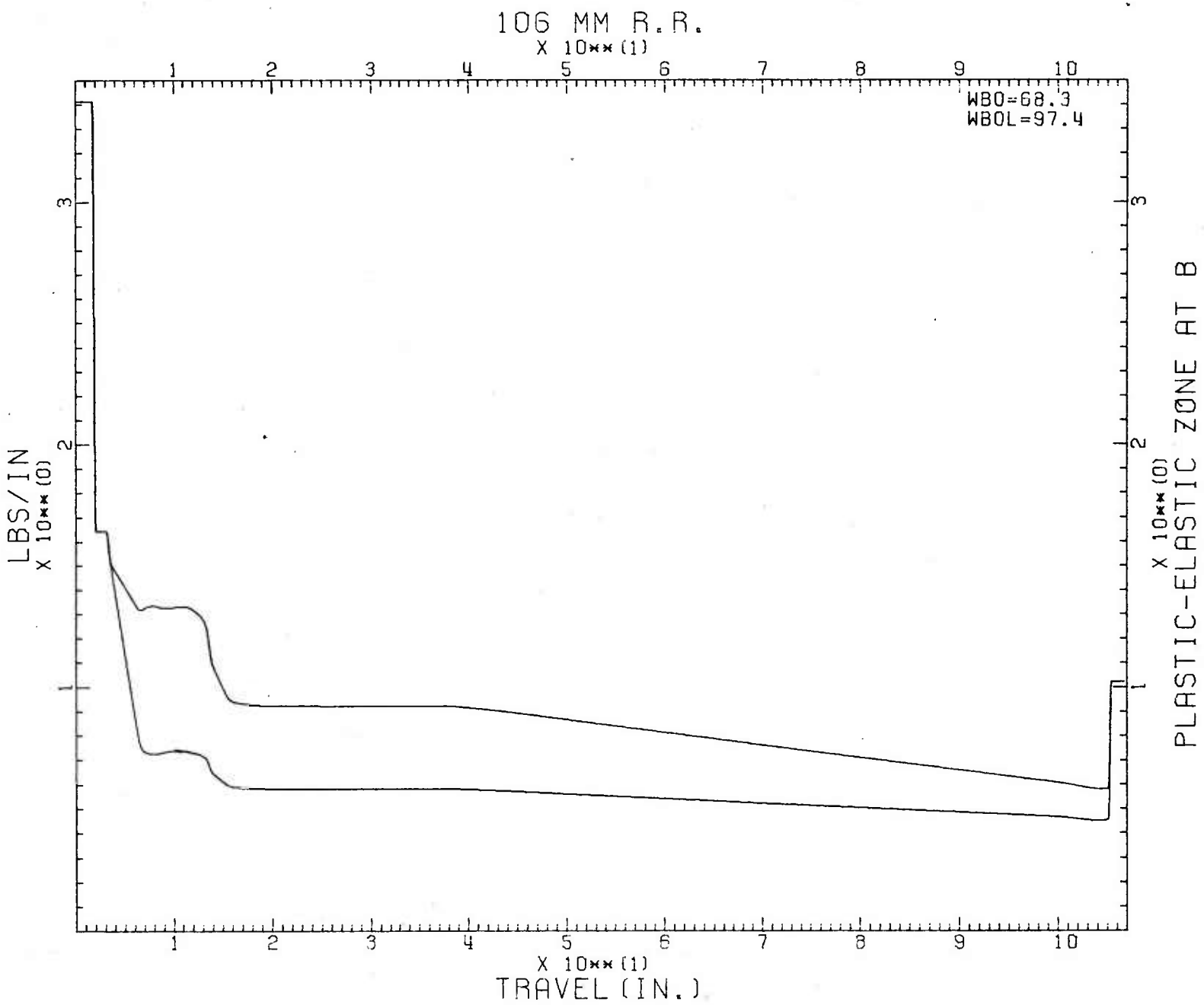

Figure 8. Weight of composite vs conventional tubes using autofrettaged liner.

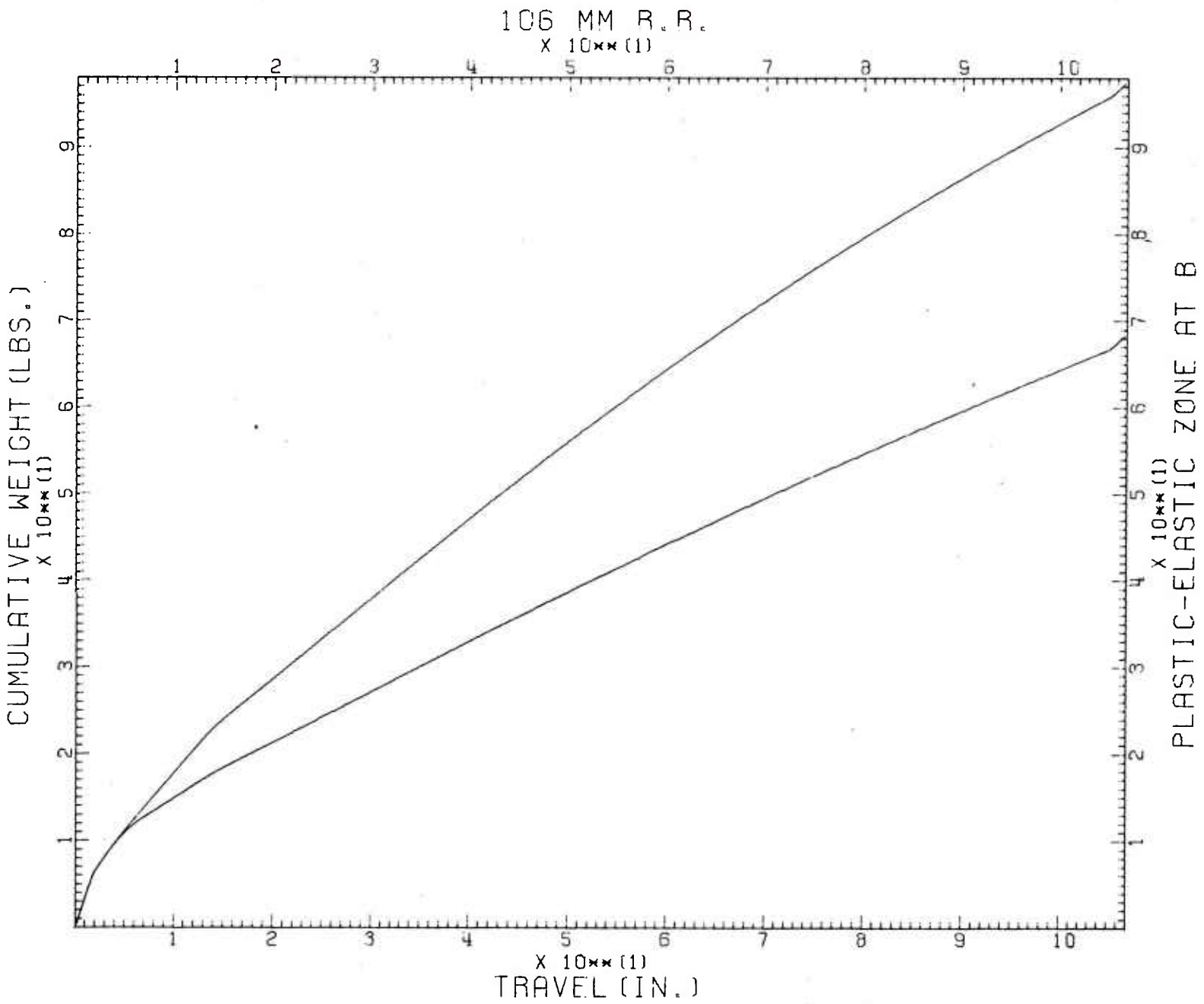

Figure 9. Cumulative weights of composite and conventional tubes using autofrettaged liner.

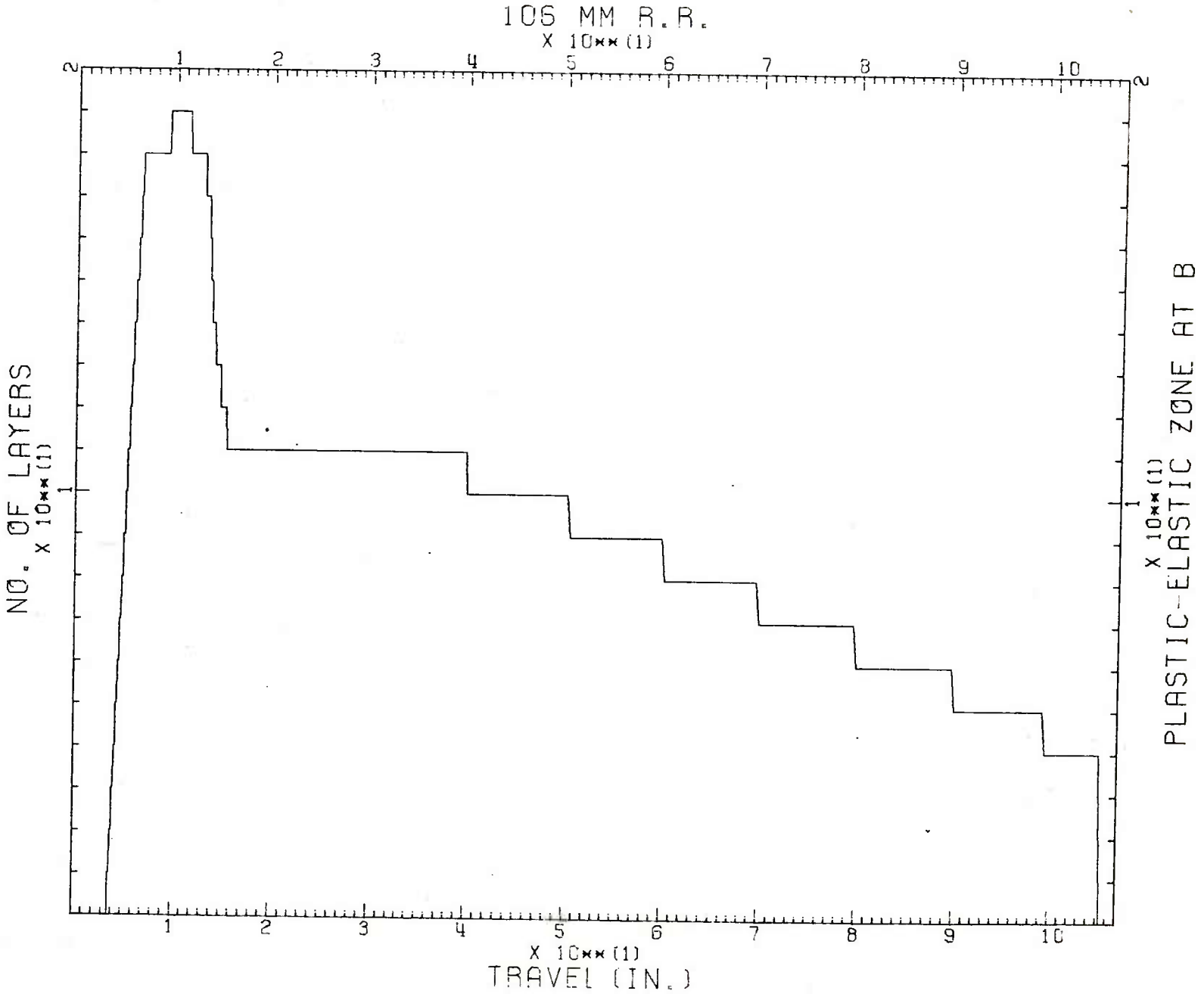

Figure 10. Fabrication pattern for winding composite tube with 0.100" autofrettaged liner.

results for the 106mm Recoilless Rifle having a liner thickness of 0.050 in., while Figures A-11 through A-20 depict results for a liner thickness of 0.075 inches.

b. "TENZAUTO" program compares "GUNTUC" residual stress output with the actual residual stresses introduced during the filament winding operation and displays it in a graphical form. It also determines and displays the tensile stresses in the composite tube when subjected to a predetermined internal service pressure. Three different liner thicknesses were investigated for the 106mm Recoilless Rifle application: the 0.050", 0.075", and 0.100".

Results from TENZAUTO are presented in Figures 11, 12 and 13 for the 0.100" liner. Figure 11 shows the ideal hoop stress distribution for a 0.100" thick liner and a 14 layer composite jacket. It exhibits a tangential or hoop service stress A-A when the residual stresses of the form B-B are present. With these residual stresses, the cylinder will rupture simultaneously at the bore, liner-jacket interface, and jacket outside diameter. Curve C-C represents the elastic stresses that prevail upon release of the applied pressure (in this case 20,000 psi).

Figure 12 depicts the theoretical residual stresses B-B obtained during the filament winding process. These stresses are produced by a constant filament winding tension of 3.8 lb. Knowing these residual stresses, the elastic stress equations (C-C curve), and the yielding criterion at the bore, a limit pressure can be obtained which produces yielding of the liner at the bore. This pressure is obtained from the

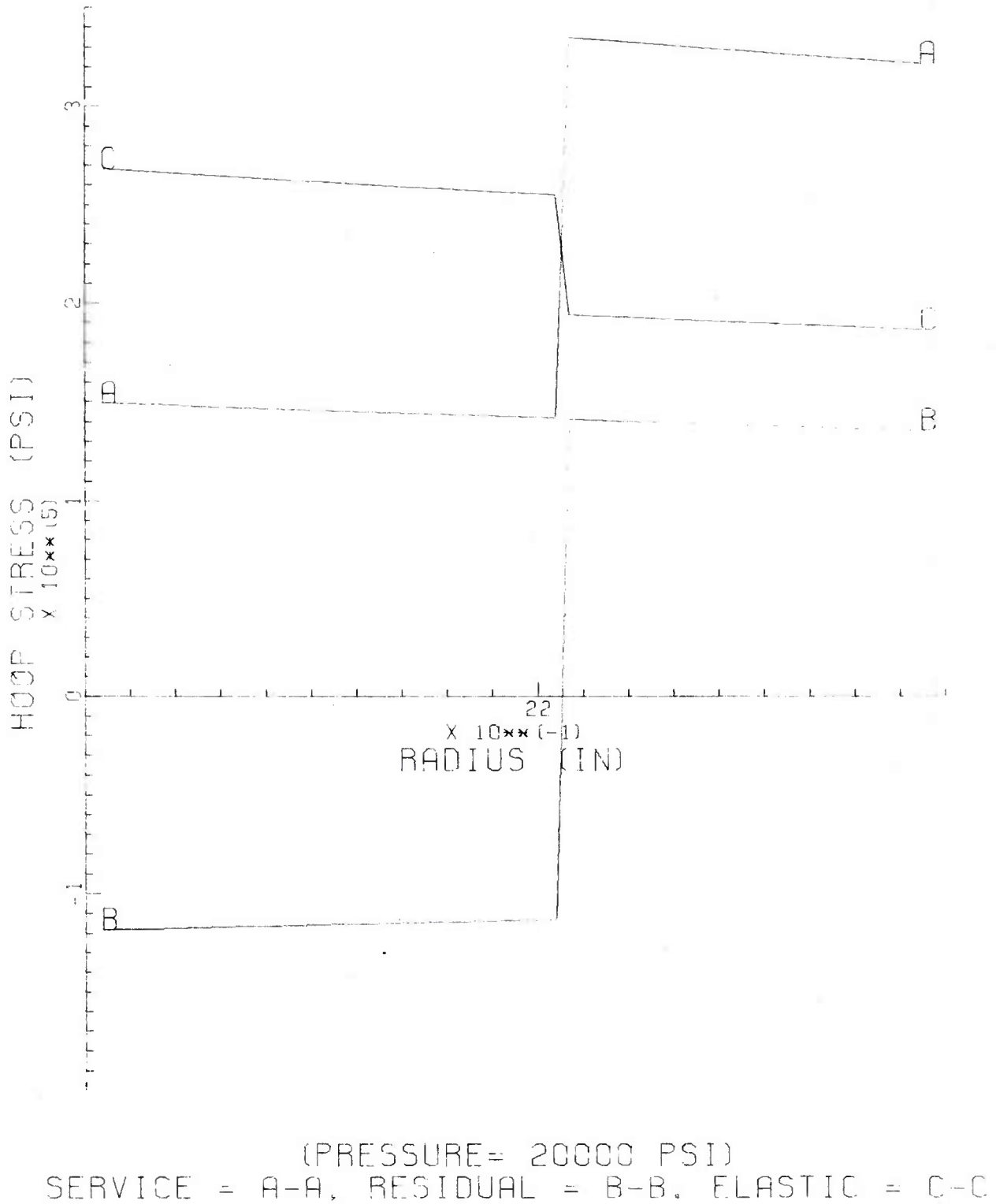

Figure 11. Plot of ideal stress distribution for "GUNTUC" designed composite cylinder with 0.100" steel liner.

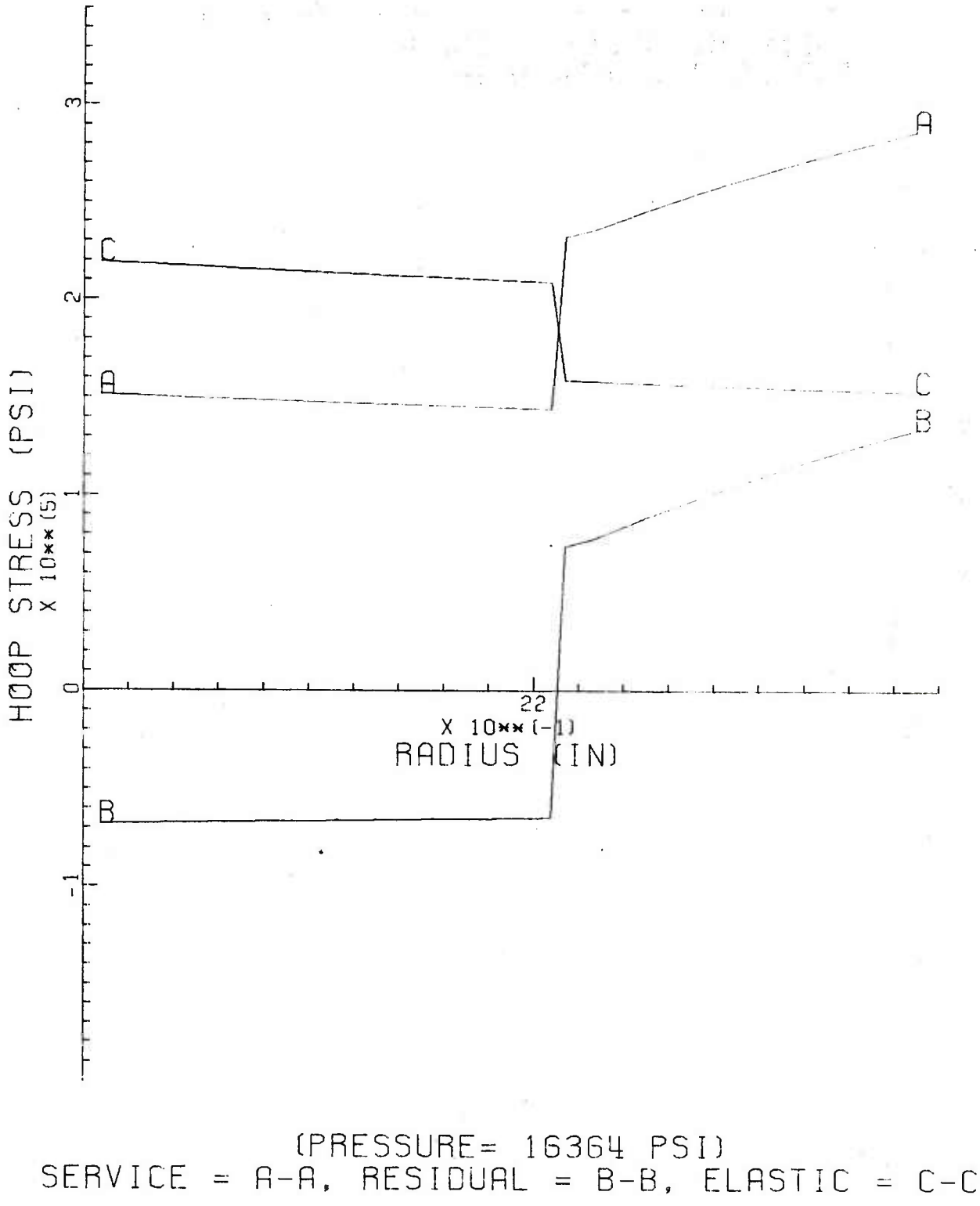

Figure 12. Plot of stress distribution for actual fabricated composite cylinder.

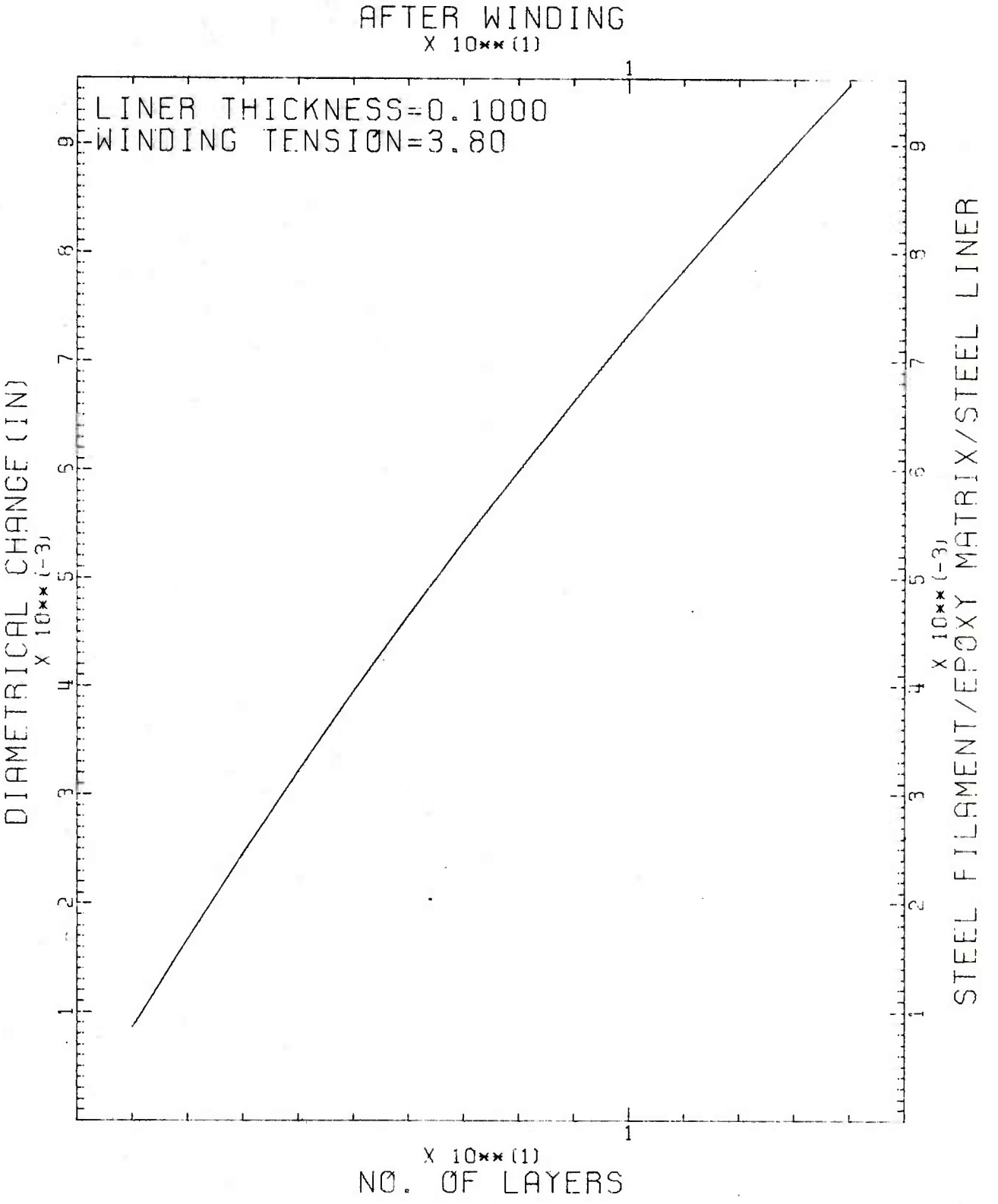

Figure 13. Plot of the 0.100" liner's diametrical change vs number of layers.

following equations outlined in Reference 2.

i.e., $\sigma_\theta\Big|_{\text{BORE}}^{\text{RESIDUAL}} + \sigma_\theta\Big|_{\text{BORE}}^{\text{ELASTIC}} = \sigma_\theta\Big|_{\text{BORE}}^{\text{YIELDING}}$

from Figure 12 $\sigma_\theta\Big|_{\text{BORE}}^{\text{RESIDUAL}} = -69 \text{ KSI}$

then $-69 \text{ Ksi} + (A^* + \frac{B^*}{2}) = \frac{1}{2}\left[\sigma_r + \sqrt{3}\sqrt{\frac{4}{3}\sigma_o^2 - \sigma_r^2}\right]$

where A* and B* are the Lame' constants and

$\sigma_\theta\Big|_{\text{BORE}}^{\text{YIELDING}}$ ➡ is the resultant limit stress based on the Von Mises yielding criterion

The solution of this equation produces an internal pressure of 16,364 psi as shown in Figure 12. Inspecting Figure 12 one finds that at a pressure of 16,342 psi, the liner is at its limit stress, however the jacket has not yet reached its limit stress as depicted in Figure 11. For the jacket to be at its limit, the residual stresses (the B-B curve) have to be increased to a magnitude similar to the one in Figure 11. This can be done by increasing the 3.8 lb tension per filament or by increasing the internal pressure from 16,364 psi to 20 KSI.

---

[2] D'Andrea, G., et al, "Application of Filament Winding to Cannon and Cannon Components. Part II: Residual Stress Analysis." October 1975, WVT-TR-75058.

Any internal pressure within this range will plastically deform the liner, and will stress the jacket from the A-A curve of Figure 12 to the A-A curve of Figure 11. When the pressure within this range is released, the cylinder will follow Hooke's Law and the stresses will behave in a manner described by the C-C curve. As the pressure is released the A-A curve is subtracted by the C-C curve and a new B-B curve is obtained. The new B-B curve can only be pushed or extended to the B-B curve depicted in Figure 11. Although this process does not alter the stress state in the liner, it will produce a diametrical change of the bore greater than the change shown in Fig 13.

Diametrical change has to be considered when selecting liners to hold a predetermined pressure. For instance, if the liner of the 106mm composite RR is manufactured by turning a conventional 106mm tube to a wall thickness of 0.050" for a pressure capacity of approximately 16 KSI the diametrical change is 18.5×10^{-3} inches (See Appendix B). For the same pressure capacity in a 0.100" thickness, the diametrical change is 9.5×10^{-3} inches (see Fig 13). Although from a minimum weight point of view, the 0.050" liner and jacket looks attractive; this increased deflection could cause interference with the 106mm round and a probable tube failure would occur if fired. Figure 13 represents the theoretical results of the diametrical change of the liner as a function of the number of layers. This graphical output is a very important one since it allows the filament winding operator to monitor the product as it is being fabricated.

In Appendix B, figures B-1 and B-6 present similar results for two other liners thicknesses: the 0.050" and the 0.075".

c. "LAMCOMB" program described in Ref 3 offers techniques for obtaining the Composite Moduli of composite structures. A summary of the theory used in "LAMCOMB" is next presented. This summary is useful if experimental results are to be checked with the theory.

From Anisotropic Elasticity, it can be shown that at any location across the thickness of the composite, the stress and strain relationship can be expressed in one of the following ways:

$$\begin{bmatrix} N \\ \hline M \end{bmatrix} = \left[\begin{array}{c|c} A & B \\ \hline B & D \end{array}\right] \cdot \begin{bmatrix} \epsilon^{\circ} \\ \hline \chi \end{bmatrix} \qquad 1$$

$$\begin{bmatrix} \epsilon^{\circ} \\ \hline M \end{bmatrix} = \left[\begin{array}{c|c} A^* & B^* \\ \hline H^* & D^* \end{array}\right] \cdot \begin{bmatrix} N \\ \hline \chi \end{bmatrix} \qquad 2$$

$$\begin{bmatrix} \epsilon^{\circ} \\ \hline \chi \end{bmatrix} = \left[\begin{array}{c|c} A' & B' \\ \hline H' & D' \end{array}\right] \cdot \begin{bmatrix} N \\ \hline M \end{bmatrix} \qquad 3$$

where

A = In-plane stiffness matrix, lb/in = A_{ij}

A^*= Intermediate in-plane matrix, in/lb = A^*_{ij}

A'= In-plane compliance matrix, in/lb = A'_{ij}

B = Stiffness coupling matrix, lb = B_{ij}

B^*= Intermediate coupling matrix, in = B^*_{ij}

B'= Compliance coupling matrix, 1/lb = B'_{ij}

[3] D'Andrea, G., et al, "Development of: Design Analyses, Manufacturing and Testing of the 81mm XM73 Fiberglass-Epoxy Recoilless Rifle" June 1974, WVT-TR-74014.

D = Flexural stiffness matrix, lb-in = D_{ij}

D^*= Intermediate flexural matrix, lb-in = D^*_{ij}

D'= Flexural compliance matrix, 1/lb-in = D'_{ij}

H^*= Intermediate coupling, matrix, in

These constants are related and obtained as it follows:

$$A^* = A^{-1}$$

$$B^* = A^{-1} B$$

$$H^* = BA^{-1}$$

$$D^* = D - BA^{-1} B \qquad 4$$

$$A' = A^* - B^* D^{*-1} H^*$$

$$B' = H^1 = B^* D^{*-1}$$

$$D' = D^{*-1}$$

where:

$$A_{ij} = \sum_{K=1}^{n} (C_{ij})_K (h_K - h_{K-1}) \qquad 5$$

$$B_{ij} = \frac{1}{2} \sum_{K=1}^{n} (C_{ij})_K (h_K^2 - h_{K-1}^2) \qquad 6$$

$$Dij = \frac{1}{3} \sum_{K=1}^{n} (Cij)_K \ (h_K^3 - h_{K-1}^3) \qquad 7$$

and

K=1, 2, ...n no. of layers,

h_K = thickness in inches

i, j = 1, 2, 6 or x, y, s in 2-dimensional space

A cylindrical shell under homogeneous loading maintains its shape, and the induced stress distribution can be represented by simpler relations. By assuming no change in curvature (i.e., $\chi = 0$) the total strain is now equal to the in-plane strain ϵ_i^o (from $\epsilon_i = \epsilon_i^o + Z\chi_i$) i.e., the strain is homogeneous across the thickness of the shell or independent of Z.

Using equations 3, one can determine the stress components

$$\sigma_i^{(K)} = Cij^{(K)} \left[Ajk \bar{N}k - \alpha_j^{(K)} T \right] \qquad 8$$

Using equation 2, the total strain caused by the load Nj is

$$\epsilon_i^o = A^*_{ij} \bar{N}j \qquad 9$$

· OBTAINING A*

Recall:

$A^* = A^{-1}$

and

$$Aij = \sum_{K=1}^{n} (Cij)_K \ (h_K - h_{K-1})$$

or

$$Aij = \begin{bmatrix} A_{11} & A_{12} & A_{16} \\ A_{21} & A_{22} & A_{26} \\ A_{61} & A_{62} & A_{66} \end{bmatrix}$$

Then:

$$A^* \quad \frac{\text{Cofactor of A}}{\text{determinant of A}} = \frac{\text{CofA}}{A} \qquad 10$$

where

$$A = A_{11} A_{22} A_{66} + A_{12} A_{26} A_{61} + A_{16} A_{21} A_{62} - A_{16} A_{22} A_{61} - A_{11} A_{26} A_{62} - A_{12} A_{21} A_{66}$$

and

CofA is the determinant of a matrix by striking the i^{th} row and j^{th} column of A, and choosing positive (negative) sign if i + j is even (odd), i.e.,

$$A^*_{11} = \frac{1}{|A|} \cdot \begin{vmatrix} A_{22} & A_{26} \\ A_{62} & A_{66} \end{vmatrix} = \frac{A_{26}\,A_{66} - A_{26}\,A_{62}}{|A|}$$

$$A^*_{12} = \frac{1}{|A|} \cdot \begin{vmatrix} A_{21} & A_{26} \\ A_{61} & A_{66} \end{vmatrix} = A^*_{21}$$

$$A^*_{22} = \frac{1}{|A|} \cdot \begin{vmatrix} A_{11} & A_{16} \\ A_{61} & A_{66} \end{vmatrix}$$

$$A^*_{16} = \frac{1}{|A|} \cdot \begin{vmatrix} A_{21} & A_{22} \\ A_{61} & A_{62} \end{vmatrix} = A^*_{61}$$

$$A^*_{66} = \frac{1}{|A|} \cdot \begin{vmatrix} A_{11} & A_{12} \\ A_{12} & A_{22} \end{vmatrix}$$

$$A^*_{62} = \frac{1}{|A|} \cdot \begin{vmatrix} A_{11} & A_{16} \\ A_{21} & A_{26} \end{vmatrix} = A^*_{26}$$

or

$$A^*_{ij} = \begin{vmatrix} A^*_{11} & A^*_{12} & A^*_{16} \\ A^*_{21} & A^*_{22} & A^*_{26} \\ A^*_{61} & A^*_{62} & A^*_{66} \end{vmatrix}$$

OBTAINING ϵ_i^o

$$\epsilon_i^o = A_{ij}^* \; Nj$$

or

$$\epsilon_1^o = \epsilon\Big|_{\text{LONGITUDINAL}} = A_{1j}^* \; Nj$$

$$= A^*_{11} \; N_1 + A^*_{12} \; N_2 + A^*_{16} \; N_6$$

$$\epsilon_2^o = \epsilon\Big|_{\text{HOOP}} = A_{2j}^* \; Nj$$

$$= A^*_{21} \; N_1 + A^*_{22} \; N_2 + A^*_{26} \; N_6$$

For a cylindrical pressure vessel, assuming that $N_6 = 0$ and

$$\frac{N_2}{N_1} = \text{HTLSR}$$

then:

$$\epsilon_H = N_2 \left(A^*_{22} + \frac{A^*_{21}}{\text{HTLSR}} \right) \qquad 11$$

and

$$\epsilon_L = N_2 \left(A^*_{12} + \frac{A^*_{11}}{\text{HTLSR}} \right) \qquad 12$$

where N_2, the stress resultant is equal to $t\sigma_H = PR$

Example: 106mm Composite Recoilless Rifle

Find:

a. The theoretical composite moduli.

b. Derive an expression which will determine the experimental modulus of elasticity in the hoop direction once the hoop to longitudinal strain ratio is known.

SOLUTION

a. Material properties for Layer 1 (Liner) and Layer 2 (Jacket) are:

Modulus of Elasticity of	Liner = 30×10^6 psi
	Filament = 30×10^6 psi
	Matrix = $.5 \times 10^6$ psi
Poisson's ratio of	Liner = .30
	Filament = .28
	Matrix = .36

Since the hoop direction corresponds to the direction of the filaments, the ply angle for both layer 1 and 2 is 90°, while the filament volume ratio is 99.99% and 75% respectively.

When this information is fed into LAMCOMB the output shown in Table 2 is displayed for the OCL specimens and the 106mm RCLR.

TABLE 2. "LAMCOMB" OUTPUT FOR STEEL LINER COMPOSITE CYLINDERS

S/N	Layer No	Thickness inches	A^*_{11} x10^{-6}	A^*_{12} in/lb	A^*_{22}	A^*_{66}
OCL 4, OCL 5	1	.050	.4996	.0786	.2626	1.0906
	2	.102				
OCL 6	1	.075	.3692	.0699	.2333	.8581
	2	.090				
OCL 10	1	.100	.2747	.0512	.1709	.6354
	2	.078				
OCL 7	1	.100	.2769	.0524	.1750	.6436
	2	.084				
106mm RCLR Stub-tube	1	.100	.2909	.0612	.2041	.6974
	2	.120				
106mm RCLR Full Size	1	.100	.2934	.0629	.2099	.7073
	2	.126				

From Table 2 the following composite moduli can then be obtained:

$$E_H = \frac{1}{A^*_{22}}$$

$$E_L = \frac{1}{A^*_{11}}$$

$$\nu_{HL} = - E_H A^*_{12} \qquad 13$$

$$G_{HL} = \frac{1}{A^*_{66}}$$

For the 106mm full size composite R.R.

$$E_H = \frac{1 \quad x\ 10^6}{.266(0.175)} = 25{,}284{,}450 \text{ psi}$$

$$E_L = \frac{1 \quad x\ 10^6}{(.226)(.277)} = 15{,}973{,}930 \text{ psi}$$

$$\nu_{HL} = - E_H (.226)(-.052 \times 10^{-6}) = .297$$

$$G_{HL} = \frac{\quad x\ 10^6}{(.226)(.643)} = 6{,}881{,}459 \text{ psi}$$

b. From

$$\epsilon_i = A^*_{ij} \ Nj$$

(i, j = 1, 2, 6)

Let subscript 2 depict the hoop direction and

1 depict the longitudinal direction, then

$$\epsilon_1 = A^*_{11}\ Ni + A^*_{12}\ N_2 + A^*_{16}\ N_6$$

$$\epsilon_2 = A^*_{21}\ Ni + A^*_{22}\ N_2 + A^*_{26}\ N_6 \qquad 14$$

since no shearing stresses are present the term N_6 is equal to zero. At this point the Hoop-To-Longitudinal-Stress-Ratio (HTLSR) is introduced, i.e.,

$$HTLSR = \frac{N_2}{N_1}$$

then

$$\epsilon_1 = N_2\left(\frac{A^*_{11}}{HTLSR} + A^*_{12}\right)$$

and

$$\epsilon_2 = N_2\left(\frac{A^*_{21}}{HTLSR} + A^*_{22}\right)$$

or

$$\frac{\epsilon_2}{\epsilon_1} = \frac{A^*_{21} + A^*_{21}\ (HTLSR)}{A^*_{12}\ (HTLSR) + A^*_{11}} = K \qquad 15$$

Since the OCL specimens and 106mm RCLR were strain gaged in the hoop and longitudinal direction the K ratio is then known, consequently the HTLSR can be determined by the following equation

$$HTLSR = \frac{A^*_{21} - K\ A^*_{11}}{K\ A^*_{21} - A^*_{22}} \qquad 16$$

Knowing the HTLSR the modulus of Elasticity in the hoop direction can be easily evaluated:

Recall the Hooke's law equation

$$\sigma = E \epsilon$$

in our particular case

$$\sigma = \frac{PR}{t} \quad \text{or} \quad t\sigma = PR = N_2$$

then

$$\epsilon_2 = N_2 \left(\frac{A^*_{21}}{HTLSR} + A^*_{22} \right)$$

becomes

$$\epsilon_2 = t\sigma \left(\frac{A^*_{21}}{HTLSR} + A^*_{22} \right)$$

or

$$\frac{1}{E_{Hoop}} = t \left[A^*_{22} + \frac{A^*_{21}}{HTLSR} \right] \qquad 17$$

This analysis will be used in the section on Testing.

3. Fabrication and Inspection

The fabrication of a composite gun tube is the translation of the design into a finished product that will perform the required function. Materials, theory, facilities and procedures are now integrated in a systematic way to ensure that the desired quality is obtained for a minimum cost. The problems that must be evaluated are:

(1) Integrating the filaments with the matrix to obtain desired properties.

(2) Ensuring that the composite tube is uniform without voids.

(3) Ensuring that the composite tube has good structural and chemical balance so that it is not damaged during fabrication and cure.

(4) Compensation for normal variation of materials within batches.

(5) Choosing the proper filament winding procedure to get maximum filament volume ratio and composite homogeneity.

(6) Winding tension studies as well as wrapping or winding approaches.

(7) Curing techniques to determine the best and most efficient way to obtain a high quality tube.

References 1 and 2 explain in details through many illustrations the original fabrication procedures used in the development of the 106mm Composite Recoilless Rifle. This following write up will describe the latest technology developed under this MMT project.

A summary of all the 106mm burst cylinders tested along with the additional fatigue cylinders is given in Appendix C.

Earlier reports [1,2] explain some of the design, fabrication and

---

[1] Cullinan, R., et al, "Application of Filament Winding to Cannon and Cannon Components. Part I: Steel Filament Composites," April 1972 WVT-7205.

[2] D'Andrea, G., et al, "Application of Filament Winding to Cannon and Cannon Components. Part II: Residual Stress Analysis." October 1975, WVT-TR-75058.

testing of burst cylinders done throughout this project while this report explains the work accomplished on fatigue cylinders and on a full length tube. The cycled-burst cylinders OCL-5 and 7 and the fatigued cylinders OCL-4, 6 and 10 were fabricated using the same solvent-wipe process explained in Reference 1 and shown in Figure 14.

a. TEST CYLINDERS

Two cylinders, OCL-5 (0.050" wall) and OCL-7 (0.100" wall) were fabricated and tested with the intent of determining if any permament bore enlargement or contraction would occur at pressures which exceed the yield of liner itself.

OCL-5

This cylinder, designed by GUNTUC to a rupture pressure of 17.6 KSI with a 0.050" wall (see Figure 15) was wound with 17 layers of NS-355 wire. It had an average of 158.2 ends/in/layer and an average tension of 3.5#/end. Appendix D contains the fabrication and inspection sheets of this fatigue cylinder.

The cylinder was bore inspected with an air gage before and after winding. The air gage was also mounted in the center of the cylinder to monitor each individual layer deflection during winding. Details of this technique are given in Reference 2 and shown in Figure 16. The

[1]Cullinan, R., et al, "Application of Filament Winding to Cannon and Cannon Components. Part I: Steel Filament Composites," April 1972, WVT-7205.

[2]D'Andrea, G., et al, "Application of Filament Winding to Cannon and Cannon Components. Part II: Residual Stress Analysis." October 1975, WVT-TR-75058.

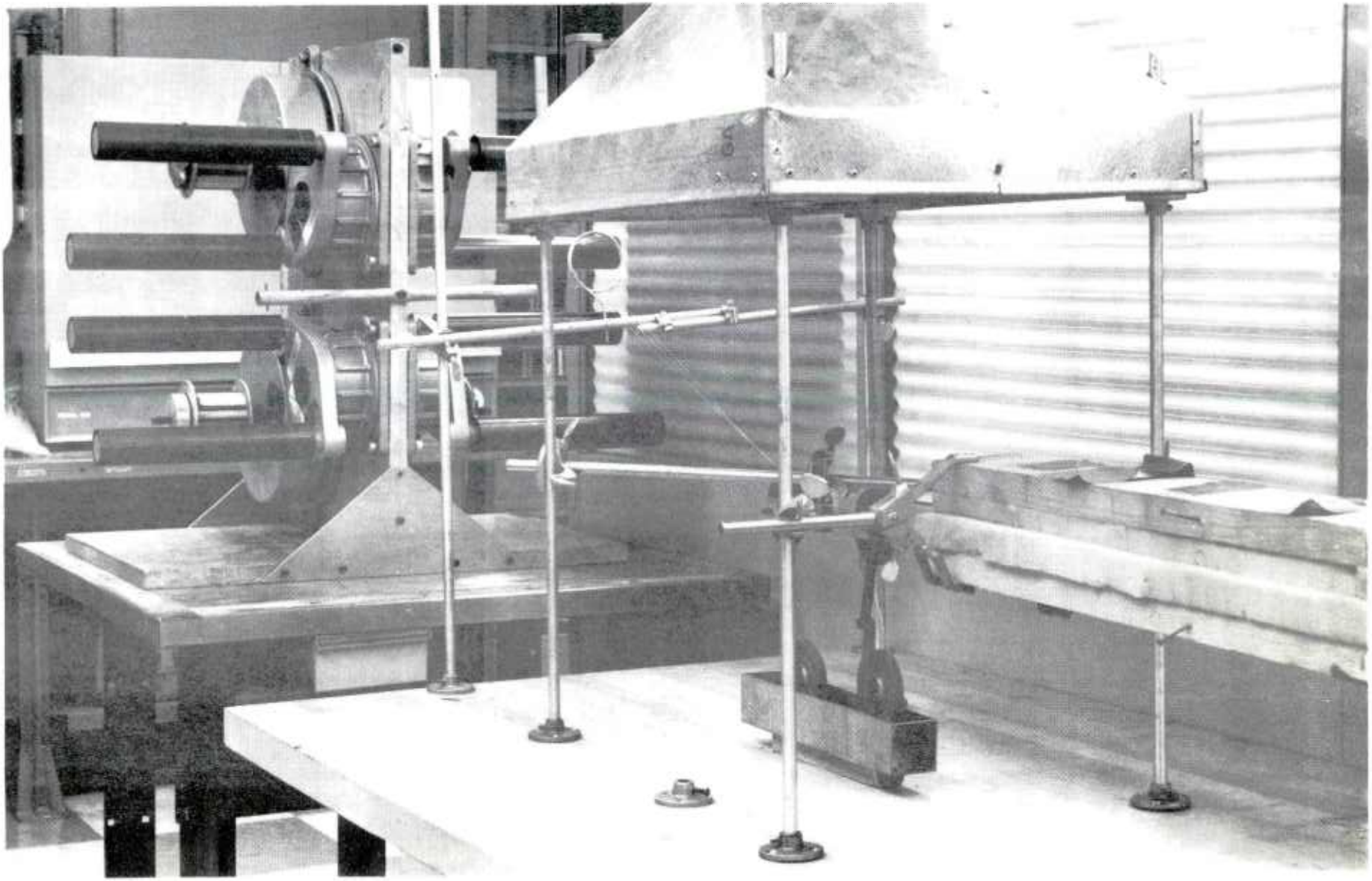

Figure 14. View of solvent-wipe cleaning process using in winding.

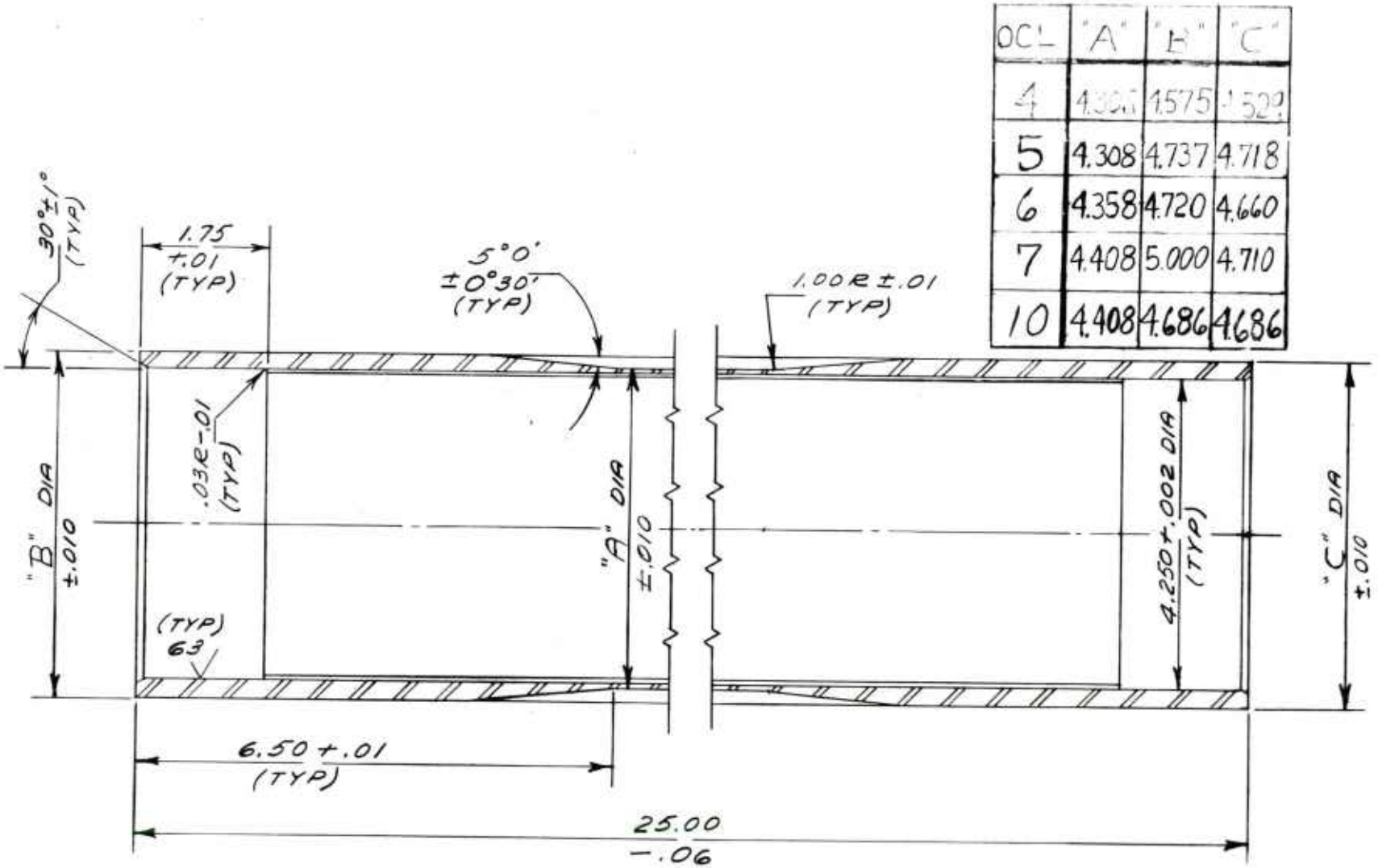

Figure 15. Dimensional drawing of steel liners used for test cylinders.

Figure 16. Modified air gage inspection assembly.

resin, E-828 (100 phr)/MNA (80 phr)/BDMA (2 phr) which was the same resin used throughout this study, was gelled under infrared lamps and placed in 350°F oven for 3 hours to develop its final cure.

OCL-7

This cylinder was machined to 0.100" wall with the dimensions given in Figure 15. It was designed to rupture at 20 KSI and wound with 14 layers of 6 mil wire (NS-355) at an average of 158.7 ends/in/layer and an average tension of 3.80#/end. (See Appendix D)

The same fabrication and inspection techniques used for OCL-5 were used again for OCL-7.

Three additional cylinders were fabricated to analyze the fatigue strength of composite cylinders designed for 19 KSI burst strength and having 0.050", 0.075" and 0.100" wall thicknesses in the gage length. The liners for the three cylinders, OCL-4, 6, and 10 were machined to the dimensions also shown in Fig 15.

OCL-4

This cylinder with a 0.050" wall was wound with 17 layers of 6 mil NS-355 wire with an average of 161.9 ends/in/layer and an average tension of 3.8#/end. Maximum deflection in middle of gage length was -0.015" at the bore (top of rifling) and -0.013" at the rifling (bottom of rifling) after full cure.

OCL-6

This 0.075" wall cylinder was wound with 15 layers of wire with an average of 161.7 ends/in/layer and with an average tension of 3.8#/end. Maximum deflection in the gage length middle, after curing, was -0.0105"

at the bore and -0.0095" at the rifling.

OCL-10

This 0.100" wall cylinder was wound with 13 layers of wire with an average of 157.6 ends/in/layer and an average tension of 3.8#/end. Maximum deflection in the middle of the gage length, after winding was -0.007" at the bore and -0.0075" for the rifling.

The fabrication and inspection sheets for these three cylinders can also be found in Appendix D.

b. FULL LENGTH TUBE

A finished machined 106mm R.R. was obtained that was 2" shorter than the conventional tube (Figure 17). Overall length was 106 3/4" instead of 108 3/4". The discrepancy in length was in the barrel as the breech's threaded section, origin of the rifling and wall thicknesses, etc. were the same as a conventional tube.

This tube was ground on the O.D. to the dimensions shown in Figure 18. The 0.100" wall thickness was selected for the full length tube after analyzing the fatigue and burst data on the 25" test cylinders.

The main reasons for selecting the 0.100" wall over the other two wall thicknesses tested, i.e., 0.050" and 0.075", were its ability to minimize liner deflection and its superior fatigue properties in the limited fatigue test.

Minimum liner deflection was important in this instance because it was felt that the 0.100" wall thickness would minimize bore deflection and enable the conventional 106mm round to pass through. As Figure 19

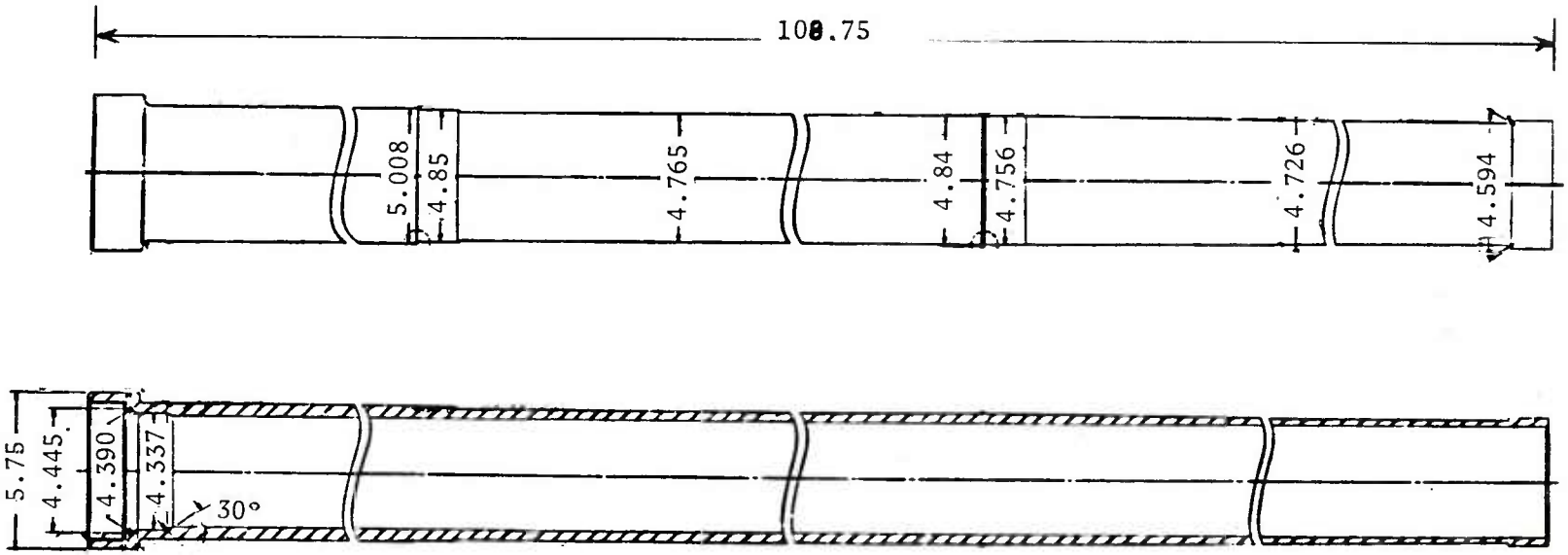

Figure 17. Drawing of Conventional 106mm M40A1 Gun Tube.

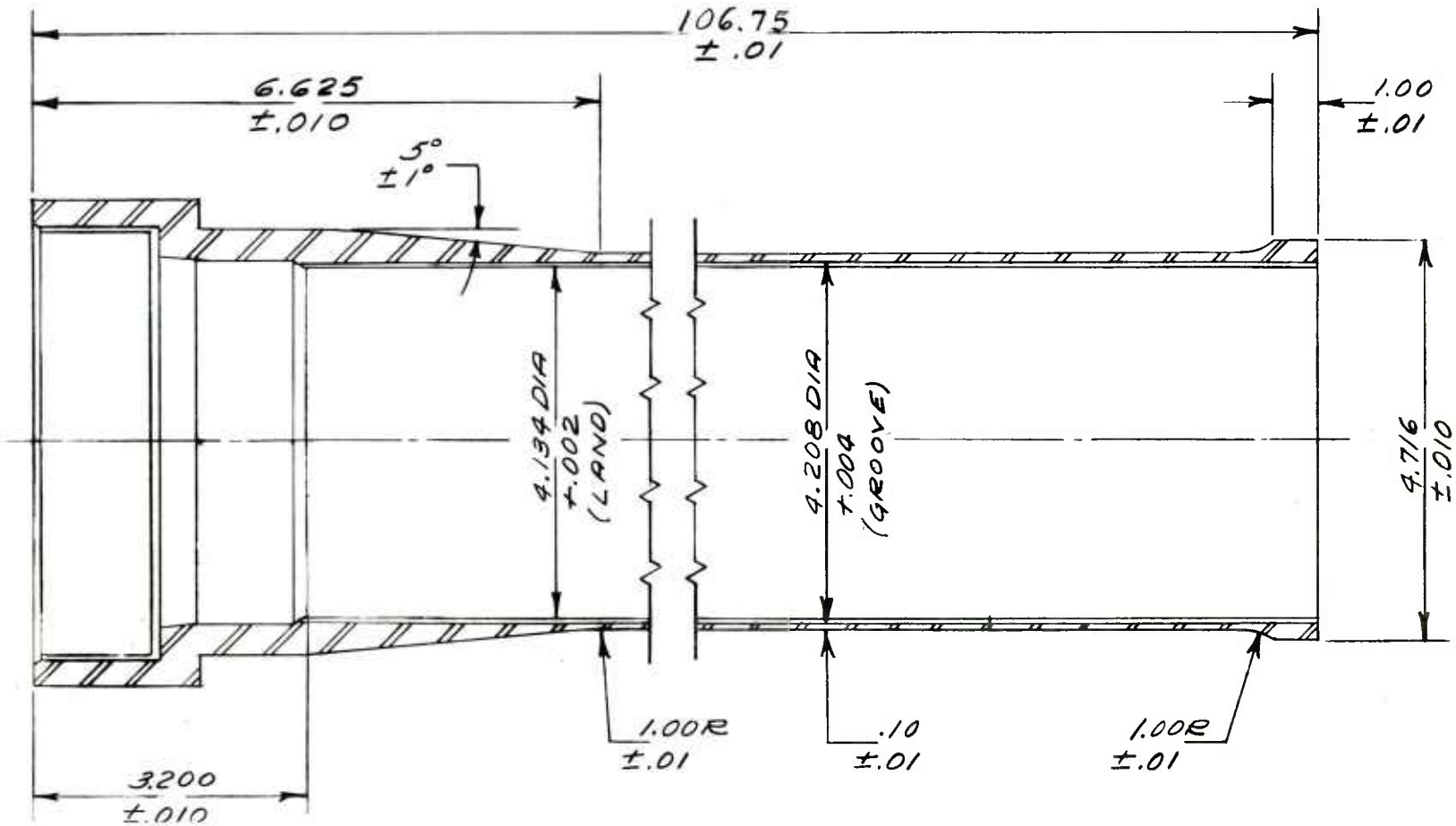

Figure 18. Dimensional drawing of 106mm gun tube liner.

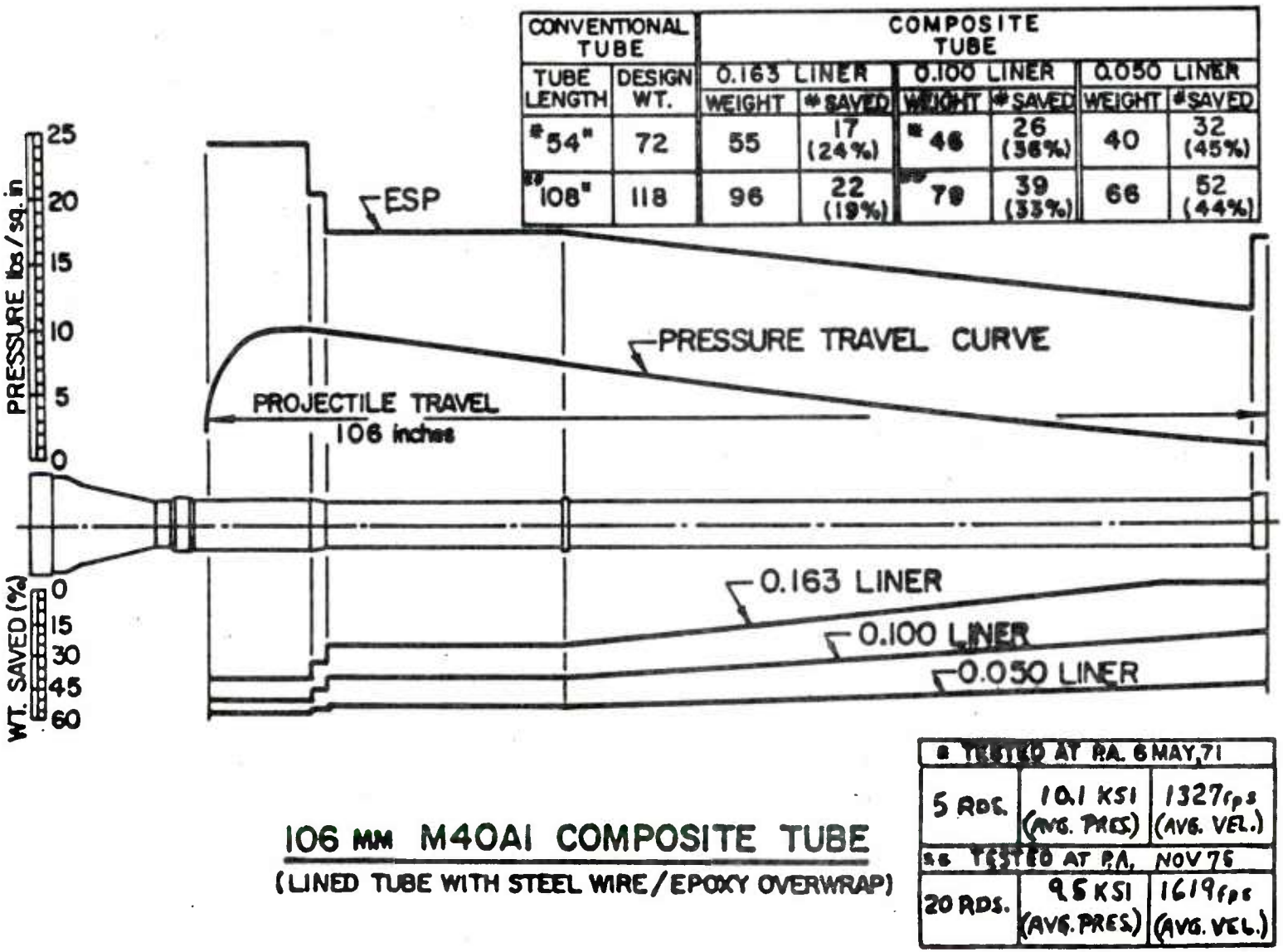

Figure 19. Pressure-travel curve of 106mm M40A1 showing weight savings of composite tubes using three different liners.

shows, the .100" liner designed to the same ESP curve, still incorporates a significant weight savings over the conventional all steel tube.

The limited testing data obtained on the three fatigued cylinders showed the 0.100" wall cylinder to have a greater fatigue capacity. As an additional safety factor in the test firing, it was decided to go with this wall thickness.

After machining the O.D., the tube was magna-flux inspected to assure that no cracks were present in the liner. The tube was also sand blasted on its entire O.D. to prepare the surface for winding. The liner weight before winding was 56 lbs.

Two aluminum end caps were machined to fit the breech and muzzle ends of the tube. These two end caps, held snug in the tube ends with a long 1/2" threaded drill rod were used to mount the tube in the winding machine.

FILAMENT WINDING MACHINE

Whereas all the burst and fatigue cylinders fabricated throughout this project were wound on the simple chain-driven winder the full length tube was wound in a larger more sophisticated winding machine.

This versatile machine, is an electronically-controlled, programmable, servo-driven unit with a high degree of winding flexibility. This machine, which is described in great detail in

Reference 3, can helically wind all stable shapes from 1° to 90° in addition to polar and hoop windings. Cones, isotensoids and objects with unequal pole diameters and varying winding angles are all within the capabilities of this machine.

This winder was used to wind the 106mm because of its greater accuracy in controlling the band advance and its overall working length of 14 ft enabled the 9 ft tube to be wound with no difficulty.

Using this machine, the solvent-wipe technique was adapted to wind the tube. Figure 20 shows the four tension devices, with the wire spools, mounted to the back of the traversing carriage. Figure 21 shows a view from the back of the carriage top. The wires from the four tensioning devices are brought together and are shown going over the solvent pick-up wheel. The two hold-down wheels are shown in the up position. Also shown in Figure 21 is the foam wiper in its open position.

Figure 22 shows this setup from the front of the carriage. Shown here is the closed wiper, the two different size pulleys which bring the four wires to a band width of 0.024-0.028 in., and on to the delivery wheel. Mounted on four legs above the carriage top is an exhaust hood. Through the use of the large flexible hose shown, which runs between the hood and a permanent exhaust line, the fumes from the solvent (trichloroethylene) are constantly evacuated throughout the winding operation. Figure 23 is a good view of the overall setup of winder,

---

[3] D'Andrea, G., et al. "Development of: Design Analyses, Manufacturing and Testing of the 81mm XM73 Fiberglass-Epoxy Recoilless Rifle" June 1974, WVT-TR-74014.

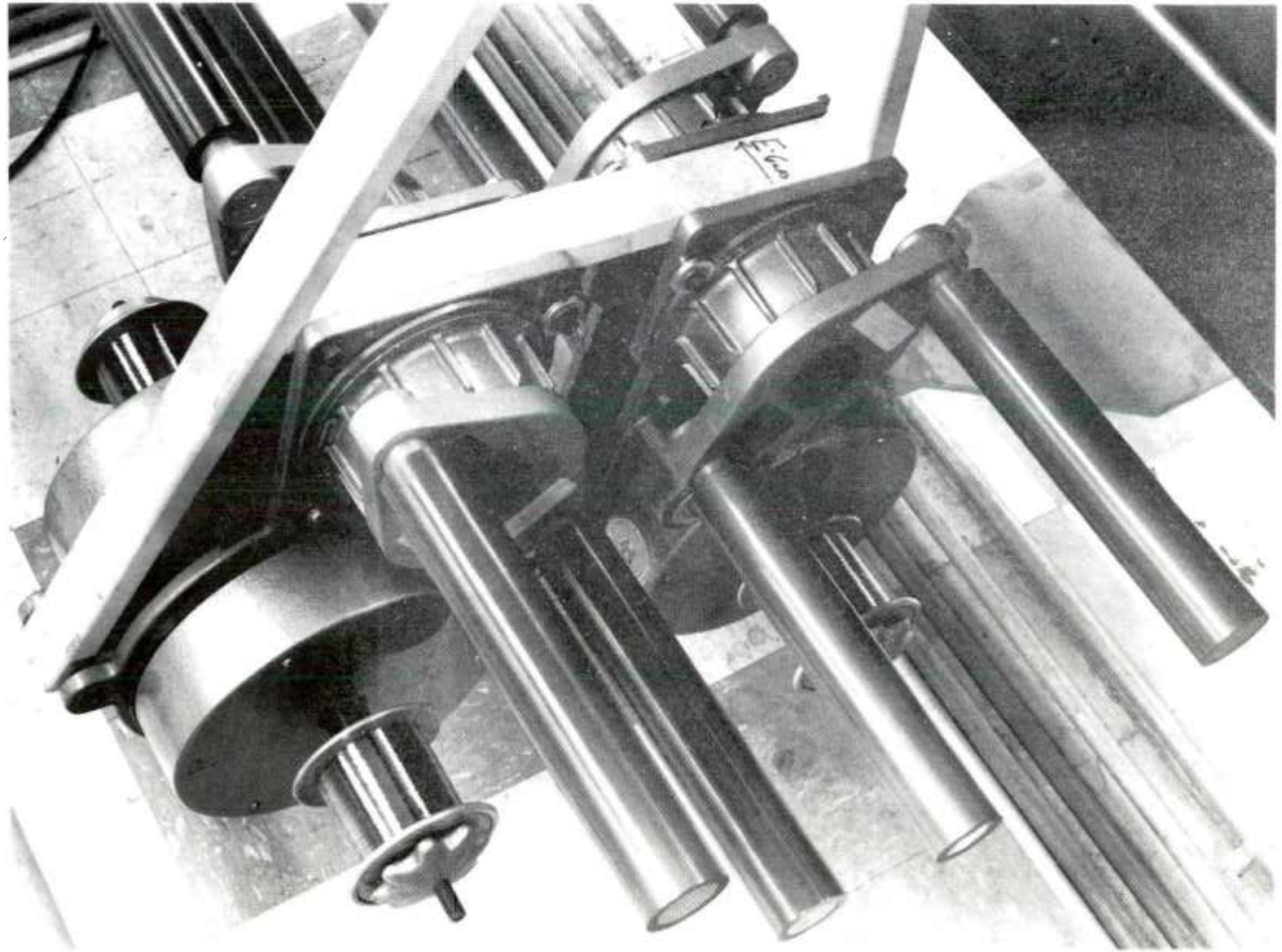

Figure 20. Filament winder's rear carriage assembly holding the four tension devices with wire spools.

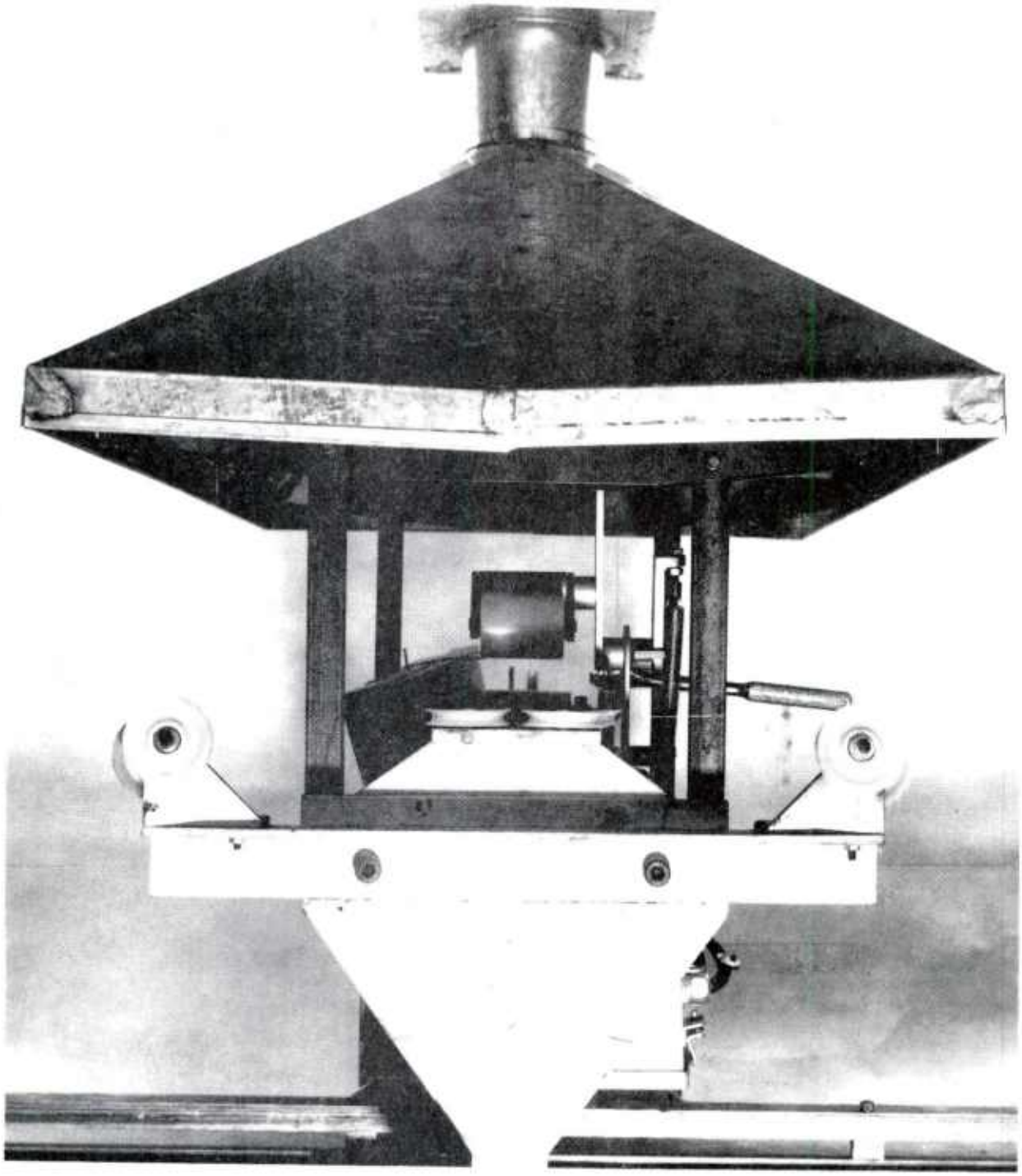

Figure 21. Rear view of carriage top showing path of filaments through the solvent-wipe cleaning process.

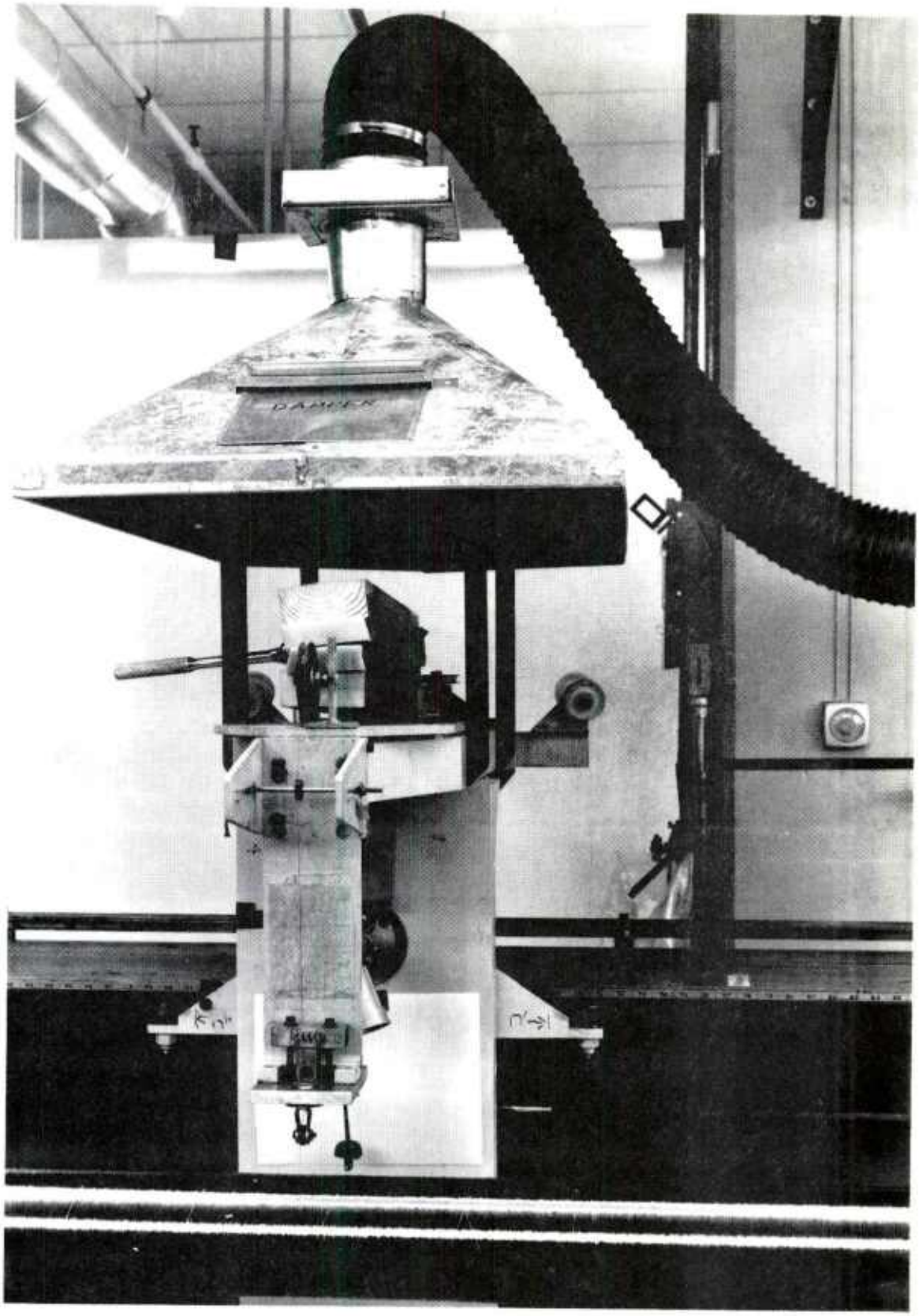

Figure 22. Front view of carriage showing path of filaments to the tube.

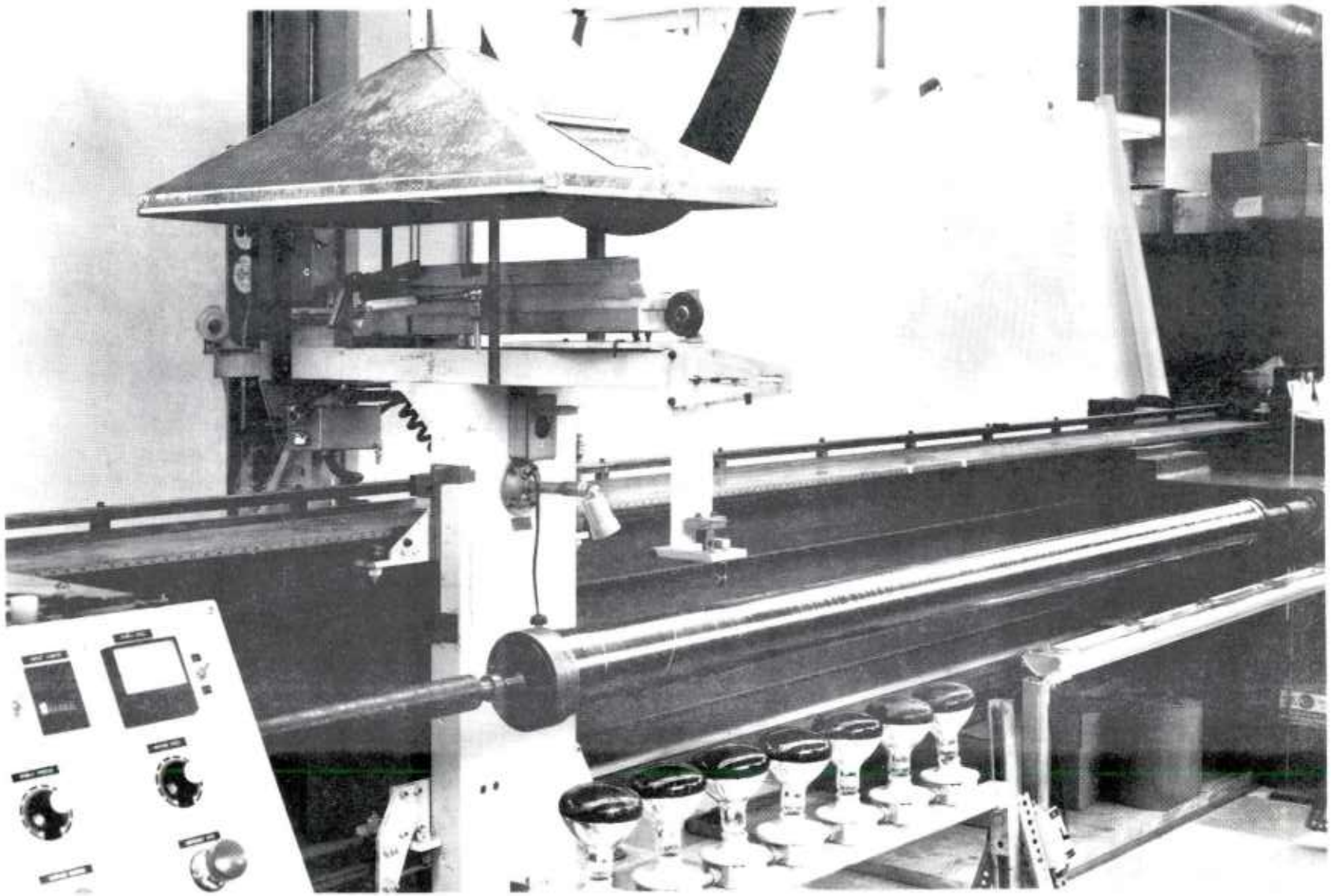

Figure 23. Overall view of winder and wound composite tube.

winder attachments, and the tube with its end caps.

The NS-355 6 mil wire and epoxy-anhydride-amine resin were used on the full scale tube. The band width consisted of four wires which were hoop wound using the solvent wipe technique, at an average tension of 3.8#/end of wire. The resin was painted on between layers as shown in Figure 24a. The actual fabrication sheet for this tube is shown in Figure 25 while Figure 26 is a schematic showing of the number of layers with regard to their position along the length of the tube.

As noted in Figure 25, after the first 6 full length layers were wound, the winding was interrupted overnight. This was done by gelling the resin, using three bands of infrared lamps (16 lamps). Figure 24b shows the lamps in position under the tube with a reflective aluminum foil. The tube was gelled by the heat from these lamps while rotating in winder for 3 hours.

The next day the tube was finished wound and gelled again in same manner as described above. Final cure was accomplished by placing tube in large heat treat furnace and curing at 350°F for 3 hours.

Final weight of composite tube was 78 lb. The liner, before winding, was weighed in at 56 lb. The jacket weight was 22 lb. Filament volume ratio was calculated to be 75%.

NOTE: Discrepancy between actual weight of 78 lb and the theoretical weight of 68.9 lb (Fig 4) is due to:

a. Neglect of "GUNTUC" program to consider the weight of rifling which was explained previously. This additional liner weight amounts to ~ 6 lb.

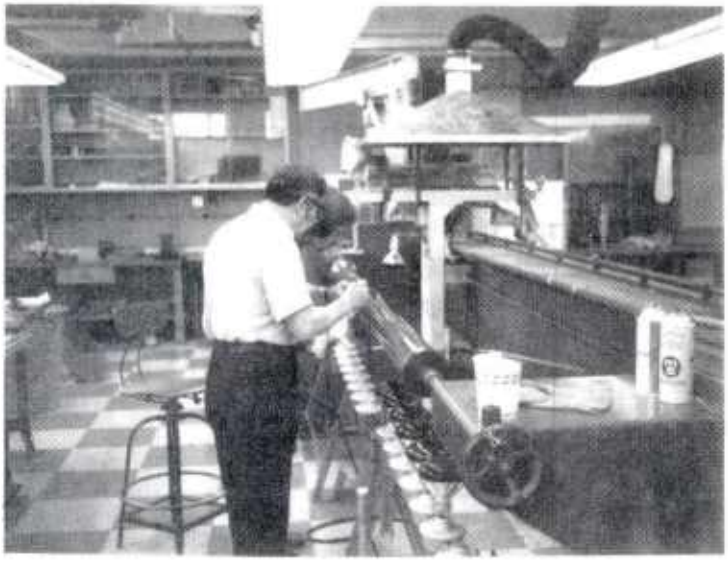

a. Application of resin during winding of a full length 106mm tube.

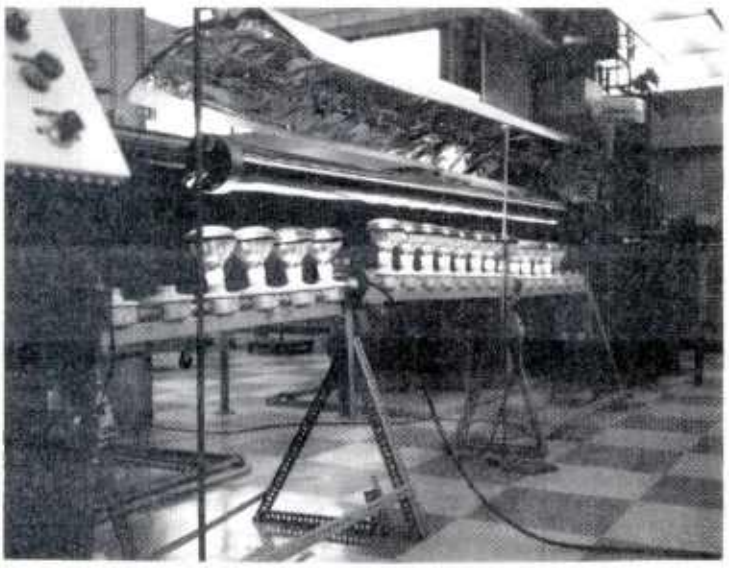

b. View of a bank of infrared lamps used to gel resin before the final cure.

Figure 24. Application and gelling of resin.

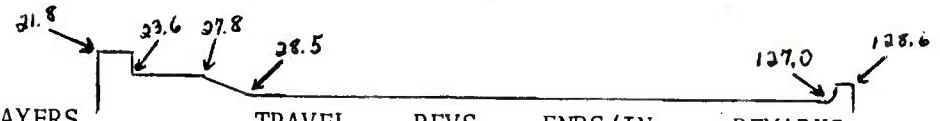

NO.	LAYERS		TRAVEL	REVS.	ENDS/IN.	REMARKS
1	23.9	28.5	4.6"	228	198	Started at bottom of slope and wound up slope to the collar
2	23.9	127.0	103.1"	4194	162.8	
3	25.0	127.0	102.0"	4848	190.0	
4	25.0	127.0	102.0"	4177	163.6	
5	25.4 *	127.0	101.6	4980	196.0	*At the 96.7" point, a heavy weight was dropped on the tube and broke a couple layers of windings.
6	25.4**	127.0	101.6	4094	161.2	
7	23.9***	127.0	103.1	5065	196.4	
8	25.8	109.8	84.0	3374	160.8	**Trimmed loose wires and rewound 4 layers over the area of broken wires.
9	26.2	109.8	83.6	5232	250.4	
10	26.2	90.8	64.6	2342	145.2	
11	26.6	90.8	64.2	2552	158.8	***Interrupted winding and gelled. Left overnight. Started at middle of shoulder between slope and collar.
12	26.6	71.8	45.2	1567	138.8	
13	27.0	71.8	44.8	1832	164.8	
14	27.0	37.8	10.8	428	154.4	
15	27.4	37.8	10.4	426	164.0	
16	27.5	37.8	10.4	411	158.0	
17	27.8	37.8	10.0	406	162.4	
18	27.8	37.8	10.0	384	153.6	
19	28.2	37.8	9.6	383	159.6	
20	28.2	37.8	9.6	390	162.4	
21	23.9	37.8	13.9	559	160.8	

Figure 25. Fabrication sheet of 106mm composite tube.

The tube was wound using pattern shown below:

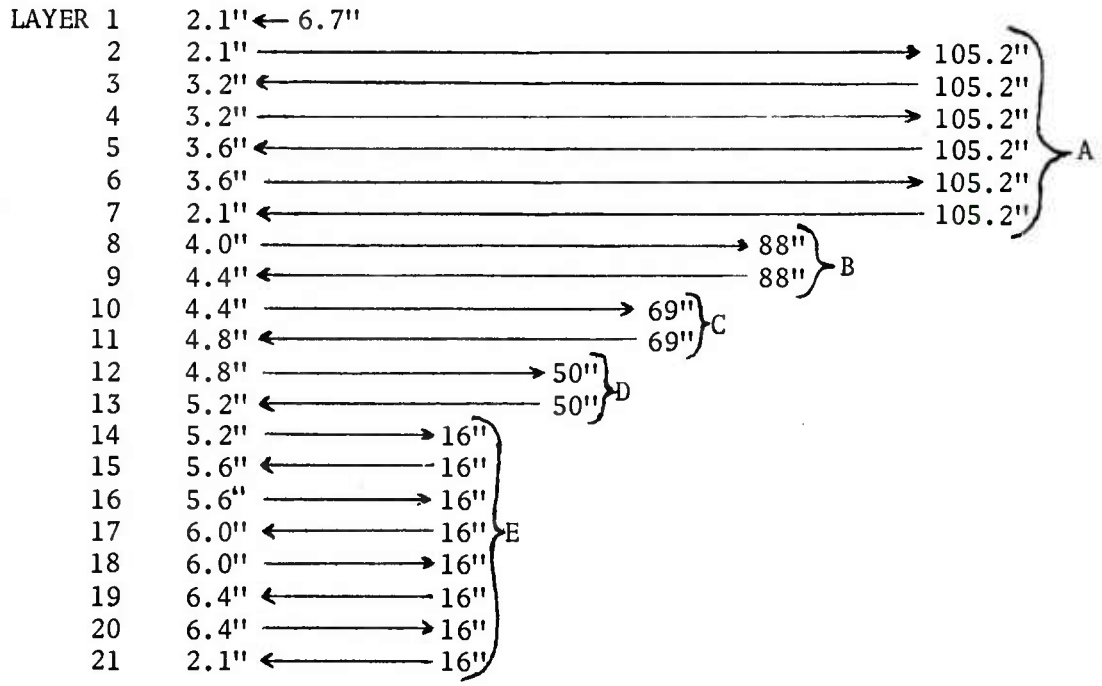

Section A - 6 layers of steel for the last 18 3/4" of the tube.
Ave A = 178.4; jacket wall thickness = 0.140;
Min O.D. = 4.488"

B - 8 layers in this section; Ave A = 185.2; wall = 0.154"
Min O.D. = 4.516"

C - 10 layers in this section; Ave A = 178.5; wall = 0.164"
Min O.D. = 4.536

D - 12 layers in this section; Ave A = 174.1; wall = 0.174"
Min O.D. 4.556

E - 20 layers in this section; Ave A = 168.2; wall = 0.218"
Min O.D. 4.643

Figure 26. Number of layers vs tube location profile of 106mm composite tube.

b. The actual winding pattern (Figure 27) did not follow the minimum weight pattern shown in Figure 6 because of fabrication simplicity. Figure 6 is based on single layer build-up along the length of the tube. The tube was actually built-up in multiples of 2 layers because this eliminates the problem of cutting the filaments which becomes necessary in single layer build-up. Figure 27 shows the actual winding pattern (dotted line) superimposed over the minimum weight pattern. This additional build-up contributed to the weight discrepancy.

A conventional 106mm M40A1 R.R. is attached to its mount and tripod through a shrunk fit clamp which fits into and locks in the mount. The mid-point of this 4" wide clamp is located 10.0" from the breech end of the tube. The O.D. of the composite tube at this location is 4.643" as compared to an O.D. of 5.008" for the conventional all steel tube. In order to utilize the standard M79 mount which controls the vertical and horizontal positioning of the 106mm R.R., it was necessary to modify the standard clamp and build up the O.D. of the composite tube.

The clamp was modified by first cutting it in half horizontally. Two each, tension adjustable, over-center latch-type clamps were riveted to the bottom half of the tube clamp.

In addition, the composite tube was built-up by the wrapping of many layers of 4 inch wide fiberglass cloth. Each layer was impregnated with a room temperature, tough curing epoxy resin (EPON 828/Versamid 140 (50/50). When the approximate O.D. value of 5.010" was reached, the mounting clamp was positioned on the build-up and clamped as tight as

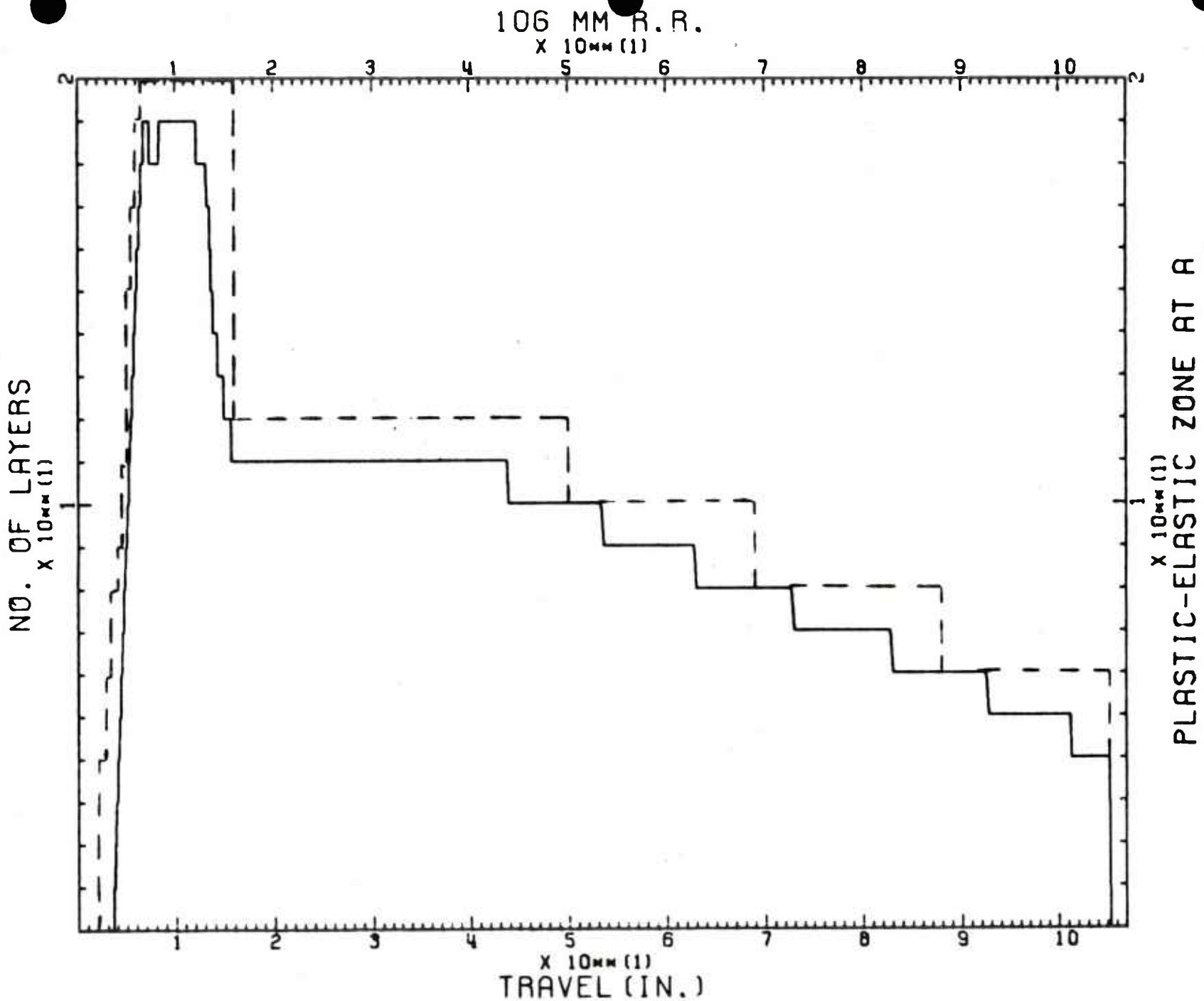

Figure 27. Actual laydown (dotted line) used in winding the composite 106mm tube.

possible. This assured a compact O.D. build-up and also assisted in bonding the clamp to the tube. Figure 28 is a close-up view of this arrangement and shows the tube actually positioned in the M79 mount. Also shown are the strain gages used to gather data during the test firing. Figure 29 is an overall view of tube, chamber, mount and tripod.

INSPECTION

As with the 25" test cylinders, the I.D. dimensions of the bare tubes were determined before and after winding with the air gage equipment mentioned previously. This inspection data is shown in Tables 3 and 4. An interpretation of this information is presented below.

With the air gage head, the rifling diameter readings are being taken in one plane, while the bore readings are simultaneously taken in the perpendicular plane. In order to determine out-of-roundness, two inspections are made. By inserting the air gage the second time, 90° apart from the original start, the rifling and bore profile along two perpendicular planes are obtained over the length of the tube.

Another aspect of this type of inspection is that the guide pins of the air gage ride in the grooves of the rifling. The rifling twist of the 106mm M40A1 is 20 calibers/twist. (1 caliber is equal to the bore diameter) Therefore every 82.68" (20 x 4.134") of travel in the barrel the rifling makes one complete twist (360°).

From the inspection point of view, this means that the air gage rotates 90° every 20.67" (82.68"/4). Every 20.67" of travel the probes are taking readings on a plane which is perpendicular to their original

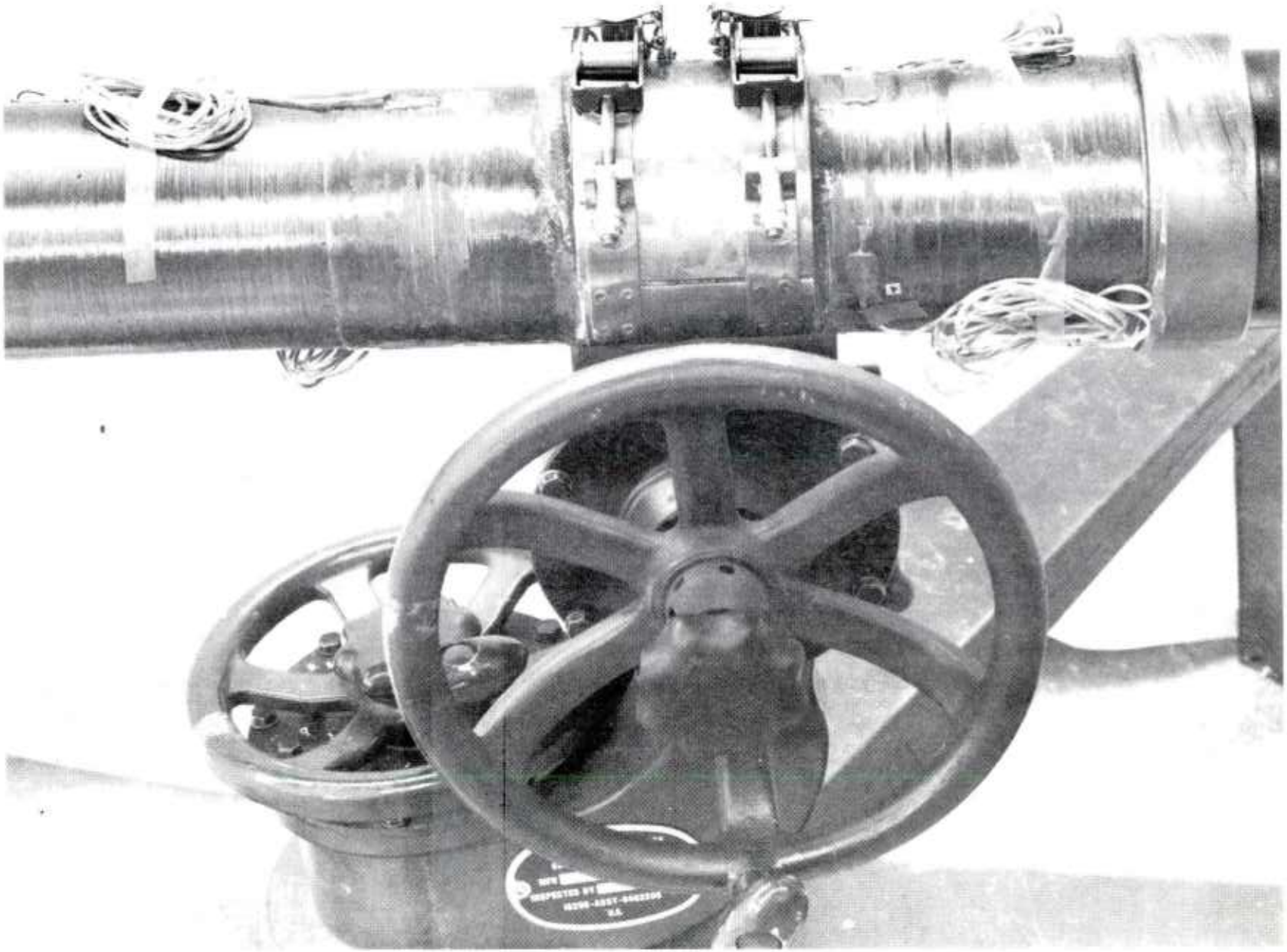

Figure 28. Close-up of modified mounting clamp on M79 mount.

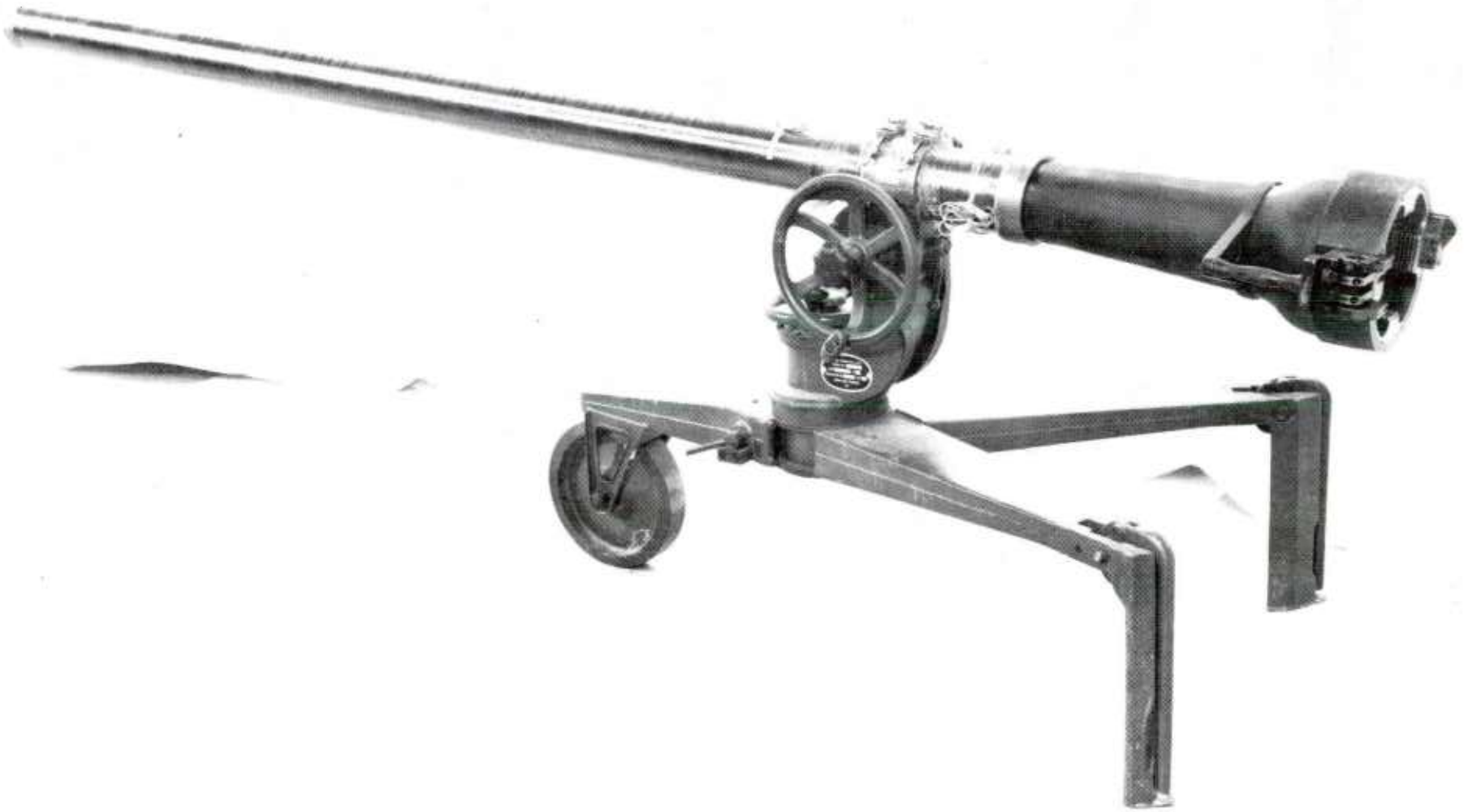

Figure 29. Overall view of composite 106mm tube with chamber and mount.

values.

With this information, and looking at Tables 3 and 4, it becomes obvious that:

Before Winding Data

a. Table 3 shows a definite out-of-roundness in the rifling values over the first 48" of travel. The initial A dimensions are undersize while the initial B (measurements perpendicular to A) are oversize.

b. After 20" of travel, the situation reverses itself and the B dimensions indicate undersize and the A dimensions show oversize. However as mentioned, after 20.67" of travel the probes rotate 90° and are now reading in planes which are perpendicular to their starting points.

c. From 50" to end of barrel, the rifling dimensions indicate roundness.

d. Table 4 presents the bore dimensions. Here we see no significant indication of out-of-roundness.

After Winding Data

A summary chart of average deflection* is shown as follows:

*For conservation of space, Tables 3 and 4 show dimensional values for every 2 in. of travel for the first 20 in. and every 4 in. of travel thereafter. In actuality, measurements were made every inch of travel. The deflection values shown in the Summary are an average from every inch of travel within each section.

SECTION	Rifling X	Rifling Y	Bore X	Bore Y
A-(20 Layers)	-5.4	-8.1	-11.1	-9.1
B-(12 Layers)	-7.1	-5.9	- 7.6	-6.6
C-(10 Layers)	-7.0	-5.1	- 8.0	-5.1
D-(8 Layers)	-4.0	-5.8	- 4.8	-6.5
E-(6 Layers)	-4.2	-4.4	- 4.6	-4.0

One can see that the winding operation attempted to eliminate the out-of-roundness that existed in the rifling for the first 44" (Sections A and B). In Section C, if we compare the X planes for the rifling and bore we see the deflection is equal to or greater than Section B which has 2 more layers. The Y plane values show too small a deflection. This indicates an egg shaped out-of-roundness.

In addition, Section D shows the same condition but in reverse. The Y plane shows a greater deflection although it has 2 less layers and the X plane shows too little a deflection. This indicates reverse out-of-roundness.

However, remembering that for every 20.67" of travel the measured planes are reversed, we find that:

1. Yes, there is out-of-roundness but it exists in the tube along the same plane.
2. The winding operation itself induced an out-of-roundness in a section of the tube which was originally round.

The tube was again inspected after honing and as shown in Tables 3 and 4. The bore diameter (top of rifling) is uniform throughout the length of the tube. Notice that the rifling diameter (bottom of rifling) has not changed. This is because the honing head in this machining operation affects only the smallest diameter which in this case is the bore diameter.

4. Testing

Testing plays a very important role in the process of evaluating and standardizing the process used in the manufacturing of the 106mm Composite Recoilless Rifle or any other composite component. Destructive testing is used to verify or evaluate proposed material, theory, fabrication, processes, to identify unknown parameters, and to assess margins of safety by overloading to failure. Firing tests are performed to verify the effectiveness of the end item as it functions in the actual environment and conditions of its end use.

References 1 and 2 explain in detail the basic in-house tests performed. Besides the numerous individual mechanical tests on filaments and resin to determine their respective properties, the composite tests performed were:

Resin Pull-out Tests - to establish best epoxy matrix system in regards to bond strength

---

[1]Cullinan, R., et al. "Application of Filament Winding to Cannon and Cannon Components. Part I: Steel Filament Composites," April 1972, WVT 7205

[2]D'Andrea, G., et al. "Application of Filament Winding to Cannon and Cannon Components. Part II: Residual Stress Analysis." October 1975, WVT-TR-758.

Flat specimen tests - to determine composite's tensile and shear strength

NOL Ring Tests - to determine composite's hoop strength

Pressure Tests - a. burst - correlate design and experimental pressure capacities of composite cylinders (Summary presented in Appendix C)

b. fatigue - explained below

In Reference 1, the details of a five round firing on a "sawed-off" composite 106mm (54" long) are also presented. This report presents the details and data gathered from destructive tests which lead to the successful test firing of a full length composite 106mm R.R. Table 5 presents a summary of the tests performed, correlation between theory and experiments, and geometry of tested components.

a. DESTRUCTIVE TESTS

(1) Cyclic-Burst Tests

Test cylinders OCL-5 and 7 were gaged on the O.D. with 3 each rosette type (0° and 90°) strain gages. These 3 gages were located in the middle of the cylinder's gage length at positions 120° apart. The hoop and longitudinal strain values, shown on pages 73 through 80, are the average of the three readings.

---

[1]Cullinan, R., et al, "Application of Filament Winding to Cannon and Cannon Components. Part I: Steel Filament Composites," April 1972, WVT-7205

TABLE 5. SUMMARY OF CYLINDERS TESTED WITH CORRELATION BETWEEN THEORY AND EXPERIMENTAL DATA

STATIC TESTS	NL	L_t	J_t	P	ϵ_H	ϵ_L	CTR	A_{11}	A_{12}	A_{22}	A_{66}	E_{HTH}	E_{HEX}
		in.	in.	KSI	%	%		x 10^{-6} in/lb				x 10^6 psi	x 10^6 psi
OCL-5	17	.050	.102	12	.716	.182	-	.499	.078	.262	1.090	25	25.24
OCL-7	14	.100	.084	12	.510	.150	-	.291	.061	.204	.697	26.6	26.6
OCL-7	14	.100	.084	10	.408	.120	-	.291	.061	.204	.697	26.6	26.6
CYCLIC TESTS													
OCL-4	17	.050	.102	12	-	-	1398	.499	.078	.262	1.090	25	-
OCL-6	15	.075	.090	12	-	-	1884	.369	.070	.233	.858	26	-
OCL-10	13	.100	.078	12	-	-	4416	.293	.063	.210	.707	26.7	-
FIRING TESTS													
STUB-106	21	.100	.126	10	.297	-	-	.274	.051	.171	.635	26	-
FULL-106	20	.100	.120	10	.315	.088	-	.277	.052	.175	.643	26	26.1

NL = No. of layers

L_t = Liner thickness

J_t = Jacket thickness

P = Pressure

ϵ_H = Hoop strain

ϵ_L = Longit. strain

CTR = Cycles to failure

A^*_{ij} = Elastic Constants

E_{HTH} = Hoop theo. Modulus

E_{HEX} = Hoop Exp. Modulus

OCL-5

This cylinder was statically pressure tested ten times by bringing the pressure up to 15 KSI, holding and releasing. The time involved for each cycle is shown in Table 6.

The cylinder was then inspected to see if any delaminations or cracks were visable in the composite jackets. None were observed. A bore inspection was performed with the air gage to determine if any additional deflection and/or buckling of the cylinder occurred. As shown in Table 7, no significant deflection was measured after the cycling.

The cylinder was returned to the in-house pressure facility for static burst testing. Pressure was allowed to increase until rupture occurred at $\sim$ 18 KSI, in the gage length.

OCL-7

This test cylinder was also statically pressure tested in the same manner as OCL-5, i.e., 10 cycles at 15 KSI. The cycle time for OCL-7 is also shown in Table 6.

The bore measurements shown in Table 7 show no significant deflection after this test. The cylinder was returned to pressure site for additional testing which involved statically pressurizing the cylinder at 20 KSI for an additional 12 cycles. Finally the cylinder was statically burst at a recorded pressure of $\sim$ 22 KSI.

Figure 30 shows the ruptured cylinders OCL-5 and 7. The windings on the upper half of OCL-5 were removed in order to pin-point the location of the top half of the circular tear. This circular tear is

TABLE 6. PRESSURE-TIME DATA ON CYCLIC-BURST CYLINDERS

CYL	CYCLE NO	PEAK PRESS. (KSI)	TIME TO PEAK PRESS. (SEC)	TIME HELD @ PEAK PRESS. (SEC)	TOTAL TIME (SEC)	CUM TOTAL TIME
O	1	14.94	13.6	7.0	20.6	
C	2	15.25	13.0	9.5	22.5	
L	3	15.56	67.2	35.2	102.4	
	4	15.37	12.0	8.1	20.1	
5	5	15.07	12.6	6.4	19.0	
	6	15.56	12.4	9.5	21.9	
	7	15.56	12.4	7.7	20.1	
	8	15.31	12.6	4.8	17.4	
	9	15.25	12.4	5.1	17.5	
	10	15.86	12.3	2.7	15.0	
	11	18.30	21.4	BURST	21.4	297.9 SEC
	1	15.86	10.6	22.6	33.2	
	2	15.86	10.0	14.0	24.0	
	3	15.86	10.0	2.4	12.4	
	4	15.86	10.0	4.0	14.0	
O	5	15.86	10.4	3.2	13.6	
C	6	15.37	10.2	1.8	12.0	
L	7	15.86	10.8	2.0	12.8	
	8	15.25	10.2	2.0	12.2	
7	9	15.25	9.8	3.6	13.4	
	10	15.55	10.2	1.6	11.8	159.4 SEC
	11	20.01	19.0	3.2	22.2	
	12	20.25	15.6	3.2	18.8	
	13	20.13	15.4	2.2	17.6	
	14	20.13	15.6	1.6	17.2	
	15	20.13	15.8	1.6	17.4	
	16	20.43	16.0	1.4	17.4	
	17	20.31	16.0	1.0	17.0	
	18	20.31	16.0	1.6	17.6	
	19	20.43	16.4	2.0	18.4	
	20	20.86	17.0	14.6	31.6	
	21	19.40	19.8	13.4	33.2	
	22	19.09	15.0	25.6	40.6	
	23	21.96	19.0	BURST	19.0	447.4 SEC

TABLE 7. INTERNAL DIMENSIONAL CHECKS OF OCL-5 AND 7 BEFORE AND AFTER CYCLING

	TRAVEL (IN.)		AFTER CURE BORE	AFTER CURE RIFLE	AFTER CYCLING BORE	AFTER CYCLING RIFLE
OCL - 5	2.5	GAGE LENGTH	4.1300	4.2070	4.1300	4.2070
	3.5		4.1300	4.2060	4.1305	4.2070
	4.5		4.1300	4.2050	4.1305	4.2050
	5.5		4.1290	4.1995	4.1280	4.1990
	6.5		4.1235	4.1920	4.2130	4.1920
	7.5		4.1150	4.1930	4.1150	4.1930
	8.5		4.1160	4.1920	4.1170	4.1940
	9.5		4.1550	4.1930	4.1170	4.1920
	10.5		4.1150	4.1940	4.1160	4.1920
	11.5		4.1160	4.1940	4.1160	4.1940
	12.5		4.1160	4.1945	4.1170	4.1930
	13.5		4.1160	4.1945	4.1160	4.1930
	14.5		4.1150	4.1950	4.1160	4.1910
	15.5		4.1160	4.1935	4.1140	4.1920
	16.5		4.1160	4.1920	4.1150	4.1915
	17.5		4.1150	4.1910	4.1155	4.1915
	18.5		4.1140	4.1970	4.1150	4.1965
	19.5		4.1210	4.2050	4.1220	4.2050
	20.5		4.1280	4.2075	4.1280	4.2060
	21.5		4.1305	4.2070	4.1290	4.2060
	22.5		4.1305	4.2070	4.1290	4.2060
OCL - 7	2.5	GAGE LENGTH	4.1320	4.2095	4.1330	4.2095
	3.5		4.1325	4.2100	4.1330	4.2100
	4.5		4.1325	4.2085	4.1330	4.2090
	5.5		4.1310	4.2050	4.1320	4.2060
	6.5		4.1275	4.2030	4.1290	4.2040
	7.5		4.1260	4.2030	4.1270	4.2045
	8.5		4.1265	4.2025	4.1280	4.2040
	9.5		4.1270	4.2020	4.1275	4.2040
	10.5		4.1265	4.2015	4.1275	4.2030
	11.5		4.1265	4.2020	4.1270	4.2035
	12.5		4.1270	4.2020	4.1275	4.2035
	13.5		4.1270	4.2020	4.1270	4.2030
	14.5		4.1270	4.2020	4.1270	4.2030
	15.5		4.1270	4.2020	4.1270	4.2030
	16.5		4.1270	4.2020	4.1270	4.2030
	17.5		4.1265	4.2020	4.1270	4.2030
	18.5		4.1260	4.2050	4.1265	4.2050
	19.5		4.1295	4.2090	4.1290	4.2085
	20.5		4.1325	4.2095	4.1320	4.2090
	21.5		4.1330	4.2095	4.1330	4.2090
	22.5		4.1330	4.2100	4.1330	4.2095

Figure 30. Cyclic-burst cylinders OCL 5 and 7 after burst.

at the exact location where the slope of the liner starts from the .050" wall up to the .255" wall. This is the only split in the cylinder.

The rupture pattern of OCL-7 is entirely different. It burst in the center of the cylinder and mushroomed out for a length of $\sim$ 2 inches. There are six longitudinal splits around the circumference of this burst.

Figures 31, 32 and 33 shows the P vs ϵ curves for the 1st, 10th and 11th (first cycle over 15 KSI and also the burst cycle) cycles on OCL-5. Figures 34 through 38 shows the P vs ϵ curves for the 1st, 10th, 11th (first cycle over 15 KSI), 12th, and 23rd (burst cycle) cycles on OCL-7.

Notice that for both cylinders, as long as the pressure remained below the lower-bound value that could cause plastic deformation of the liner (16.4 KSI), the slopes of both the first and tenth cycles are similar and linear. This indicates elastic behavior in this range. Where the pressure first exceeds this lower bound limit (the 11th cycle) the curves become non-linear.

OCL-5 ruptured at 18 KSI on the eleventh cycle which is in good agreement with theoretical prediction of 17.6 KSI. OCL-7 was pressurized 12 more cycles at 20 KSI without failure. Note that the 11th cycle shows the expected non-linearity but the 12th cycle returns to a linear but different slope. This new linear curve remains constant up to the 23rd or rupture cycle. OCL-7 was designed to rupture at 20 KSI but exceeded this limit. This discrepancy can be due to the variation of the many imput parameters needed in design.

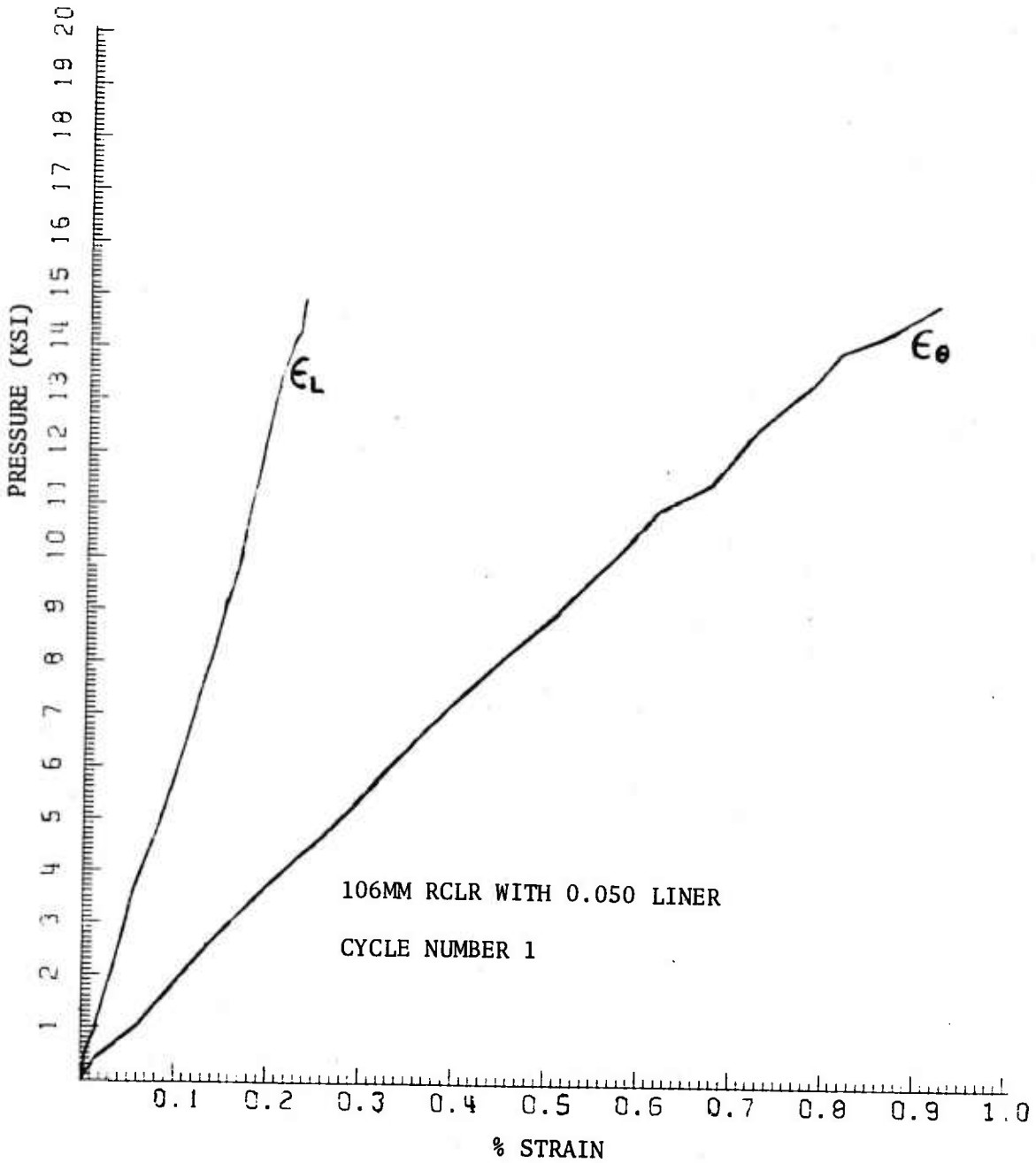

Figure 31. P vs ε curve for 1st cycle (14.9 KSI) on OCL-5.

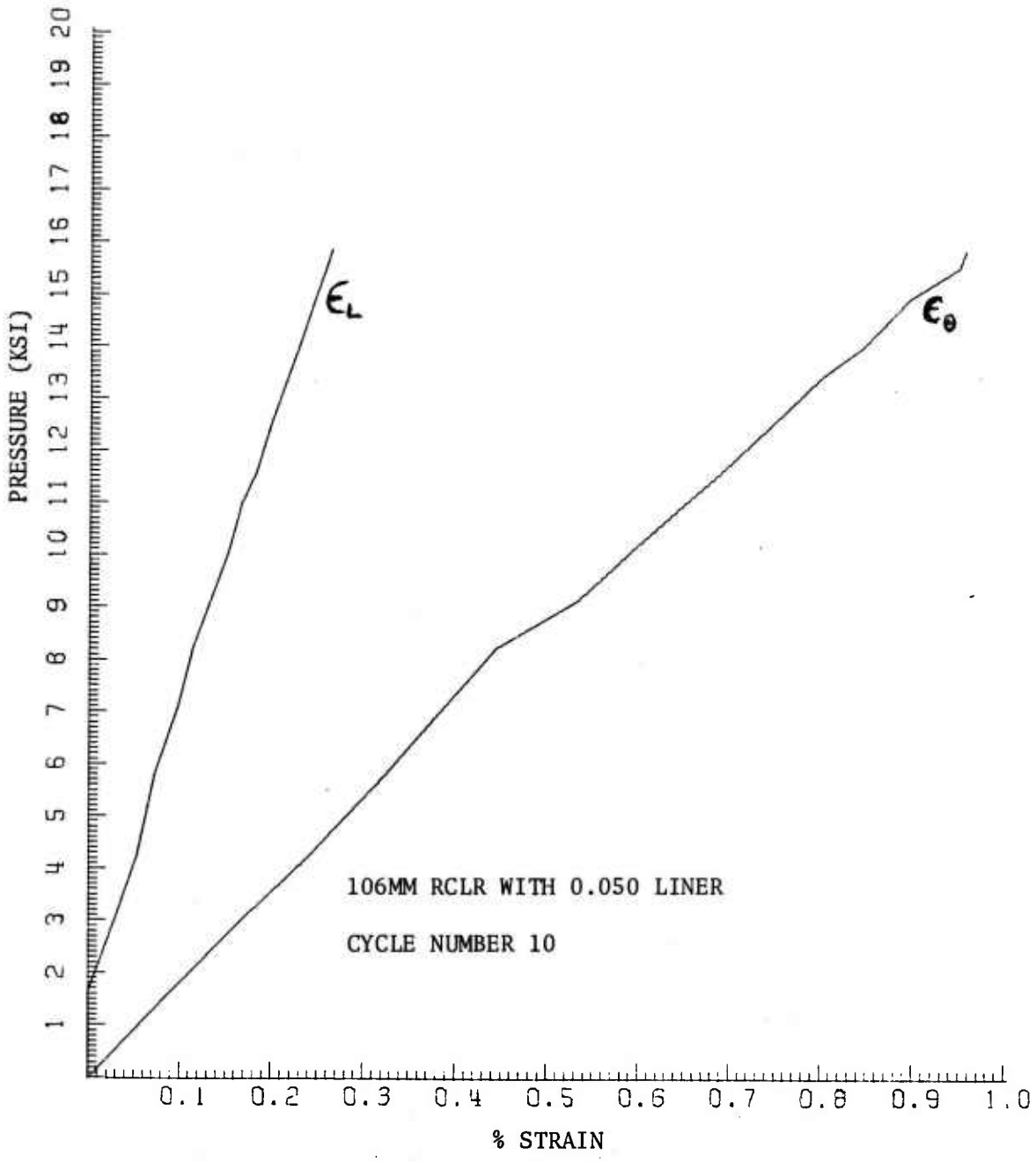

Figure 32. P vs ε curve for 10th cycle (15.9 KSI) on OCL-5.

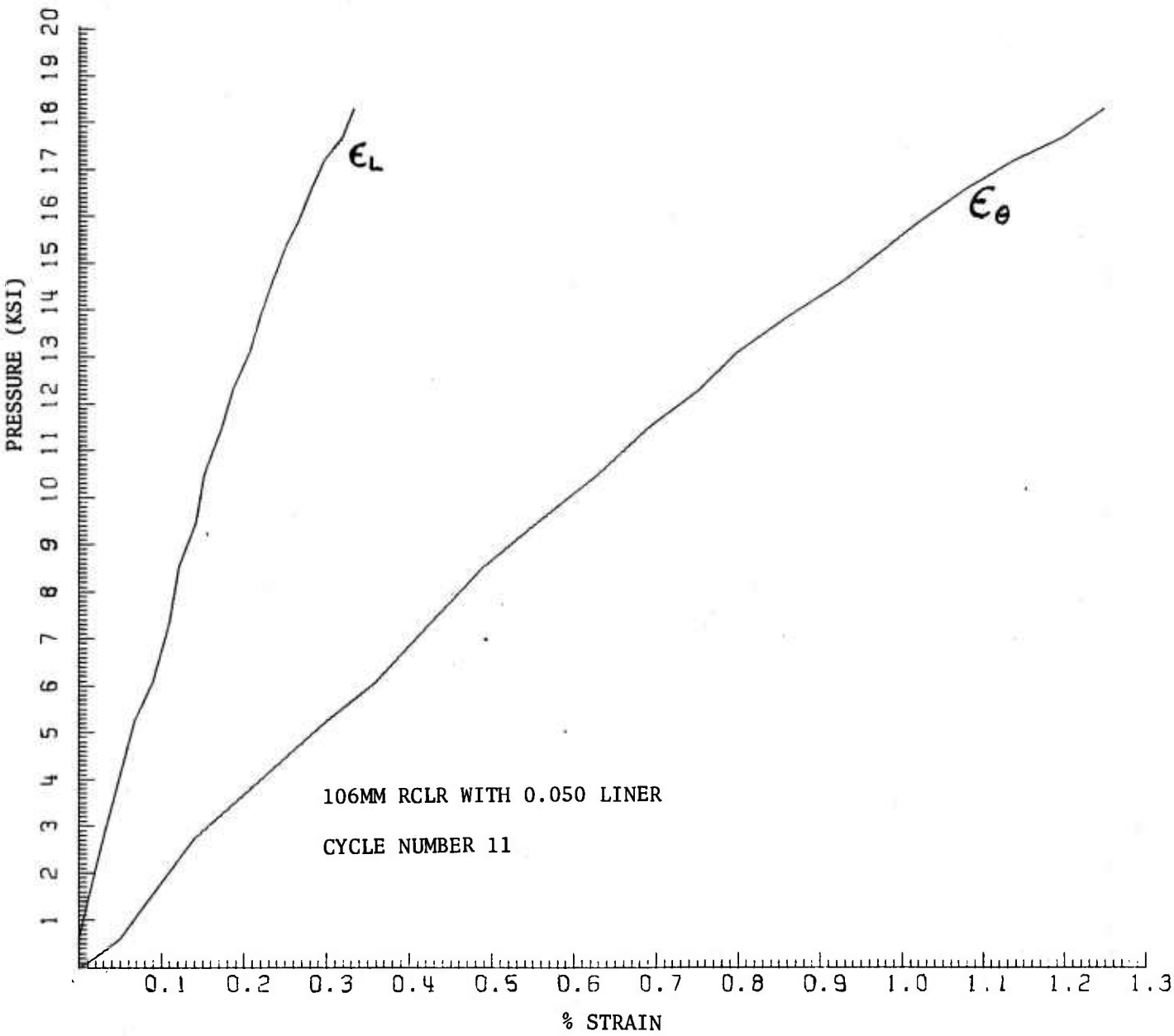

Figure 33. P vs ε curve for 11th or burst cycle (18.2 KSI) on OCL-5.

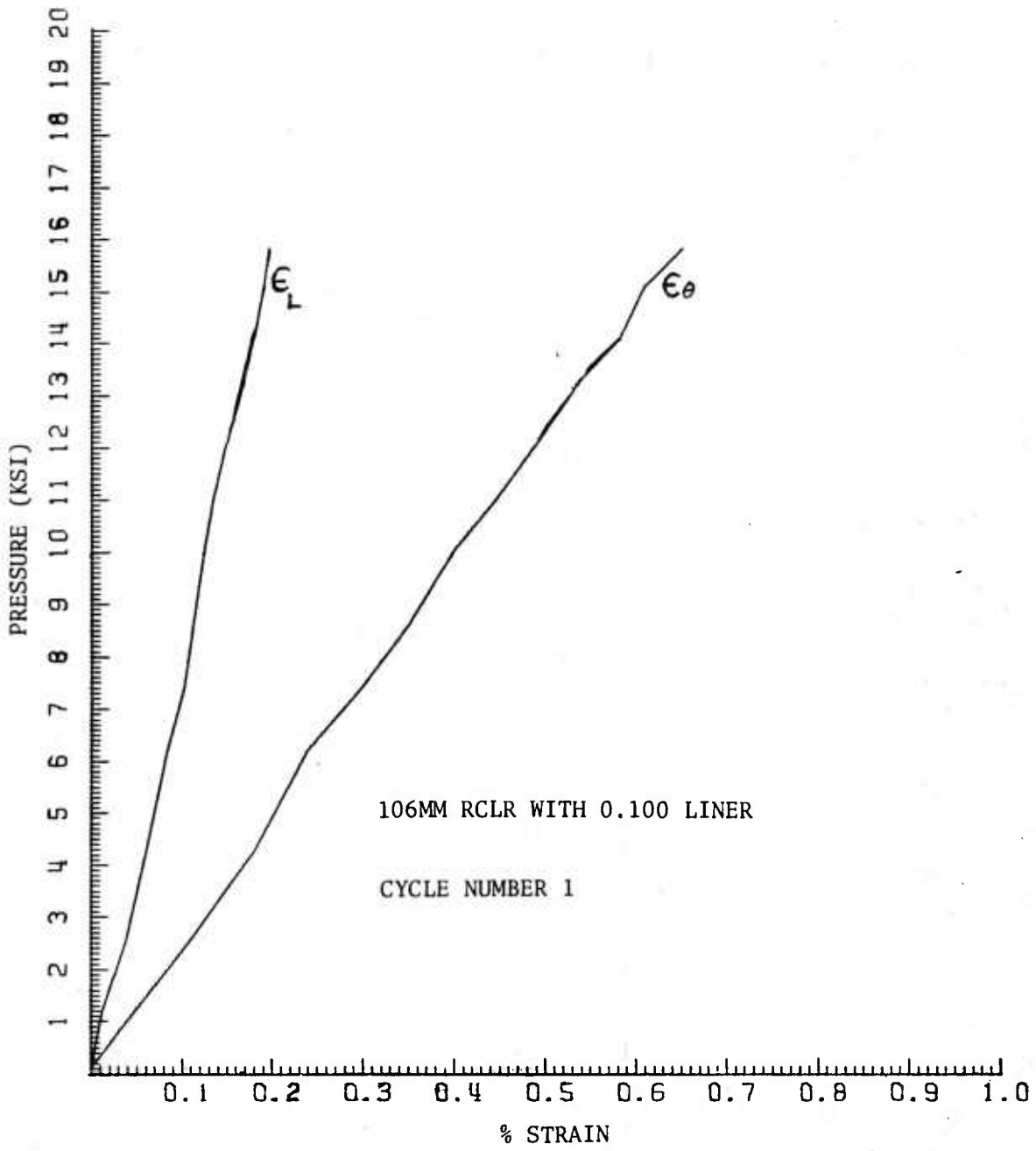

Figure 34. P vs ε curve for 1st cycle (15.6 KSI) on OCL-7.

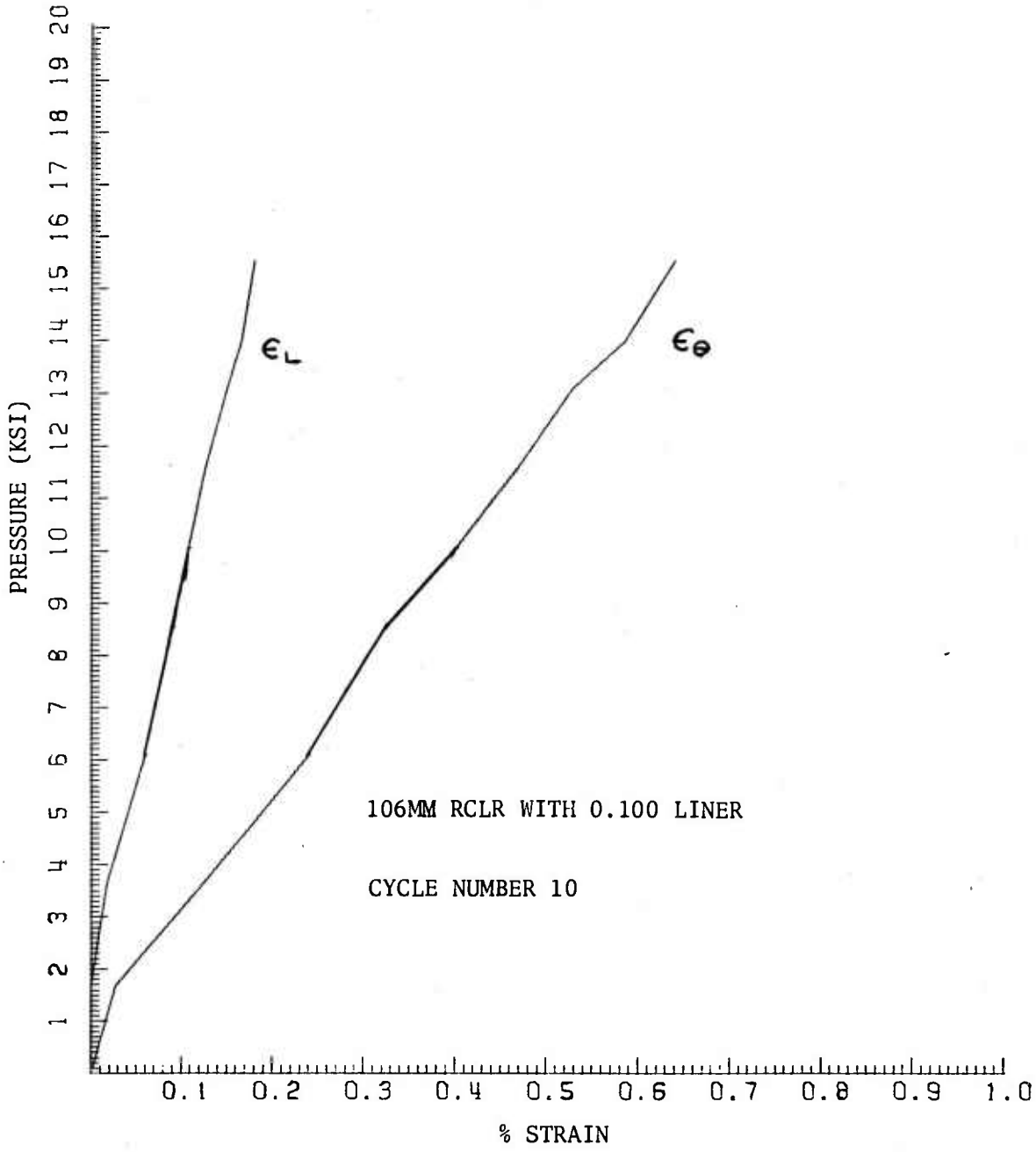

Figure 35. P vs ε curve for 10th cycle (15.6 KSI) on OCL-7.

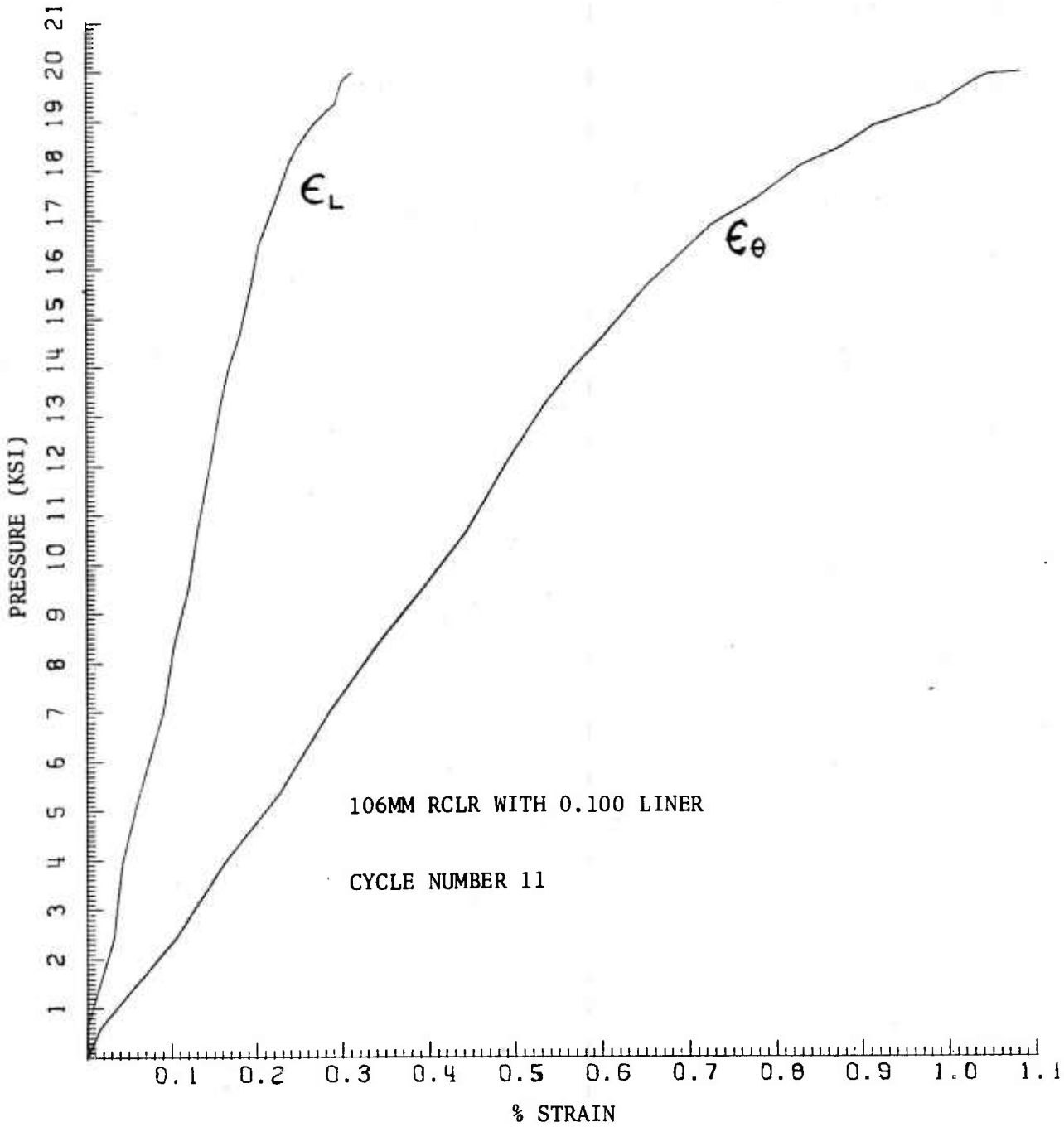

Figure 36. P vs ε curve for 11th cycle (20 KSI) on OCL-7.

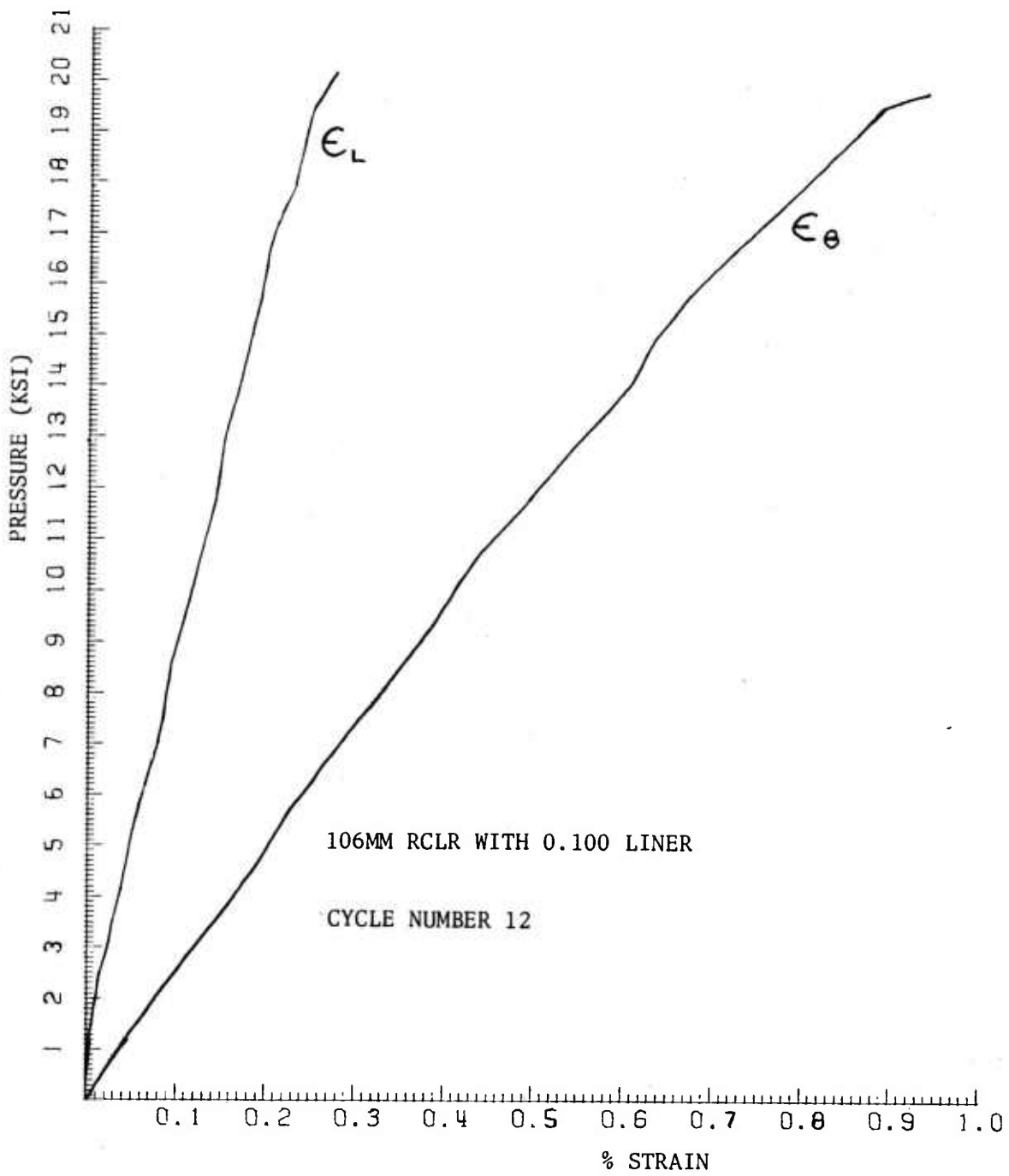

Figure 37. P vs ε curve for 12th cycle (20 KSI) on OCL-7.

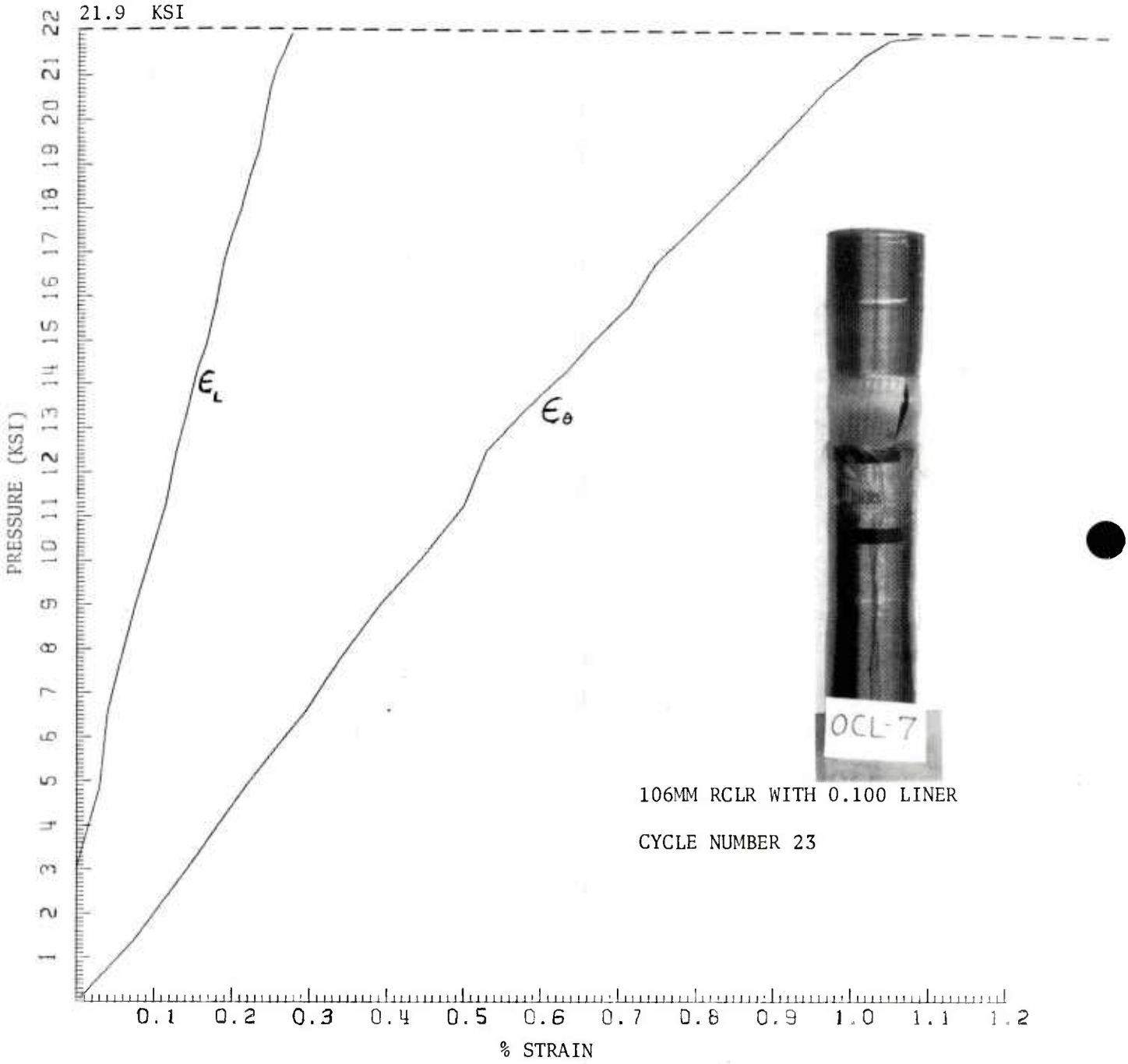

Figure 38. P vs ε curve for 23rd or burst cycle (21.9 KSI) on OCL-7.

(2) Cyclic-Fatigue Tests

Test cylinders OCL-4, 6 and 10 were tested in the high pressure fatigue facilities located here at Watervliet Arsenal. These facilities allow preselected pressures (10 to 100 KSI) to be loaded and unloaded at a much greater rate than was experienced by the previous two cylinders. Reference 9 explains in detail the capabilities of this high pressure equipment. The data from the fatigue testing was presented in Table 8.

In all three cylinders, fatigue failure occurred when the oil started to leak from a small area in the jacket. A notable finding was the distinct lack of any type of catastrophic failure. In fact, failure was determined in each case when a large loss of pressure within the system was observed and oil was visually noticed leaking from the composite jackets. Upon close observation of the cylinders, small areas of crazing and chipped resin indicated where the hydraulic oil leaked through the jackets (see circled areas in Figure 39). In this crazed area, not one filament appeared to be broken.

Boroscope examination of the I.D. of the cylinders showed no visual evidence of a crack. Air gage dimensional check of the bore as shown in Table 9 showed no significant change in any of the cylinders. Liquid dye inspection of the bore was unable to pick up any evidence

[9]Brown, B.B., et al. "4.2 Inch Mortar M30 Fatigue Test" Dec 1972 WVT-TR-7237

TABLE 8. FATIGUE DATA ON CYCLIC-FATIGUE CYLINDERS

CYL	DESIGN PRESS (KSI)	LINER THICK (IN.)	JACKET THICK (IN.)	RATE (CPM)	NO CYCLES	REMARKS
OCL-4	17.625*	.050	.102	8	1398	O.D. leak located 9 1/2" from end
OCL-6	19.075	.074	.090	9	1884	O.D. leak located 14" from end
OCL-10	19.075	.100	.078	7	4416	O.D. leak located 11 1/2" from end

All three cylinders were pressure cycled at 12,000 psi. This pressure amounts to

a. 68% ultimate for OCL-4

b. 63% ultimate for OCL-7

c. 63% ultimate for OCL-10

*The original minimum weight construction from "GUNTUC" indicated that a 0.050" liner with a 0.102" (17 layers) jacket would contain 19.1 KSI. However this construction leads to "reverse yielding" which limits its effective pressure capacity to 17.6 KSI. In this case, "reverse yielding" indicates that if this cylinder were to see 19 KSI it might not burst, but upon pressure release the liner would plastically deform from the induced compressive residual stresses in the jacket (See explanation in Section 2B and Appendix B).

TABLE 9. INTERNAL DIMENSIONAL CHECKS OF FATIGUED CYLINDERS

OCL-4

TRAVEL (IN.)	BEFORE BORE	BEFORE RIFLE	AFTER CURE BORE	AFTER CURE RIFLE	AFTER FATIGUE* BORE	AFTER FATIGUE* RIFLE
2	-	4.2110	-	4.2075	-	4.2075
4	4.1350	4.2110	4.1310	4.2080	4.1315	4.2070
6	4.1350	4.2120	4.1285	4.2000	4.1290	4.2010
7					4.1240	
8	4.1360	4.2120	4.1195	4.1980	4.1205	4.1975
9					4.1205	4.1975
10	4.1350	4.2115	4.1200	4.1980	4.1200	4.1970
11					4.1200	4.1970
12	4.1350	4.2110	4.1190	4.1970	4.1200	4.1965
14	4.1350	4.2110	4.1185	4.1965	4.1200	4.1965
16	4.1350	4.2110	4.1170	4.1960	4.1185	4.1950
18	4.1350	4.2100	4.1155	4.1975	4.1175	4.1965
20	4.1350	4.2095	4.1255	4.2080	4.1270	4.2065
22	4.1350	4.2110	4.1300	4.2070	4.1300	4.2075

Leakage

OCL-6

TRAVEL (IN.)	BEFORE BORE	BEFORE RIFLE	AFTER CURE BORE	AFTER CURE RIFLE	AFTER FATIGUE* BORE	AFTER FATIGUE* RIFLE
2	-	4.2120	-	4.2100	-	4.2095
4	4.1350	4.2120	4.1335	4.2100	4.1335	4.2095
6	4.1350	4.2110	4.1310	4.2030	4.1295	4.2025
8	4.1360	4.2105	4.1245	4.2005	4.1240	4.2005
10	4.1360	4.2100	4.1245	4.2010	4.1240	4.2010
12	4.1360	4.2100	4.1240	4.2010	4.1240	4.2025
13					4.1250	4.2030
14	4.1360	4.2100	4.1260	4.2025	4.1265	4.2030
15					4.1265	4.2025
16	4.1360	4.2100	4.1270	4.2020	4.1260	4.2020
18	4.1360	4.2100	4.1270	4.2010	4.1265	4.2015
20	4.1360	4.2100	4.1285	4.2065	4.1275	4.2065
22	4.1355	4.2115	4.1330	4.2095	4.1325	4.2090

Leakage

TABLE 9. INTERNAL DIMENSIONAL CHECKS OF FATIGUED CYLINDERS (Cont)

OCL-10

TRAVEL (IN.)	BEFORE BORE	BEFORE RIFLE	AFTER CURE BORE	AFTER CURE RIFLE	AFTER FATIGUE* BORE	AFTER FATIGUE* RIFLE
2	-	4.2105	-	4.2085	4.1330	4.2085
4	4.1350	4.2110	4.1335	4.2085	4.1330	4.2090
6	4.1340	4.2110	4.1315	4.2040	4.1310	4.2050
8	4.1340	4.2115	4.1285	4.2040	4.1290	4.2055
9					4.1305	4.2055
10	4.1340	4.2120	4.1295	4.2045	4.1305	4.2065
11					4.1305	4.2065
12	4.1340	4.2115	4.1295	4.2045	4.1295	4.2060
13					4.1290	4.2050
14	4.1340	4.2115	4.1285	4.2040	4.1290	4.2045
16	4.1340	4.2110	4.1275	4.2025	4.1275	4.2035
18	4.1345	4.2110	4.1275	4.2030	4.1270	4.2035
20	4.1340	4.2110	4.1300	4.2085	4.1300	4.2085
22	4.1345	4.2105	4.1335	4.2085	4.1330	4.2085

Leakage

* OCL-4 - 1398 cycles @ 12 KSI
OCL-6 - 1884 cycles @ 12 KSI
OCL-10 - 4416 cycles @ 12 KSI

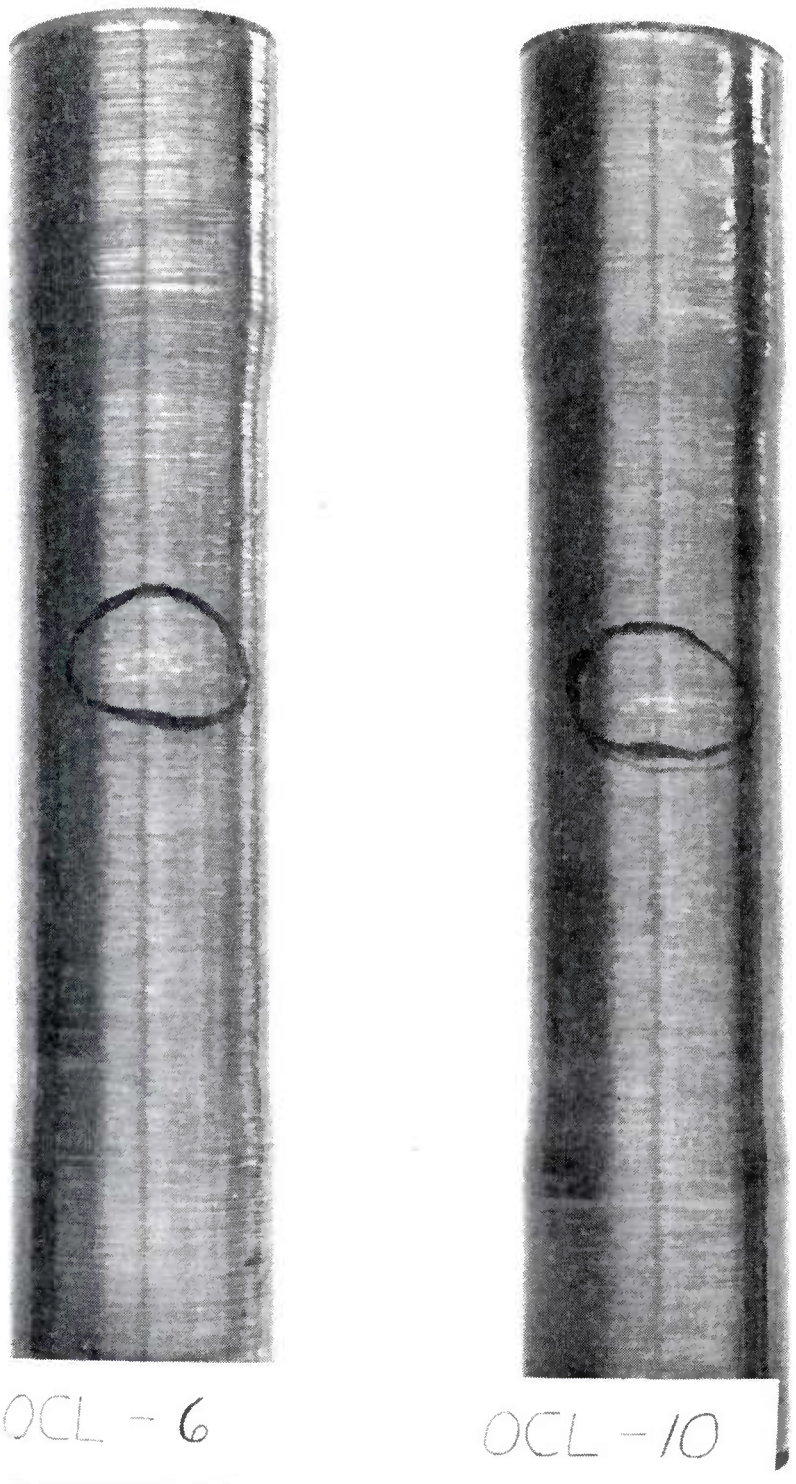

Figure 39. Fatigued cylinders OCL-6 and 10 after failure.

Figure 40. Fatigued cylinder OCL-4 showing indication of a liner crack after liquid penetrant (dye) inspection.

of a crack. Since there had to be some type of crack in the liners to allow the oil to escape, the composite jacket of OCL-4 was stripped from one end to a point beyond the jacket's leak area. Liquid (dye) penetrant inspection of the liner's O.D. surface brought out a distinct crack, as shown in the circled area in Figure 40. This crack fell directly under the area in the jacket where the crazing was observed.

This crack is about an inch long and initiates and follows the fillet of one twist of rifling. The fillet is the point where the bottom of the lands meets the groove. In all rifling, this is a point of high stress concentration because of the sharp corners involved. For a summary on the Static and Cyclic test and correlation between theory and experiment see Table 5.

b. TEST FIRING

Arrangements were made with the Artillery and Mortar Branch, Picatinny Arsenal to test fire 20 rounds through the composite 106mm tube. For the test firing, a conventional 106mm R.R. chamber section along with its breech and vent assembly was mated (threaded) to the breech end of the tube.

The composite tube along with a chamber and breech assembly were shipped to Picatinny Arsenal along with a firing test plan shown in Appendix E.

NOTE: The 8 strain gages mounted on the chamber section and the subsequent data gathered by these gages during the first eight rounds were for a separate engineering project which is not related to this project.

The location of the two hoop strain gages (No 3 and No 4) as shown in Figure 41 is 6 7/8" up from the breech end of the tube. The longitudinal strain gages (No 1 and No 2) are located 14 7/8" up from the breech end of the tube. Both types of gages are therefore located in the area of maximum composite build-up i.e., 20 layers of winding over .100" of liner. The length of this area extends from 6 5/8" to 16" measured from breech end of tube. The position of the tube during firing put No 1 gage at 12 o'clock, No 2 at 6 o'clock, No 3 at 3 o'clock, and No 4 at 9 o'clock as you look down the tube from the breech end.

Figure 42 is an overall view of the composite tube at the Picatinny Arsenal test area. Shown are the leads from the strain gages to a tab board for the four recording channels and the two digital ohmeters. The sand bags shown under the chamber were used only for the first round. After recoillessness was established, they were removed. The crosshairs shown at the muzzle were used for the bore sighting of the tube between rounds. Figure 43 shows one of the test personnel loading a round for firing.

The actual test data and details of the test are shown in the Picatinny Arsenal test report presented in Appendix F. A summary of the data is shown in Tables 10 and 11. Table 5, presented on page 67, shows correlation between theory and experiment.

Since only four recording channels were available for strain gage data, it was necessary to establish a plan which would maximize the amount of strain data obtained. During the eight rounds of Phase I, since two of the channels were being utilized by the gages on the

TABLE 10. SUMMARY DATA OF COMPOSITE 106MM RCLR TEST FIRING

ROUND	VEL	PRESS.	AVG % STRAIN (ϵ_L) FROM 1L & 2L GAGES	AVG % STRAIN (ϵ_H) FROM 3H & 4H GAGES
1	1600	9.5	.0828	NO READINGS
2	1629	9.6	.0760	
3	1642	9.5	.0740	
4	1631	9.7	.0804	
5	1607	9.7	.0795	
6	1639	9.6	.0825	
7	1631	9.9	.0760	
8	1610	9.5	.0819	
MEAN -	1624	9.6	.0791 - Mean	

			1L	2L	3H	4H	(AVG)
9	1620	9.9	.0878	NO READINGS	.3108	.3191	(.3150)
10	1616	9.7	.0796		.2963	.3006	(.2984)
11	1597	9.4	.0757		.2985	.3063	(.3024)
12	1618	9.5	.0759		.3036	.3106	(.3071)
13	1618	9.6	.0723		.2855	.2960	(.2908)
14	1629	9.5	.0806		.2819	.2963	(.2891)
15	1618	9.5	.0798		.2702	.2808	(.2755)
16	1595	9.2	.0791		.2666	.2763	(.2714)
17	1613	9.5	.0723		.2657	.2719	(.2688)
18	1616	9.5	.0736		.2610	.2721	(.2666)
19	1603	9.5	.0718		.2580	.2728	(.2654)
20	1642	9.3	.0670		.2650	.2763	(.2706)
MEAN -	1615	9.5	.0763				(.2851)

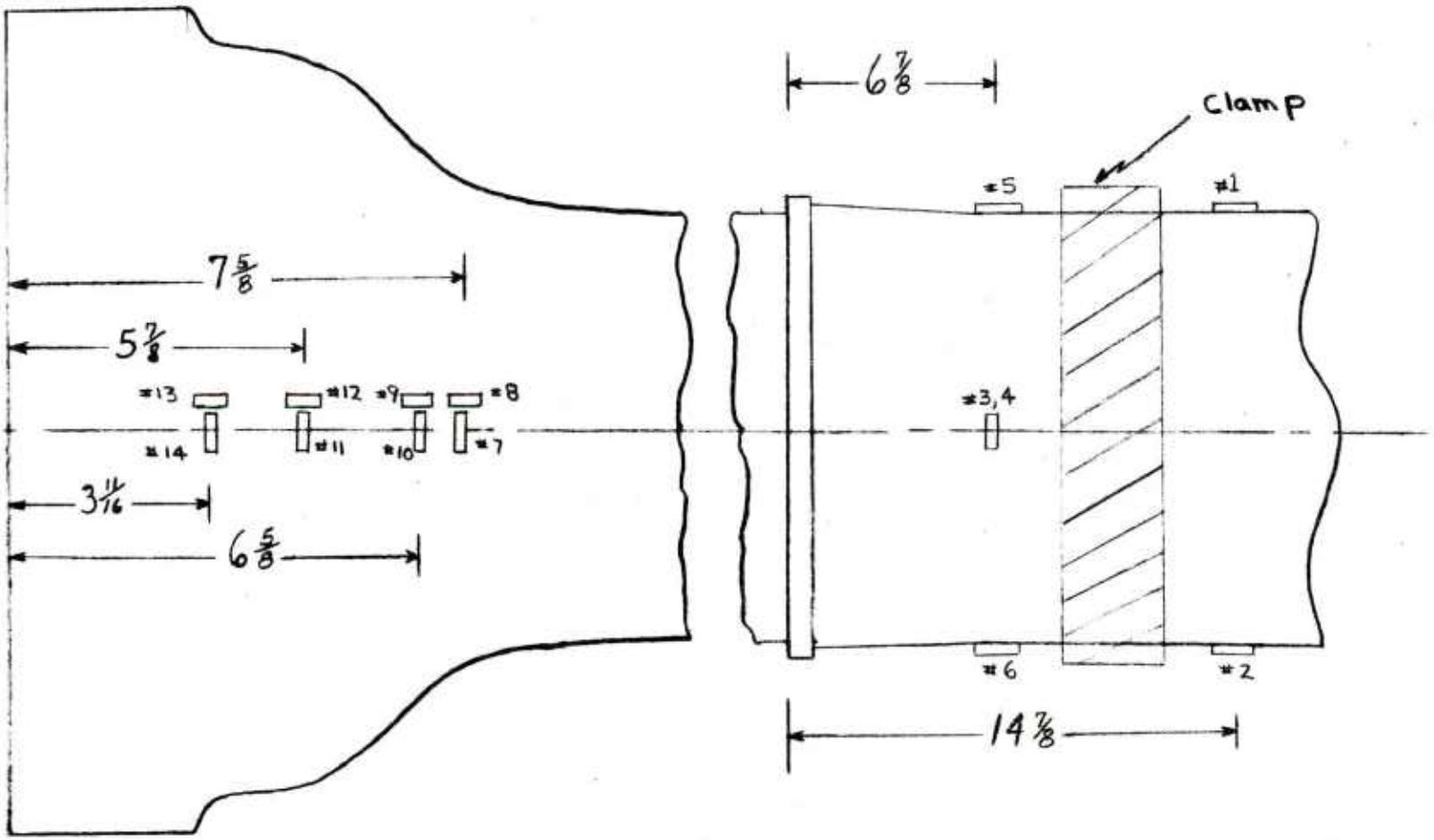

Sketch of Gage Locations
(Not to Scale)

Figure 41. Sketch showing locations of strain and temperature gages for test firing.

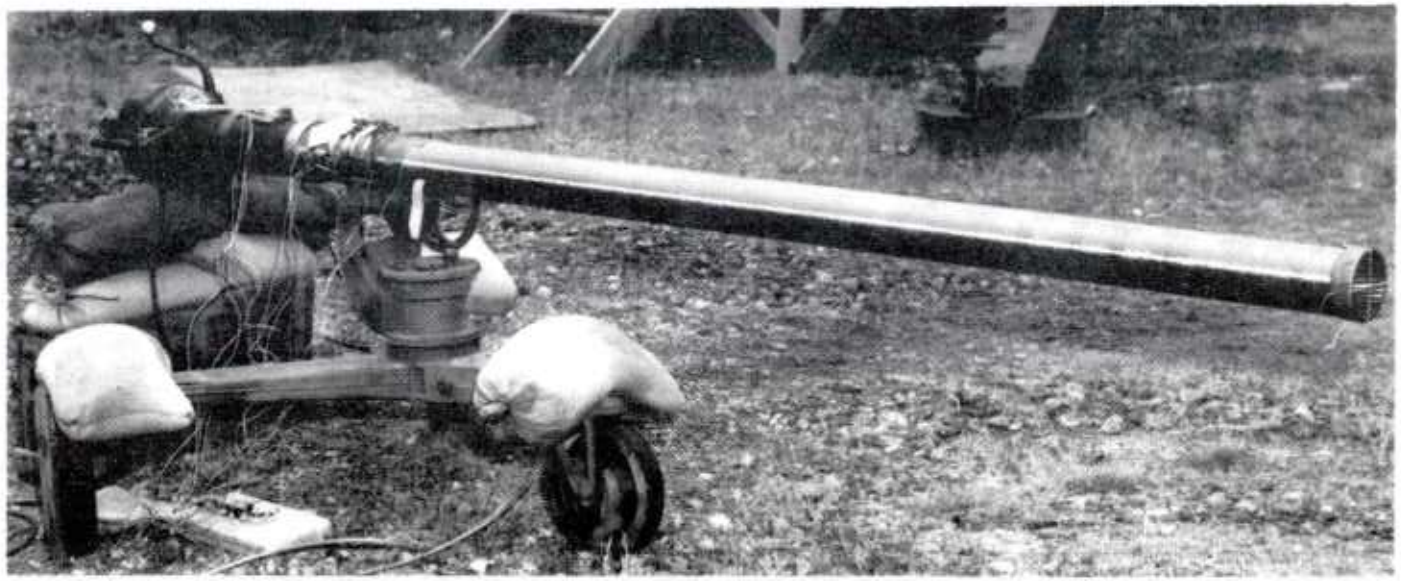

Figure 42. View of assembled 106mm composite tube ready for firing at test range.

Figure 43. Loading of inert M334A1 round in preparation for firing.

TABLE 11. TIME AND TEMPERATURE DATA ON COMPOSITE 106MM RCLR TEST FIRING

RD	TIME BETWEEN RD	BEFORE °F	MAX. AFTER °F	MAX. Δ T °F	TIME TO Δ T
1		66.5	114.7	48.2	
		65.0	112.5	47.5	
2	76 MIN	78.9	121.6	42.7	
		76.7	119.5	42.8	
3	24 MIN	81.5	122.8	41.3	
		81.2	121.6	39.4	
4	15 MIN	82.4	121.6	39.2	
		82.8	120.7	37.9	
5	20 MIN	79.9	119.5	39.6	
		77.3	117.4	40.1	
6	6 MIN	97.5	137.9	40.4	20 SEC
		95.3	133.1	37.8	
7	19 MIN	94.7	135.8	41.1	20 SEC
		89.7	131.3	41.6	
8	5 MIN	113.1	150.0	36.9	23 SEC
		108.4	148.5	40.1	
9	90 MIN	66.2	106.2	40.0	27 SEC
		65.5	105.3	39.8	
10	7 MIN	91.5	129.8	38.3	25 SEC
		92.2	129.8	37.6	
11	4 MIN	108.7	146.1	37.4	25 SEC
		108.7	147.9	39.2	
12	30 MIN	89.0	125.9	36.9	25 SEC
		86.6	126.8	40.2	
13	3 MIN	111.8	142.6	30.8	13 SEC
		112.8	148.5	35.7	
14	2 MIN	131.3	159.8	28.5	14 SEC
		130.7	168.9	38.2	
15	2.5 MIN	143.8	173.5	29.8	19 SEC
		150.5	182.2	31.7	
16	2.5 MIN	153.8	185.8	32.0	16 SEC
		160.7	191.9	31.9	
17	4 MIN	142.9	176.3	33.4	16 SEC
		157.2	192.2	35.0	
18	2.5 MIN	159.2	193.3	34.1	21 SEC
		168.7	201.2	32.5	
19	2.5 MIN	170.7	205.3	34.6	20 SEC
		177.2	209.1	31.9	
20	3.0 MIN	176.6	209.6	33.0	23 SEC
		177.7	208.8	31.1	

chamber, it was decided to connect the tube's hoop gages (No 3 and No 4) in series in one bridge and record the cummulative data on one channel. For these eight rounds, the average hoop strain would be 1/2 the total strain recorded. The tube's longitudinal gages (No 1 and No 2) were connected in a like manner.

Unfortunately, the gain for the hoop channel was set too low for the additive hoop strains obtained during firing. Therefore the recorder became saturated and no values were obtained for hoop strain during this phase. The additive longitudinal strains were obtained satisfactorily.

During Phase II, the chamber test was completed and therefore all four strain gages on the tube were individually monitored. The longitudinal gage No 2 was damaged during the firing of round 9 and no additional readings were recorded from this gage.

Set 2 in this phase of the test was to be a rapid fire test to determine the heat build-up on the O.D. of the tube. For these 9 rounds, the average rate of fire was 1 round every 2.75 min. The maximum temperature readings are shown in Table 11. It is felt however that the weather conditions, i.e., ambient temperature of 50°F and intermittent rain, prevented the tube from reaching even higher temperatures. However a maximum O.D. temperature of 209.6°F was reached and no ill effects were experienced by the composite jacket.

During this quasi-rapid fire test the average time to reach the maximum O.D. readings was 18 seconds after firing. The range was from 13 to 23 seconds and the upper and lower levels were determined more by the severity of rain than the time between rounds.

In addition to the preceding data, video tape recordings and high-speed movie film were taken of all 20 firings. Both video tape and film verified the fact that the weapon was recoilless during firing.

The M344A1 heat round is rated at a velocity of 1650 fps with an internal pressure of 10.0 KSI. The mean velocity for all rounds fired was 1619 fps and mean pressure was 9.56 KSI. The lower velocity can be attributed to the fact that the length of the barrel of the composite tube is 2" shorter than the conventional tube. The pressure discrepancy falls within the 3σ variation experienced with all types of propellants.

Upon the successful completion of this test firing, the tube was bore cleaned and returned to Watervliet Arsenal for final inspection. No significant enlargements or contractions of the I.D. are observed.

CONCLUSIONS AND RECOMMENDATIONS

The experimental and theoretical results which are shown in Table 5 clearly indicate that the filament winding technology developed through this MMT project can be readily used in fabricating any axi-symmetric composite structure.

In the course of events it was learned that other very important areas of studies should be undertaken if composites are to be used in Armament Components. The recommended areas are:

- Design Analysis, Testing and Reliability of Composite Joints and Transition Zones.
- Fatigue life of composite tubes (liner/jacket).
- Refractory liners/jacket composite tubes to decrease erosion problems.

- Computerization of the filament winding machine to provide variable tension and variable angle of wrap to produce minimum weight gun tubes and related components.
- Thermal properties study specifically related to filament wound structures.
- Circuit per pattern study: how it affects filament wound structures when subjected to a loading in Tension, Compression, Bending, Torsion, or combined loading.
- Composite Materials study related to Armament concepts and conventional components. Filament winding with Kevlar and Graphite filaments for consideration of such items as super flywheels, cartridge cases, bearings, launchers, bore evacuators, fuel tanks etc.

APPENDIX A

GRAPHICAL "GUNTUC" OUTPUT FOR THE 0.050 IN. AND 0.075 IN. LINERS

```
106 MM R.R. (STEEL LINER-STEEL FILAMENT/EPOXY MATRIX JACKET)
BORE RADIUS=2.104
FILAMENT/MATRIX VOLUME RATIO=0.750
WEIGHT PENALTY FACTOR=80.000
COMPOSITE FABRICATION COST=1.000
ALL LINER FABRICATION COST=1.000
POISSON'S RATIO(LINER)=0.300
POISSON'S RATIO(FILAMENT)=0.280
POISSON'S RATIO(MATRIX)=0.300
LINER MODULUS=30000000
FILAMENT MODULUS=30000000
MATRIX MODULUS=500000
LINER DENSITY=0.2830
FILAMENT DENSITY=0.2820
MATRIX DENSITY=0.0440
COMPOSITE DENSITY=0.2225
LINER YIELD STRENGTH=150000
FILAMENT YIELD STRENGTH=450000
MATRIX YIELD STRENGTH=10000
DOLLARS PER POUND OF LINER=0.50
DOLLARS PER POUND OF FILAMENT=8.00
DOLLARS PER POUND OF MATRIX=1.50
FACTOR OF SAFETY=1.000
```

Figure A-1. Input data for "GUNTUC" computer program (0.050" liner).

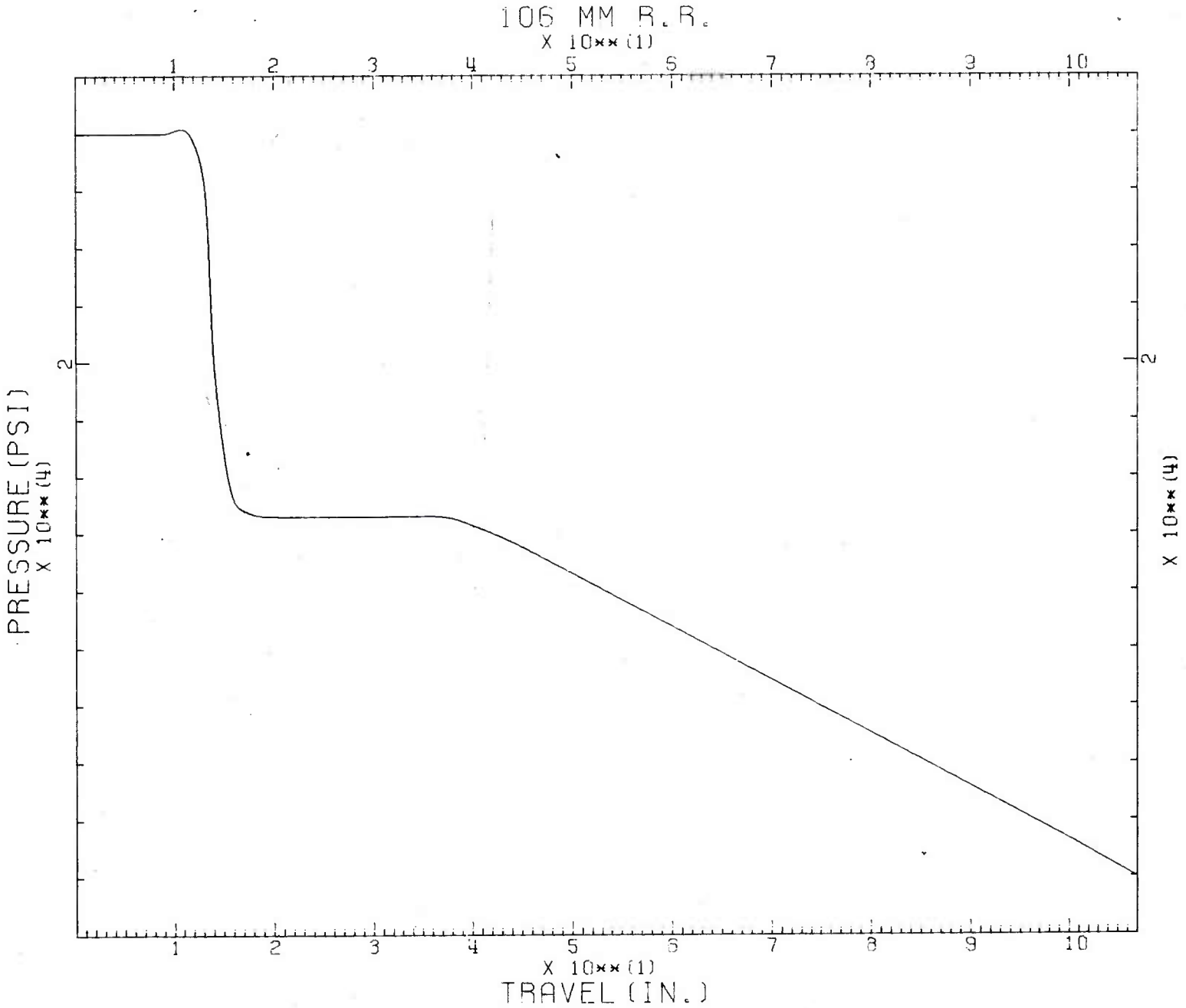

Figure A-2. ESP - travel curve for a conventional 106mm M40A1 recoilless rifle (0.050" liner).

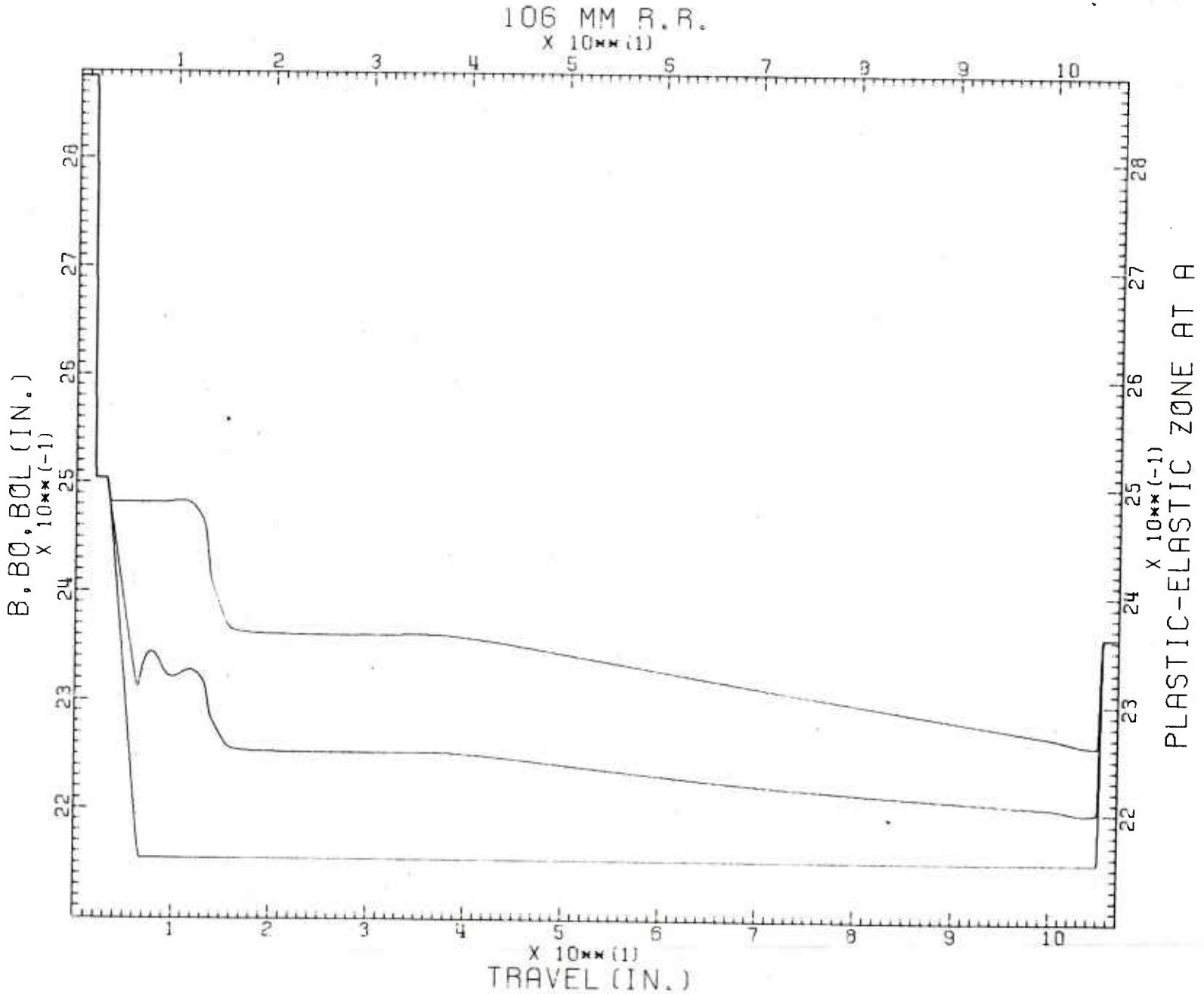

Figure A-3. O.D. values of composite vs conventional 106mm gun tubes (0.050" liner).

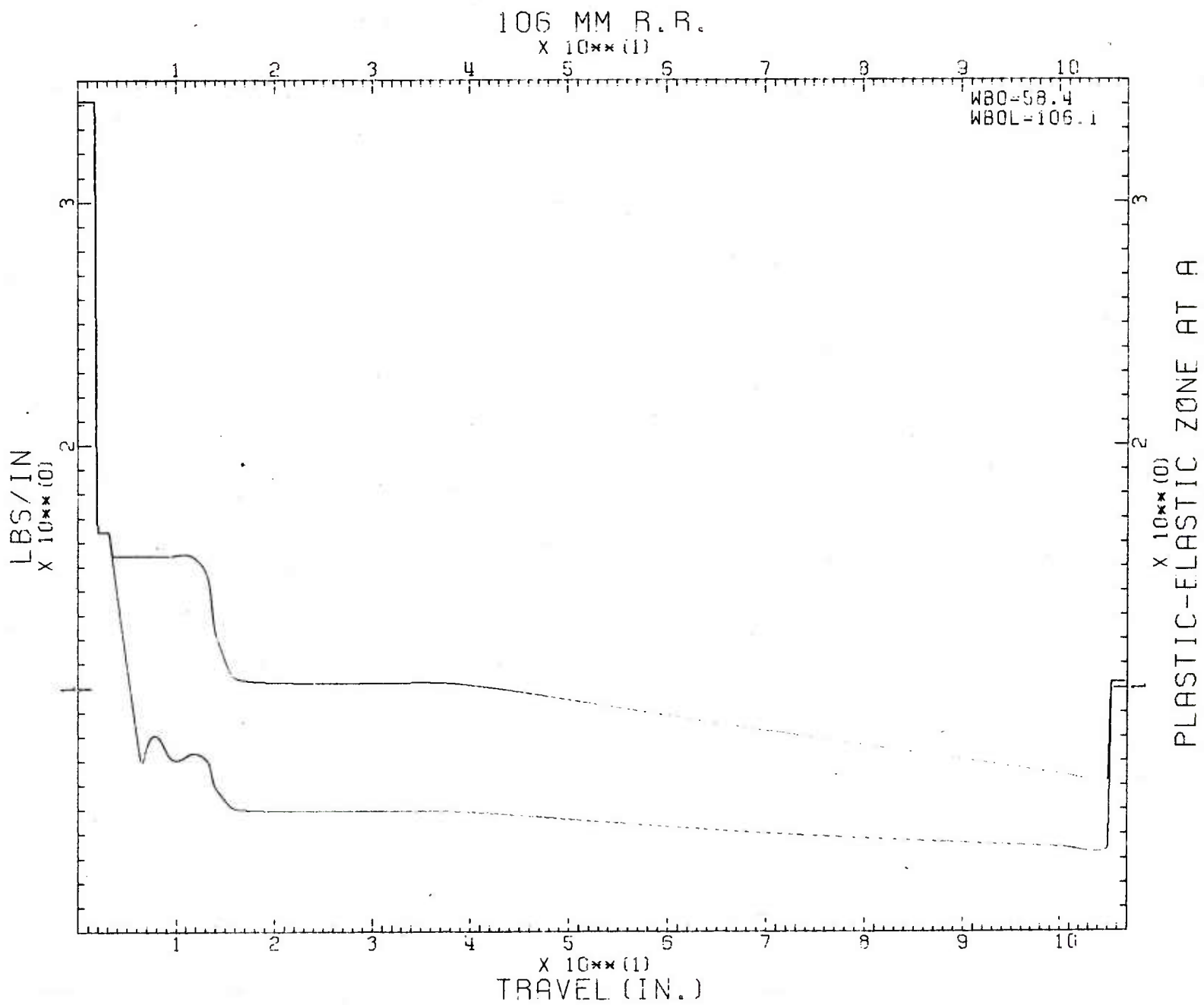

Figure A-4. Weight of composite vs conventional gun tubes (0.050" liner).

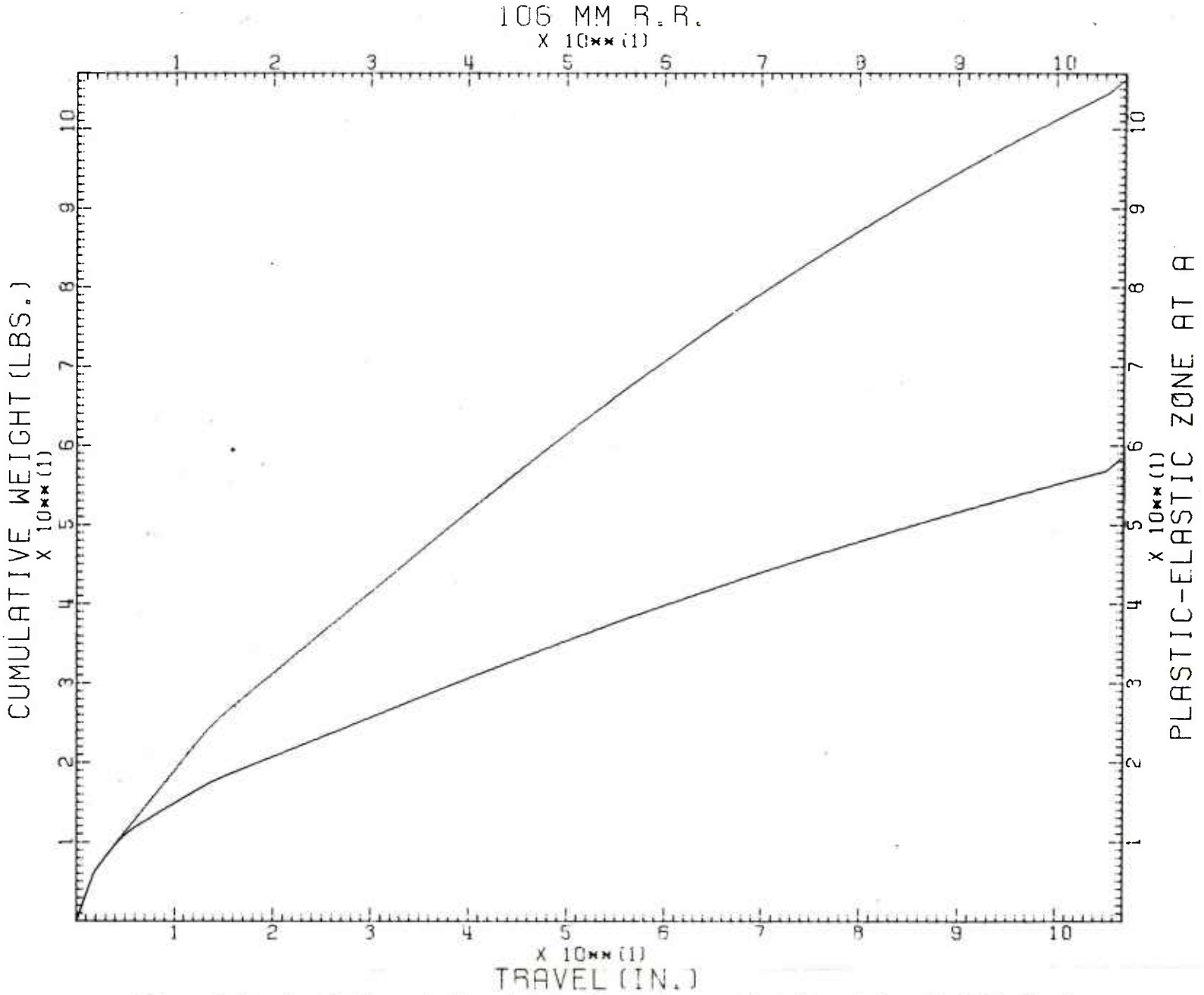

Figure A-5. Cumulative weights of composite and conventional gun tubes (0.050" liner).

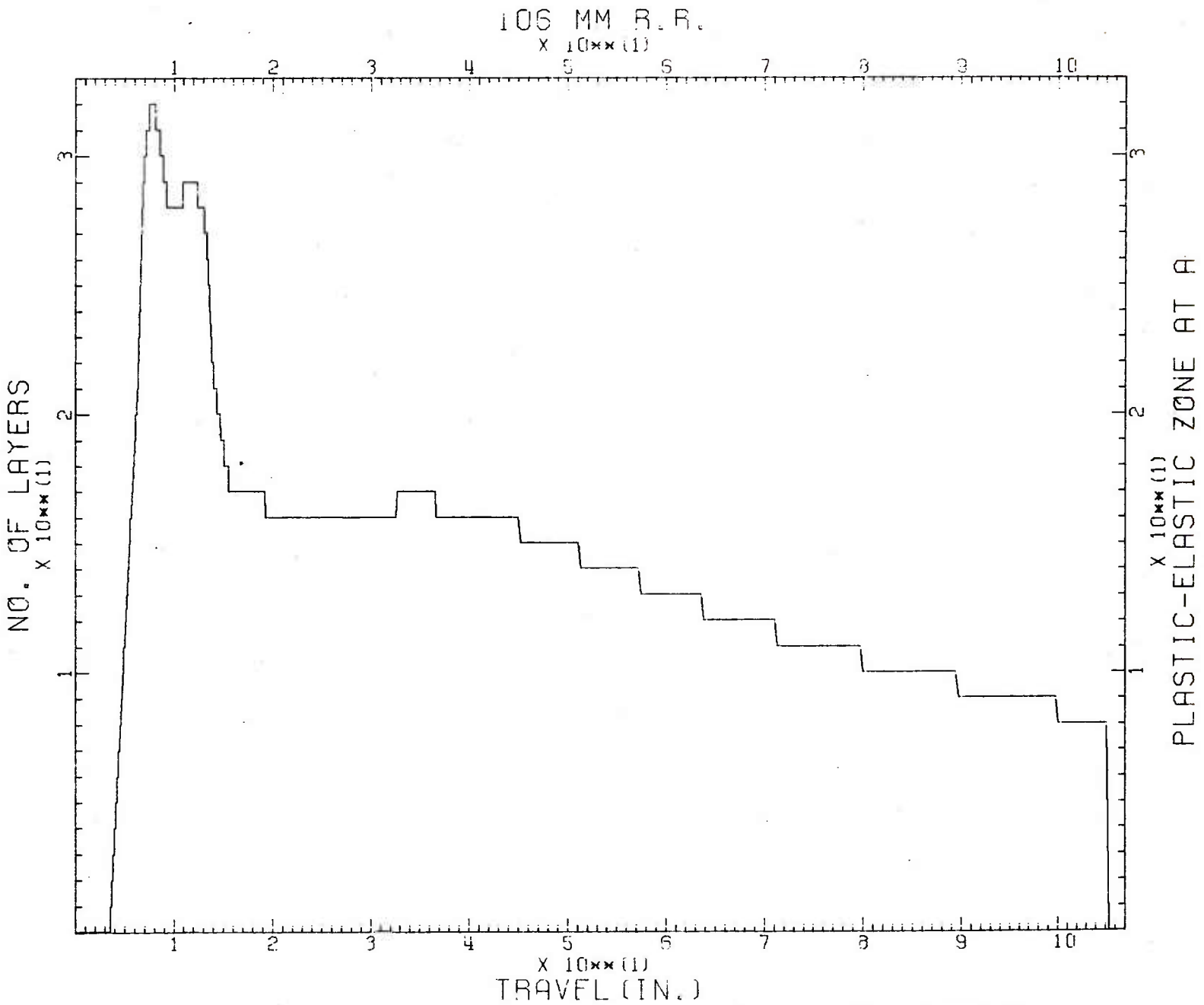

Figure A-6. Fabrication pattern for winding a composite tube with an 0.050" liner.

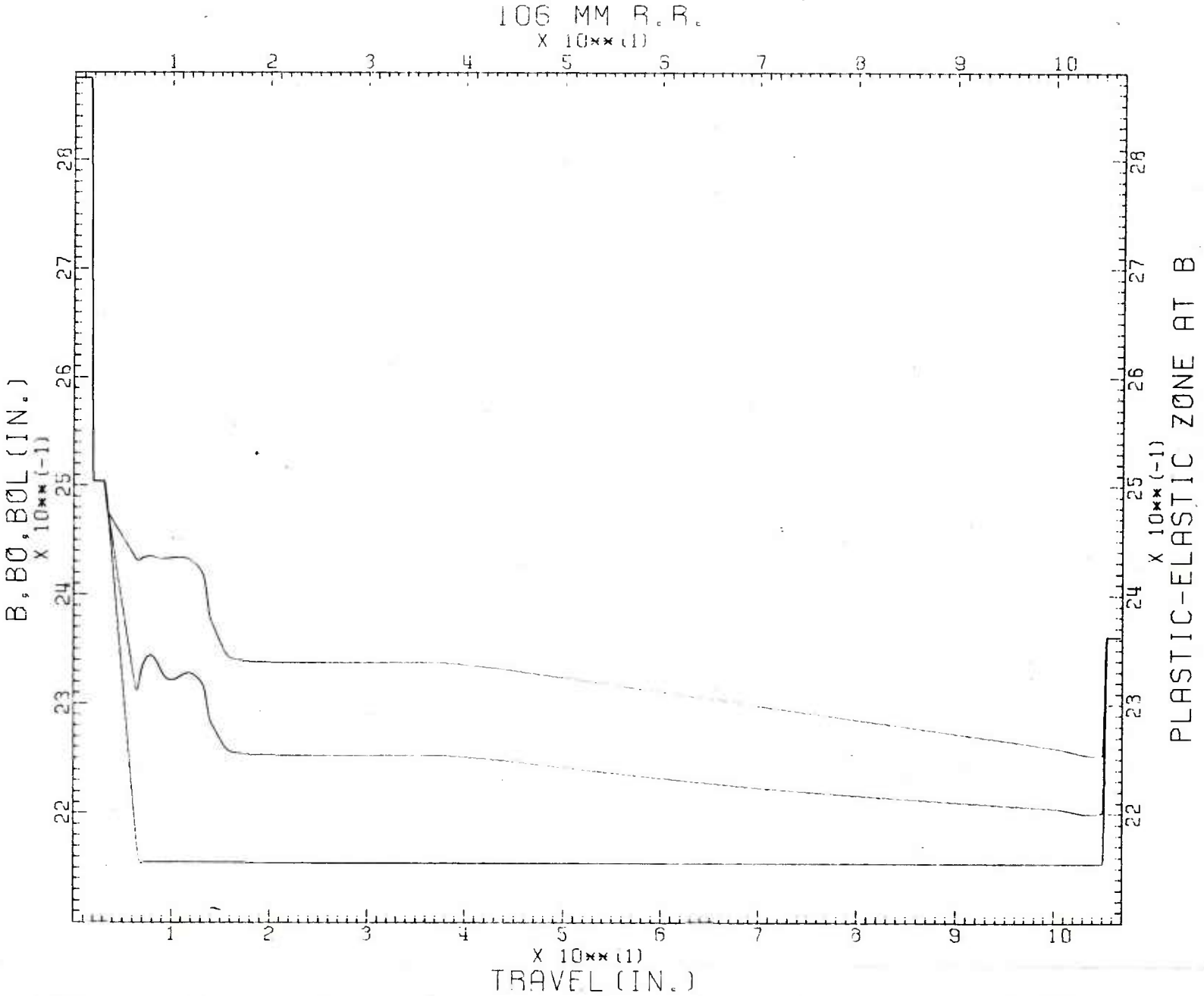

Figure A-7. O.D. values of composite vs conventional tubes using an autofrettaged liner (0.050" liner).

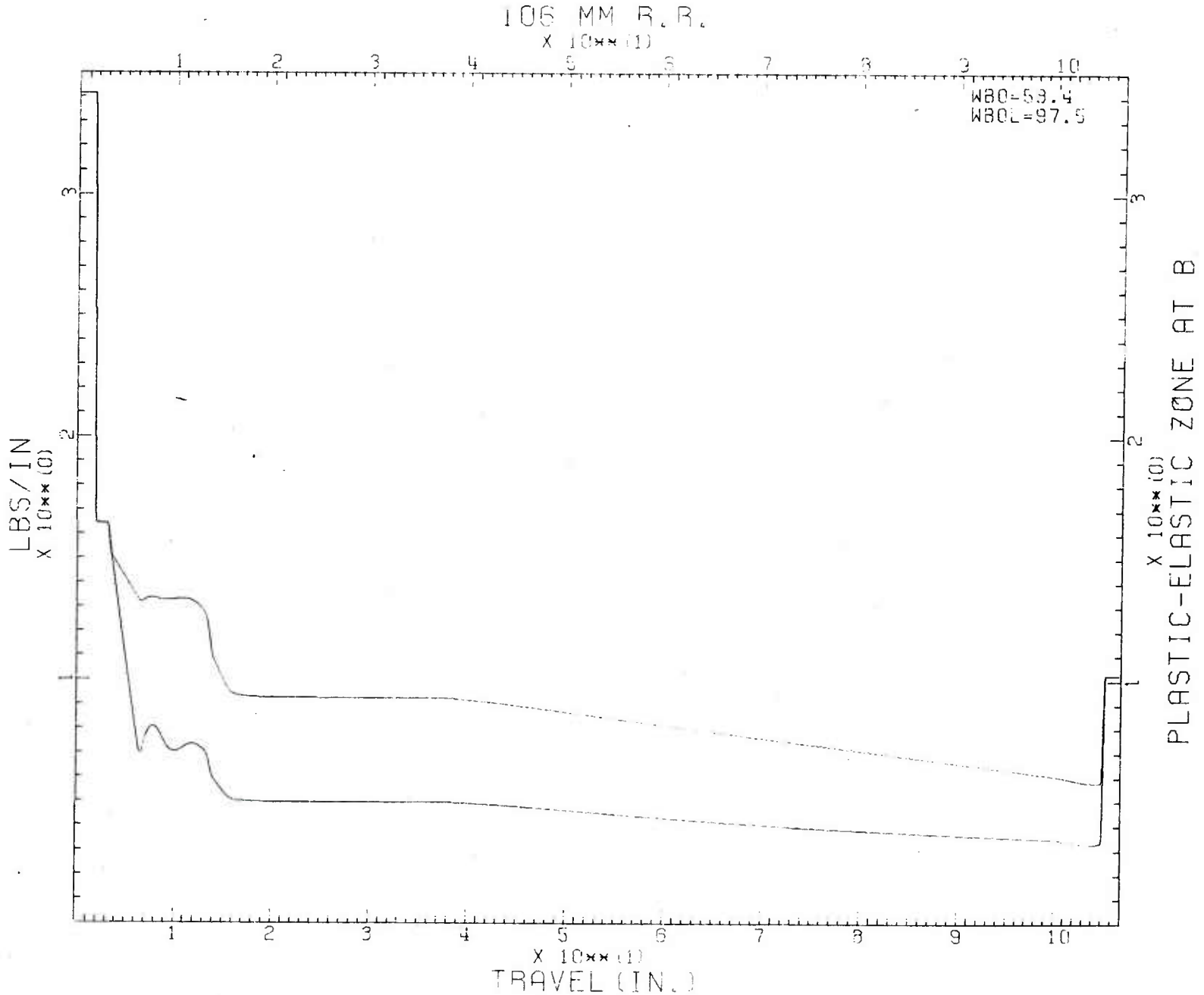

Figure A-8. Weight of composite vs conventional tubes using an autofrettaged liner (0.050" liner).

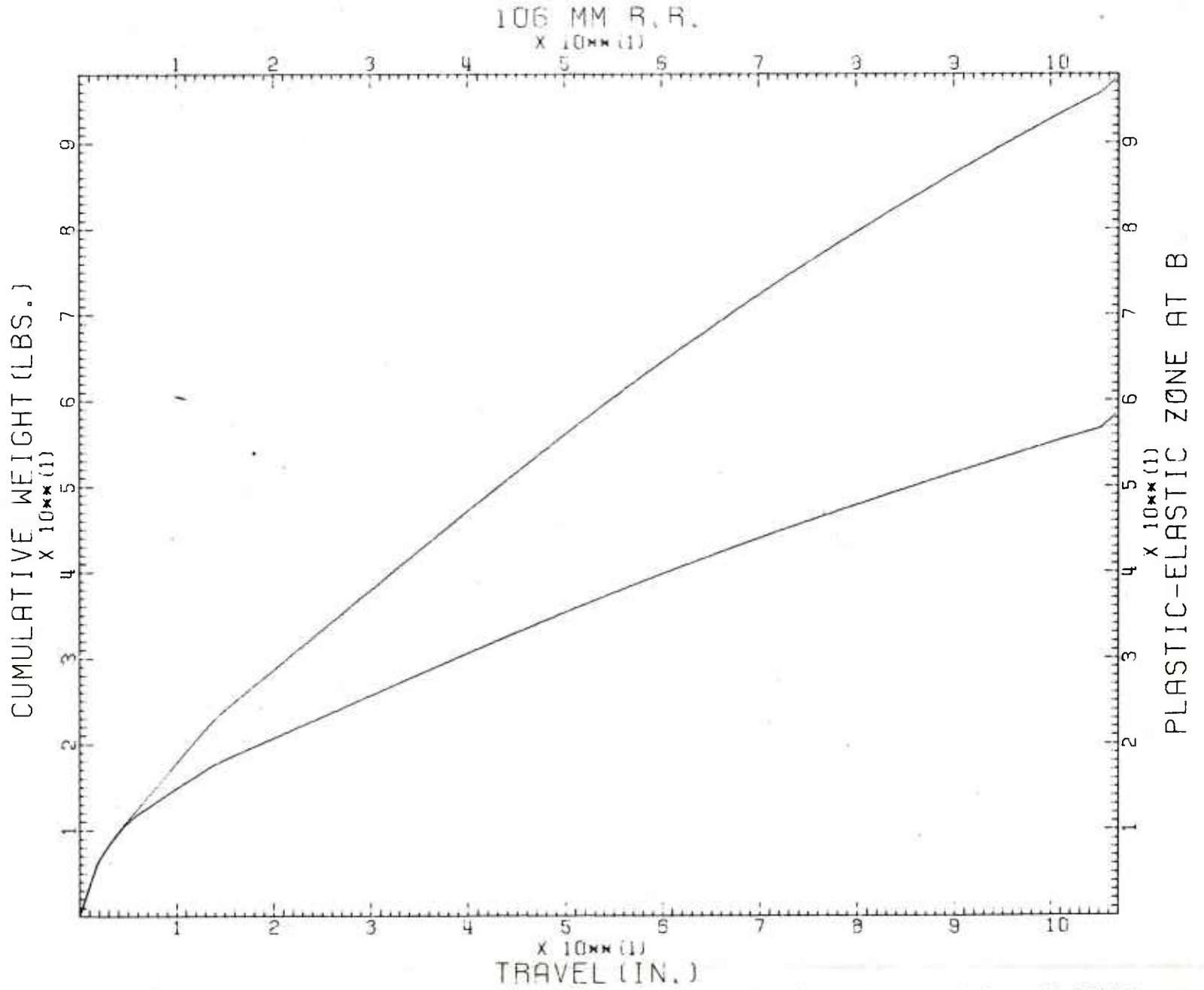

Figure A-9. Cumulative weights of composite and conventional tubes using an autofrettaged liner (0.050" liner).

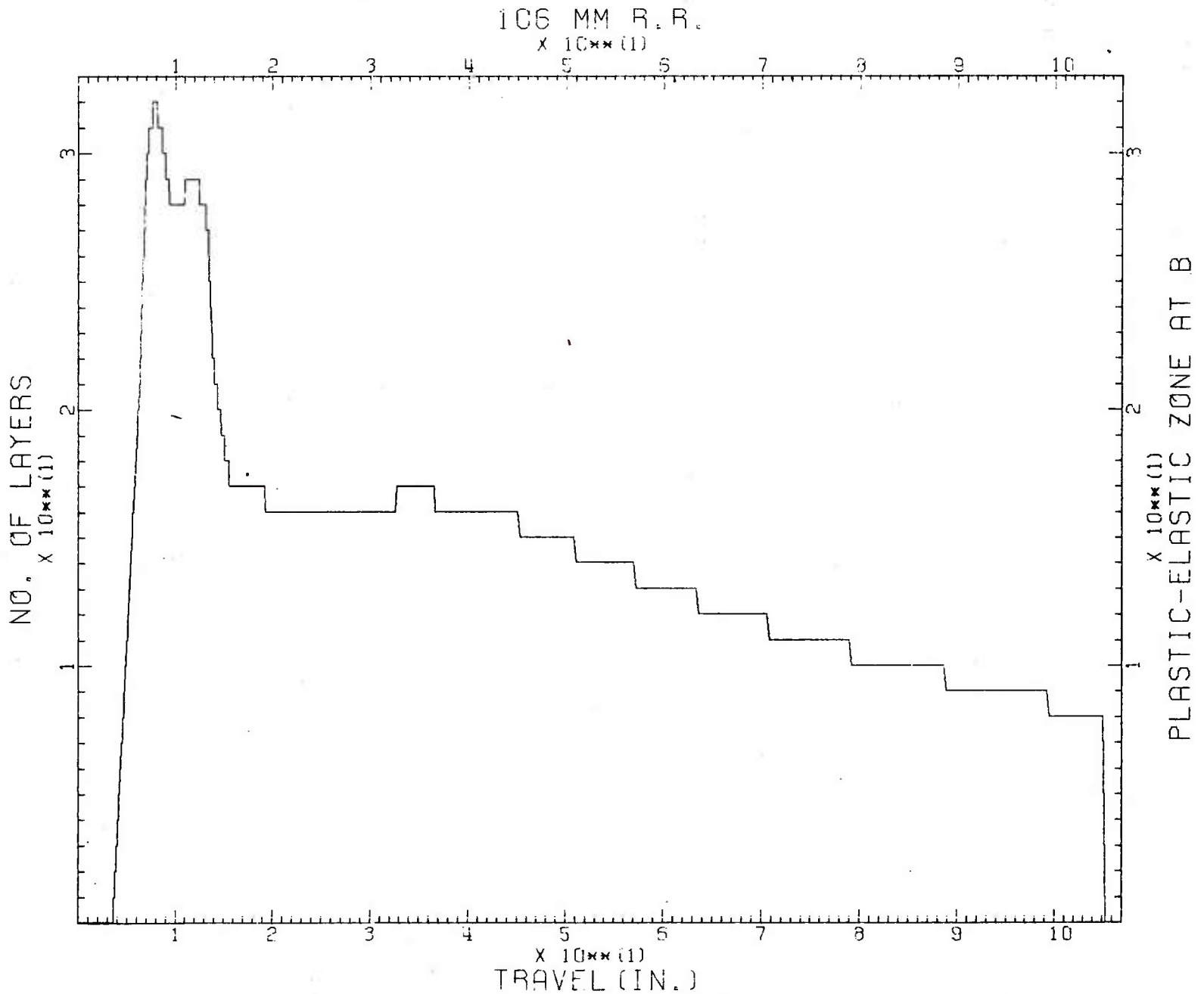

Figure A-10. Fabrication pattern for winding a composite tube with an 0.050 autofrettaged liner.

```
106 MM R.R. (STEEL LINER-STEEL FILAMENT/EPOXY MATRIX JACKET)
BORE RADIUS=2.104
FILAMENT/MATRIX VOLUME RATIO=0.750
WEIGHT PENALTY FACTOR=80.000
COMPOSITE FABRICATION COST=1.000
ALL LINER FABRICATION COST=1.000
POISSON'S RATIO(LINER)=0.300
POISSON'S RATIO(FILAMENT)=0.280
POISSON'S RATIO(MATRIX)=0.300
LINER MODULUS=30000000
FILAMENT MODULUS=30000000
MATRIX MODULUS=500000
LINER DENSITY=0.2830
FILAMENT DENSITY=0.2820
MATRIX DENSITY=0.0440
COMPOSITE DENSITY=0.2225
LINER YIELD STRENGTH=160000
FILAMENT YIELD STRENGTH=450000
MATRIX YIELD STRENGTH=10000
DOLLARS PER POUND OF LINER=0.50
DOLLARS PER POUND OF FILAMENT=8.00
DOLLARS PER POUND OF MATRIX=1.50
FACTOR OF SAFETY=1.000
```

Figure A-11. Input data for "GUNTUC" computer program (0.075" liner).

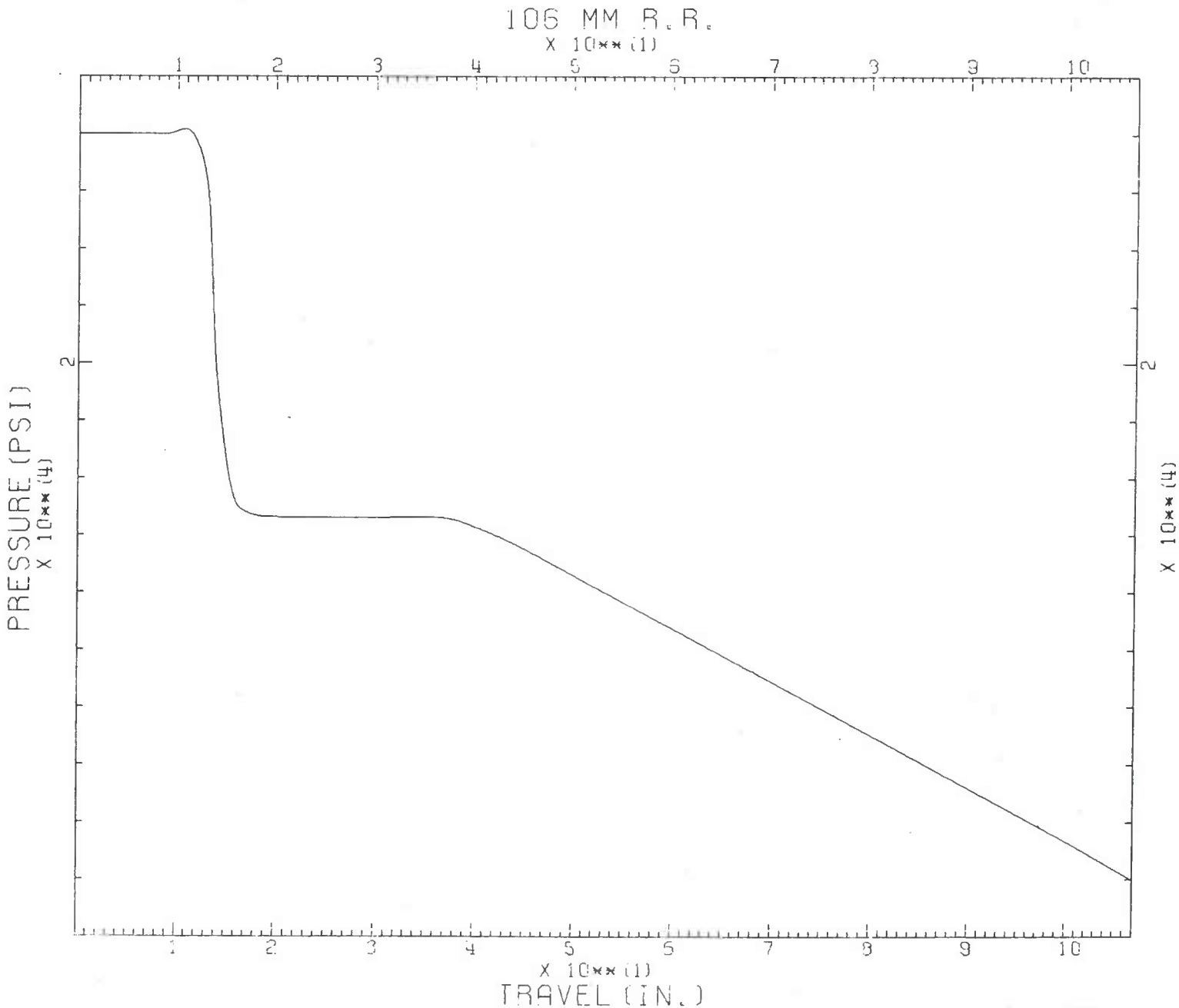

Figure A-12. ESP - travel curve for conventional 106mm M40A1 recoilless rifle (0.075" liner).

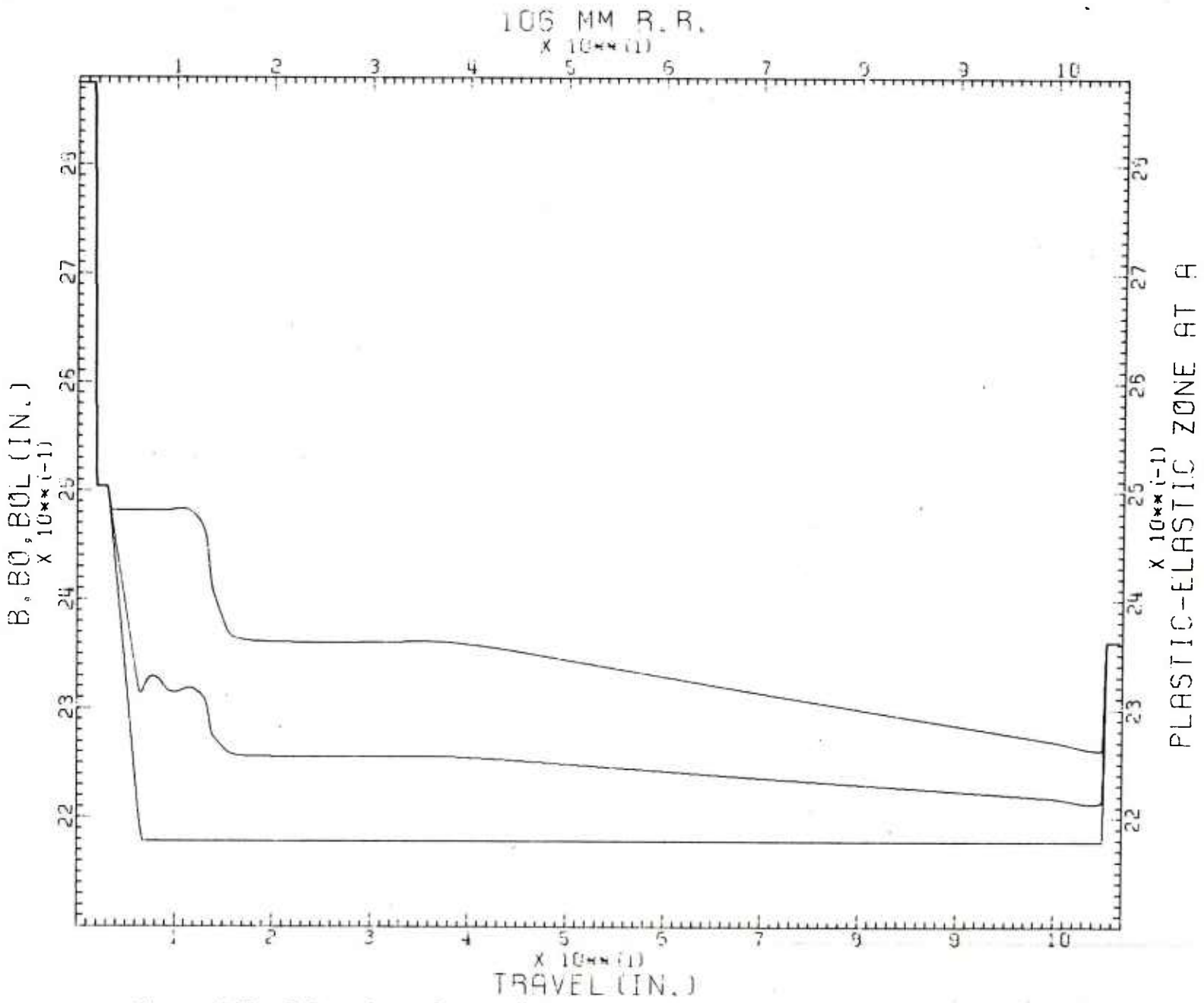

Figure A-13. O.D. values of composite vs conventional 106mm gun tubes (0.075" liner).

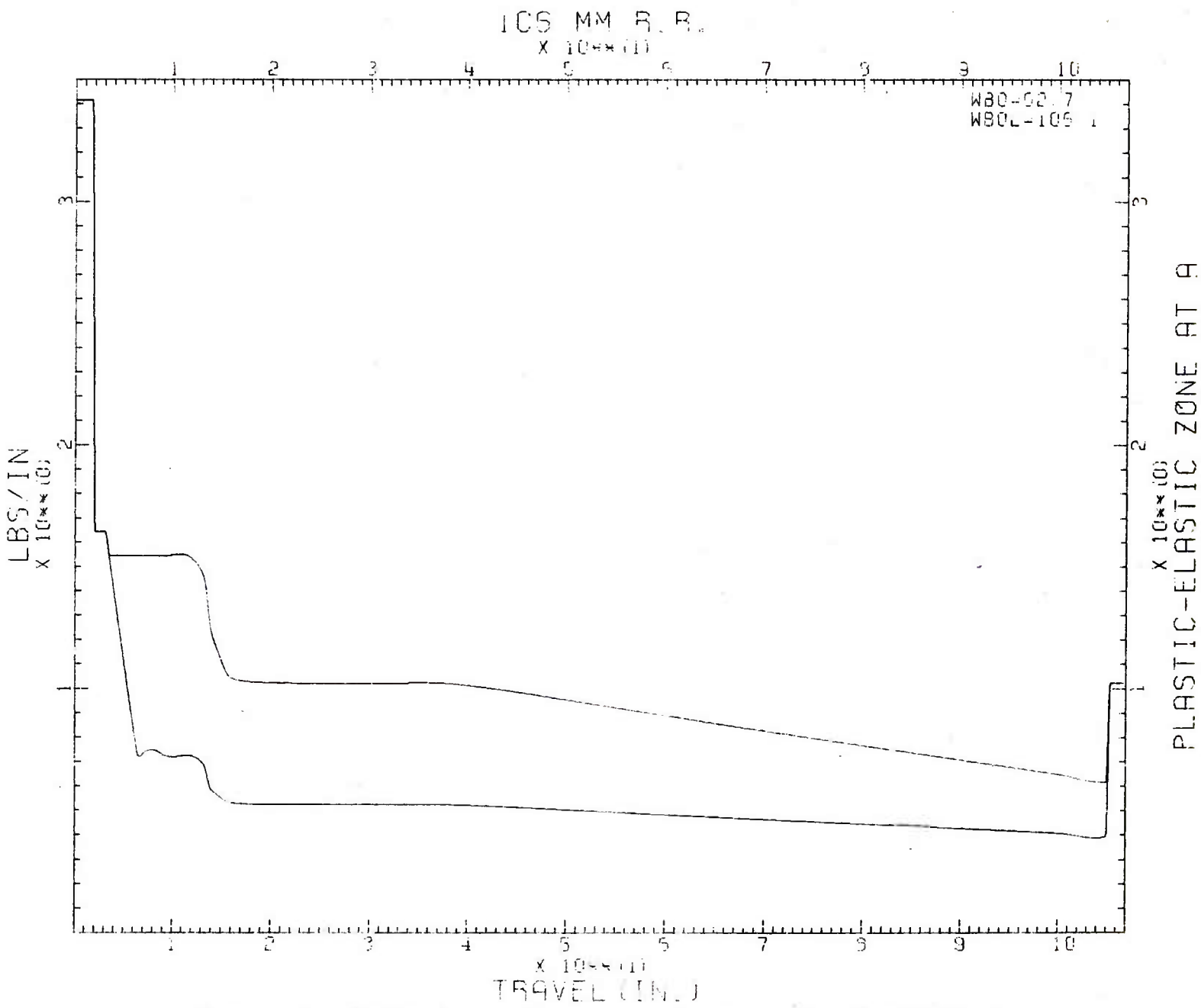

Figure A-14. Weight of composite vs conventional gun tubes (0.075" liner).

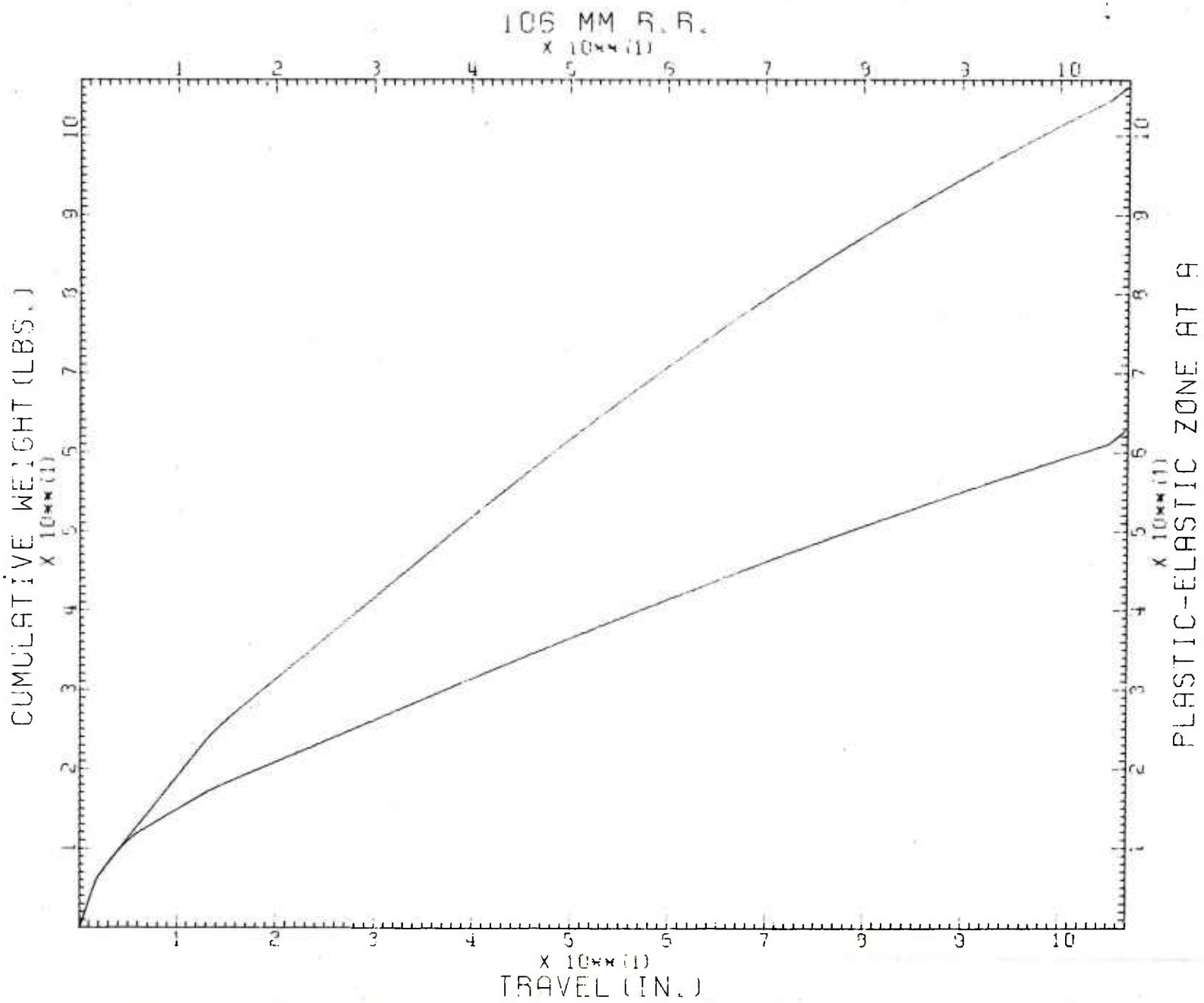

Figure A-15. Cumulative weights of composite and conventional gun tubes (0.075" liner).

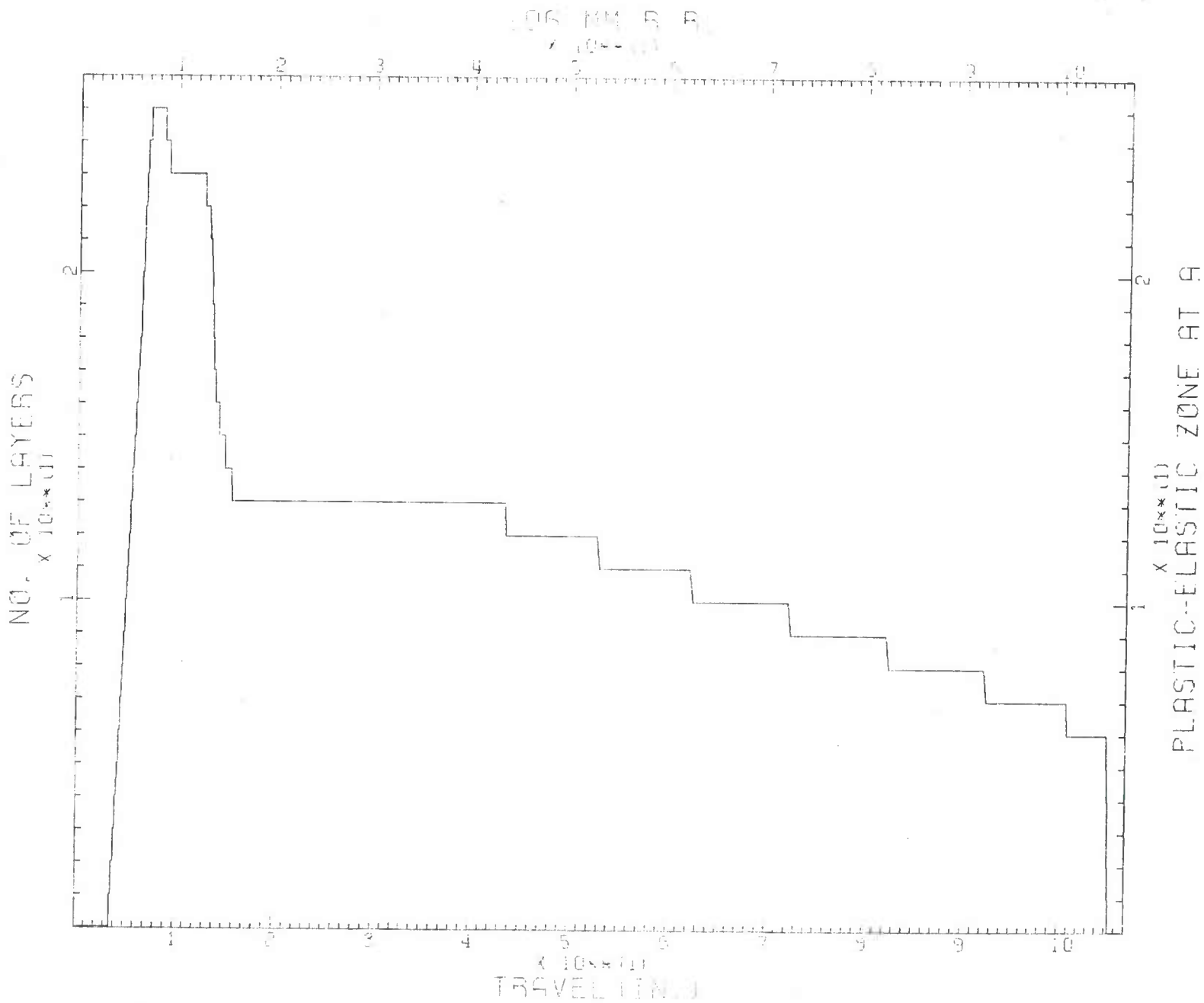

Figure A-16. Fabrication pattern for winding a composite tube with an 0.075" liner.

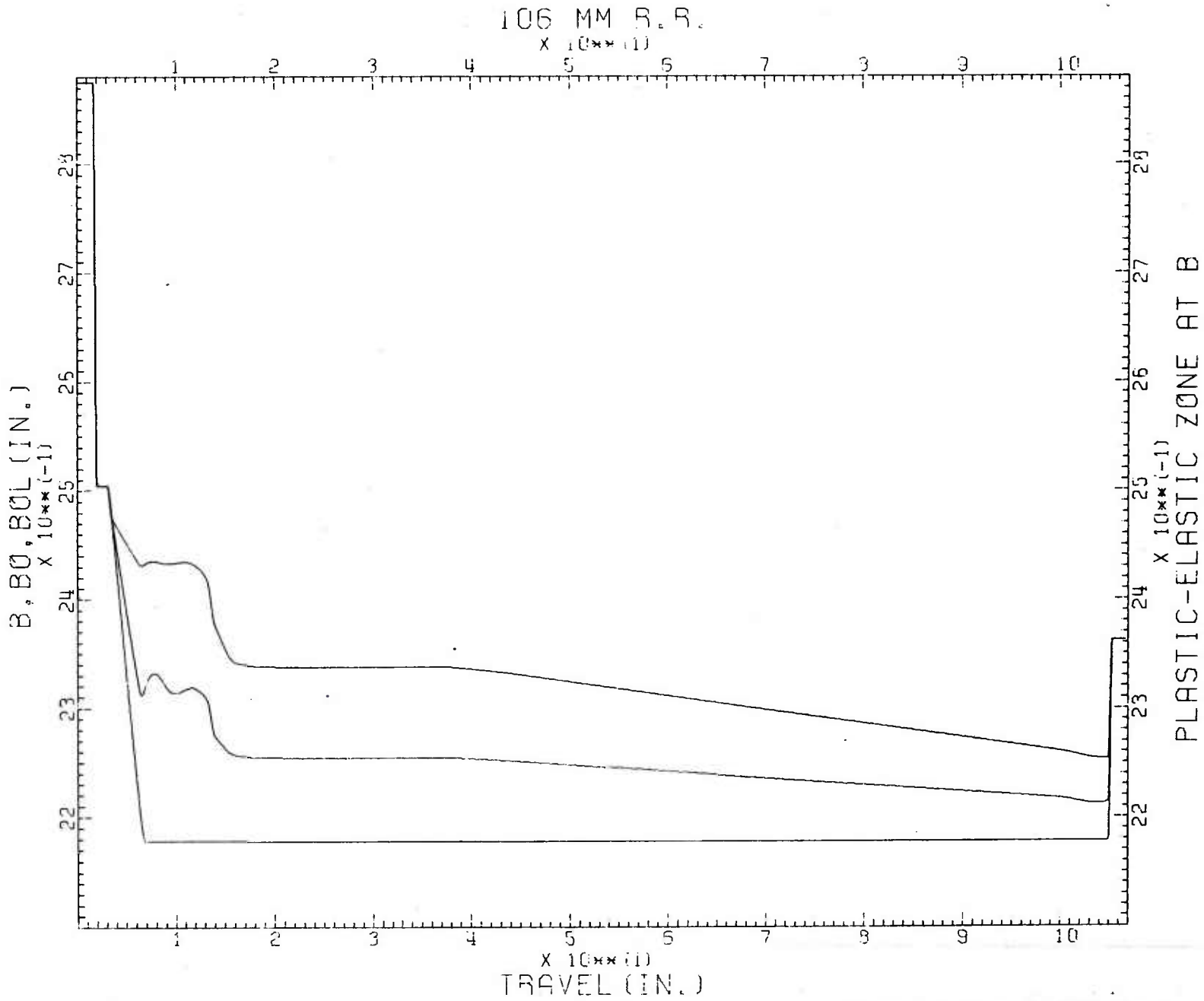

Figure A-17. O.D. values of composite vs conventional tubes using an autofrettaged liner (0.075" liner).

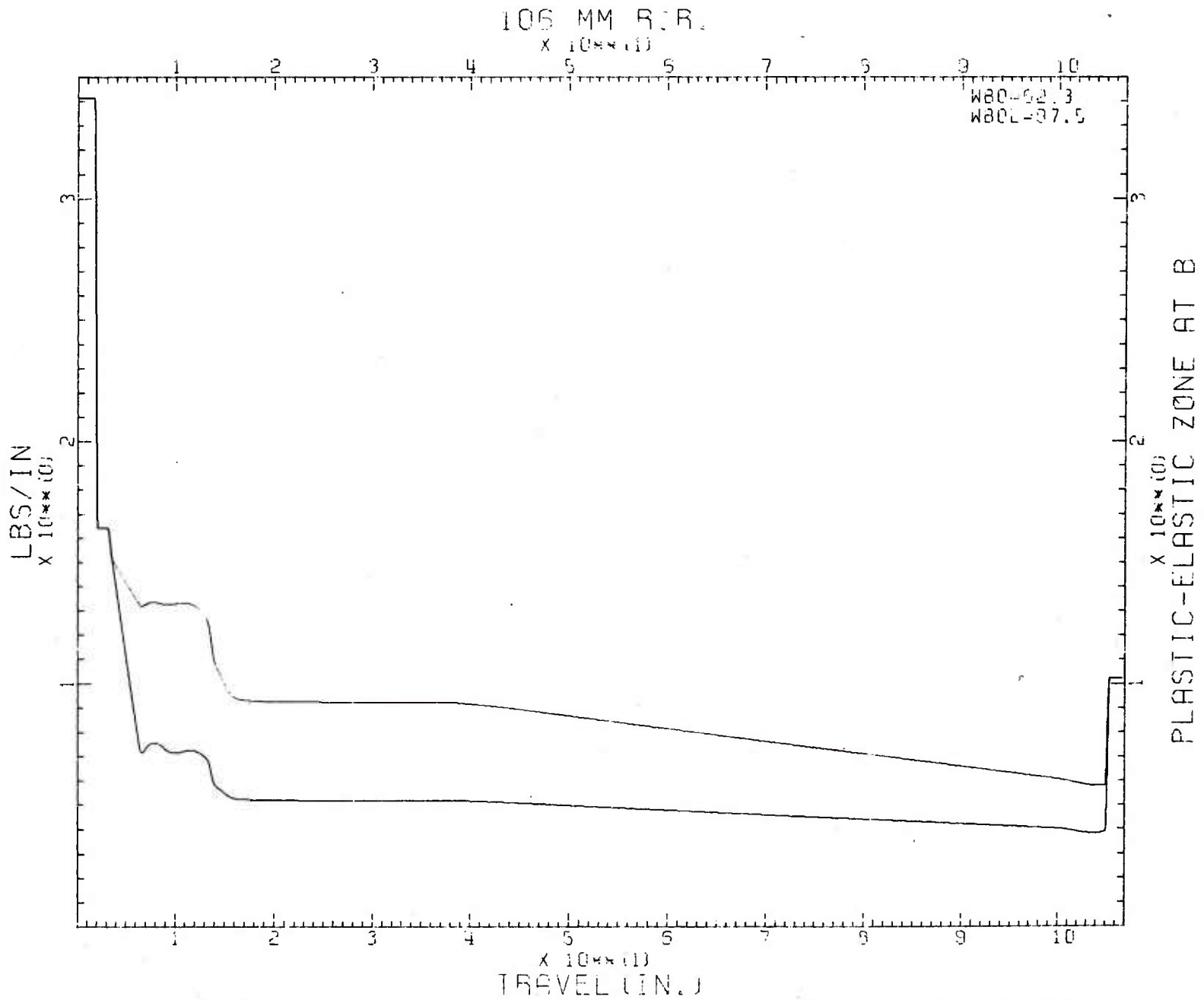

Figure A-18. Weight of composite vs conventional tubes using an autofrettaged liner (0.075" liner).

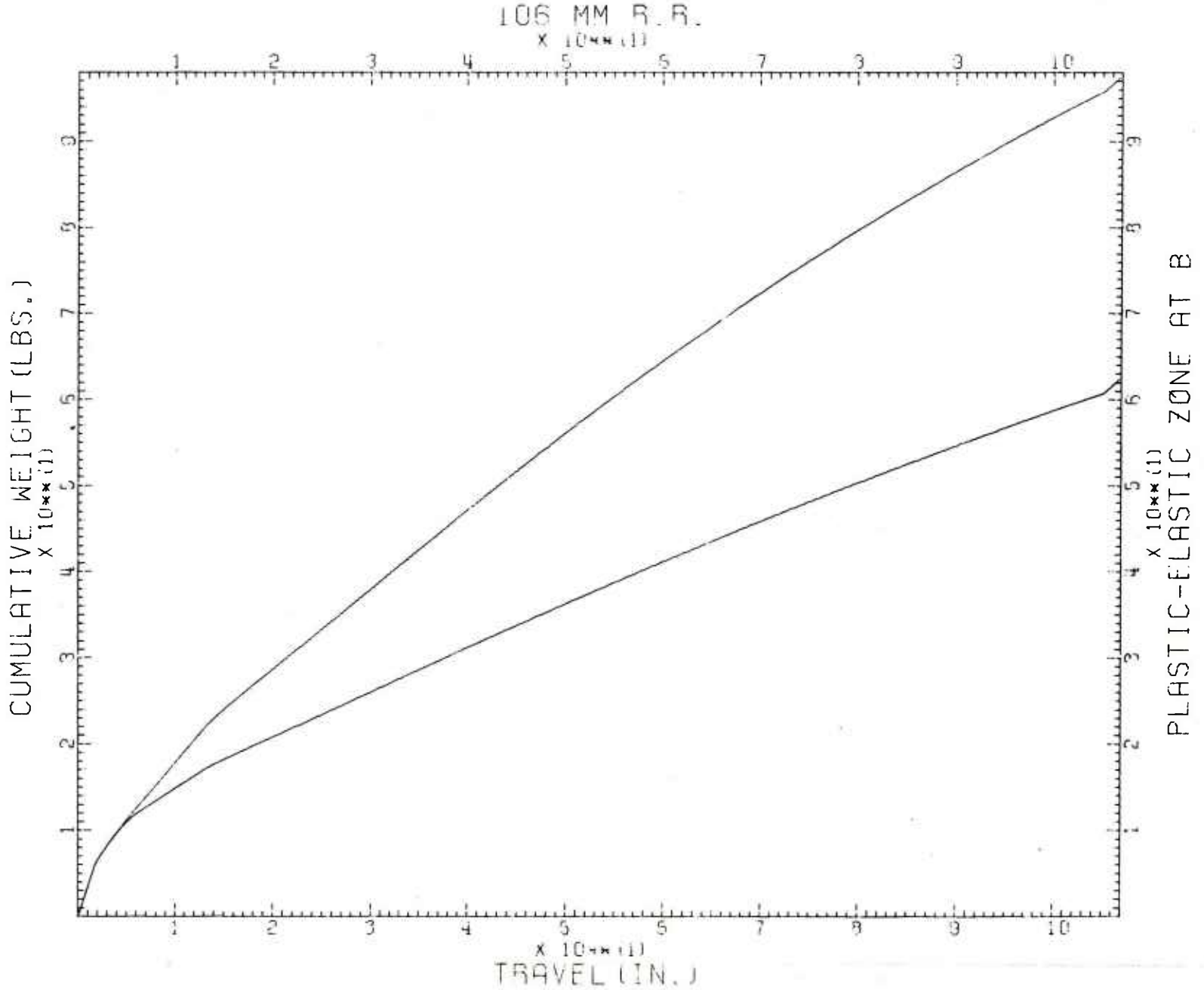

Figure A-19. Cumulative weights of composite and conventional tubes using an autofrettaged liner (0.075" liner).

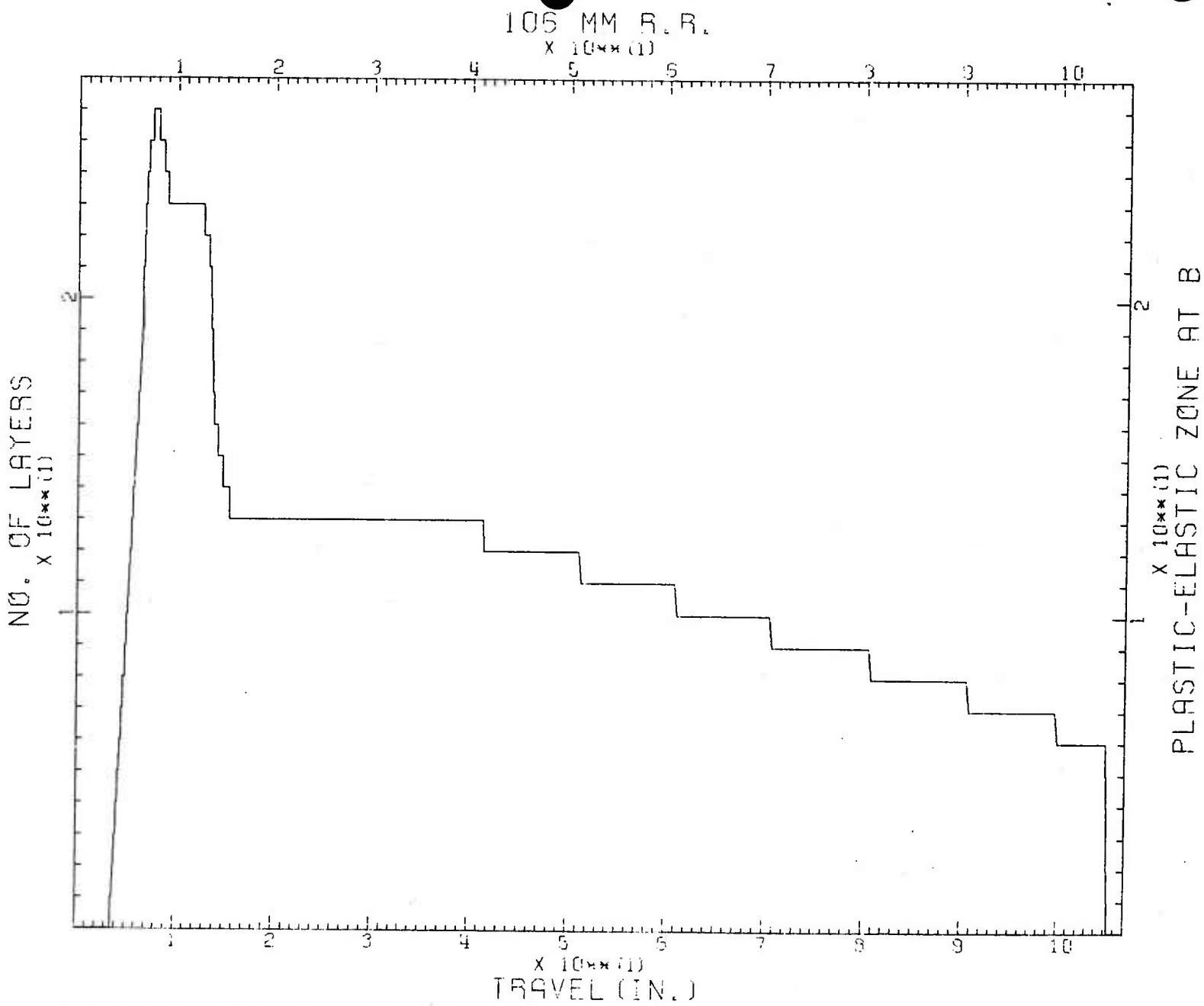

Figure A-20. Fabrication pattern for winding a composite tube with an 0.075" autofrettaged liner.

APPENDIX B

GRAPHICAL "TENZAUTO" OUTPUT FOR 0.050 IN. AND 0.075 IN. LINERS

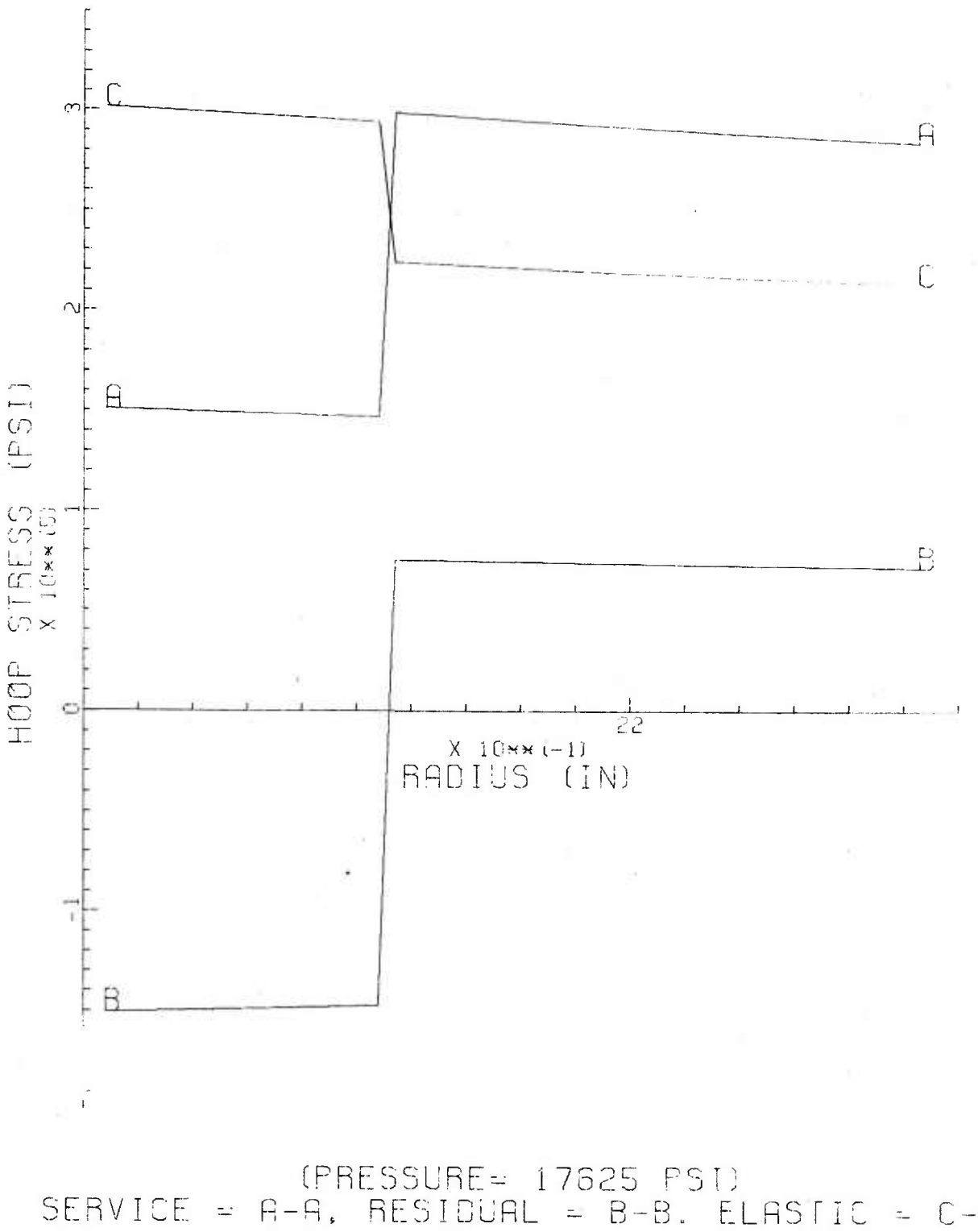

Figure B-1. Plot of ideal stress distribution for a "GUNTUC" designed composite cylinder with an 0.050" steel liner.

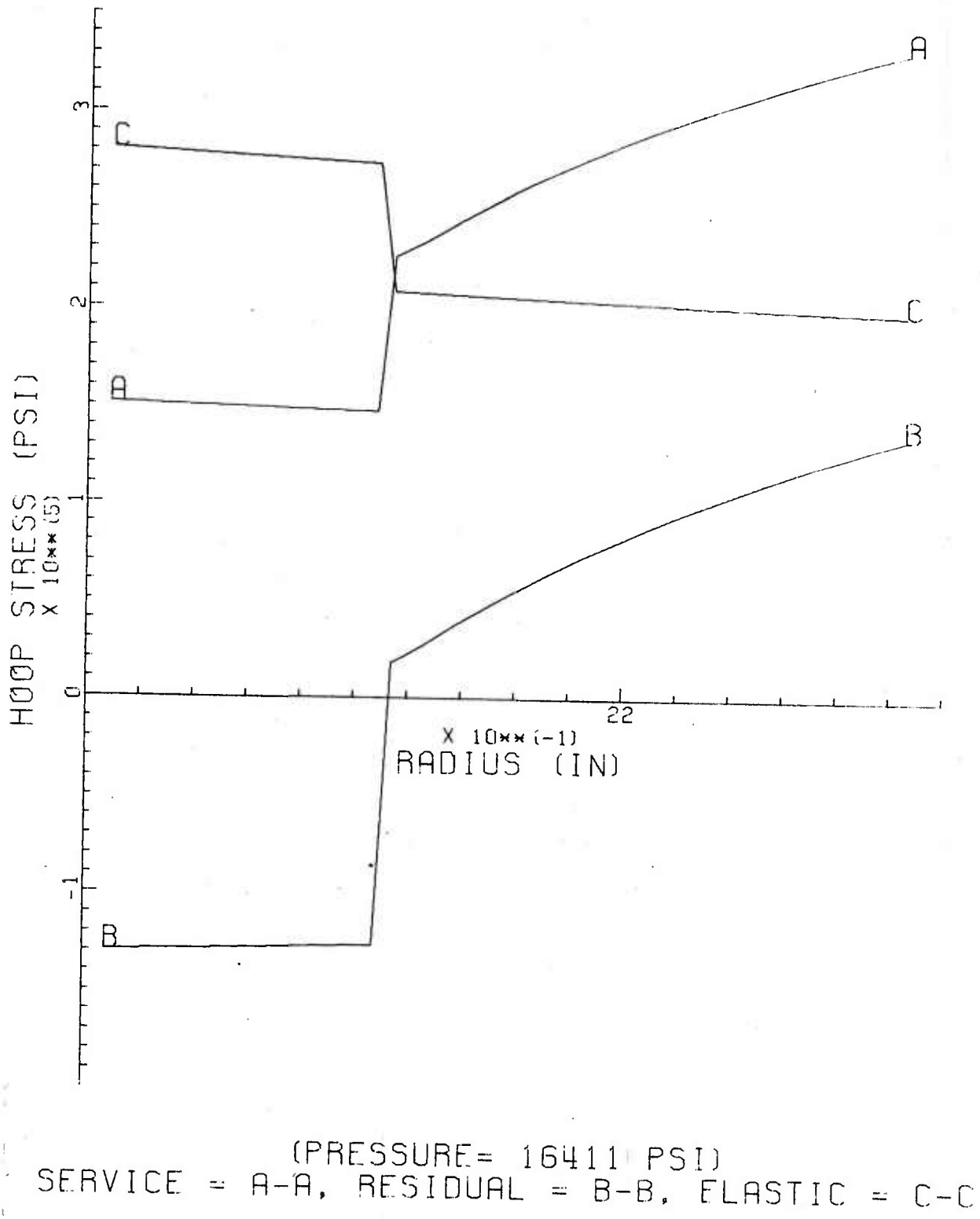

Figure B-2. Plot of stress distribution for an actual fabricated composite cylinder (0.050" liner).

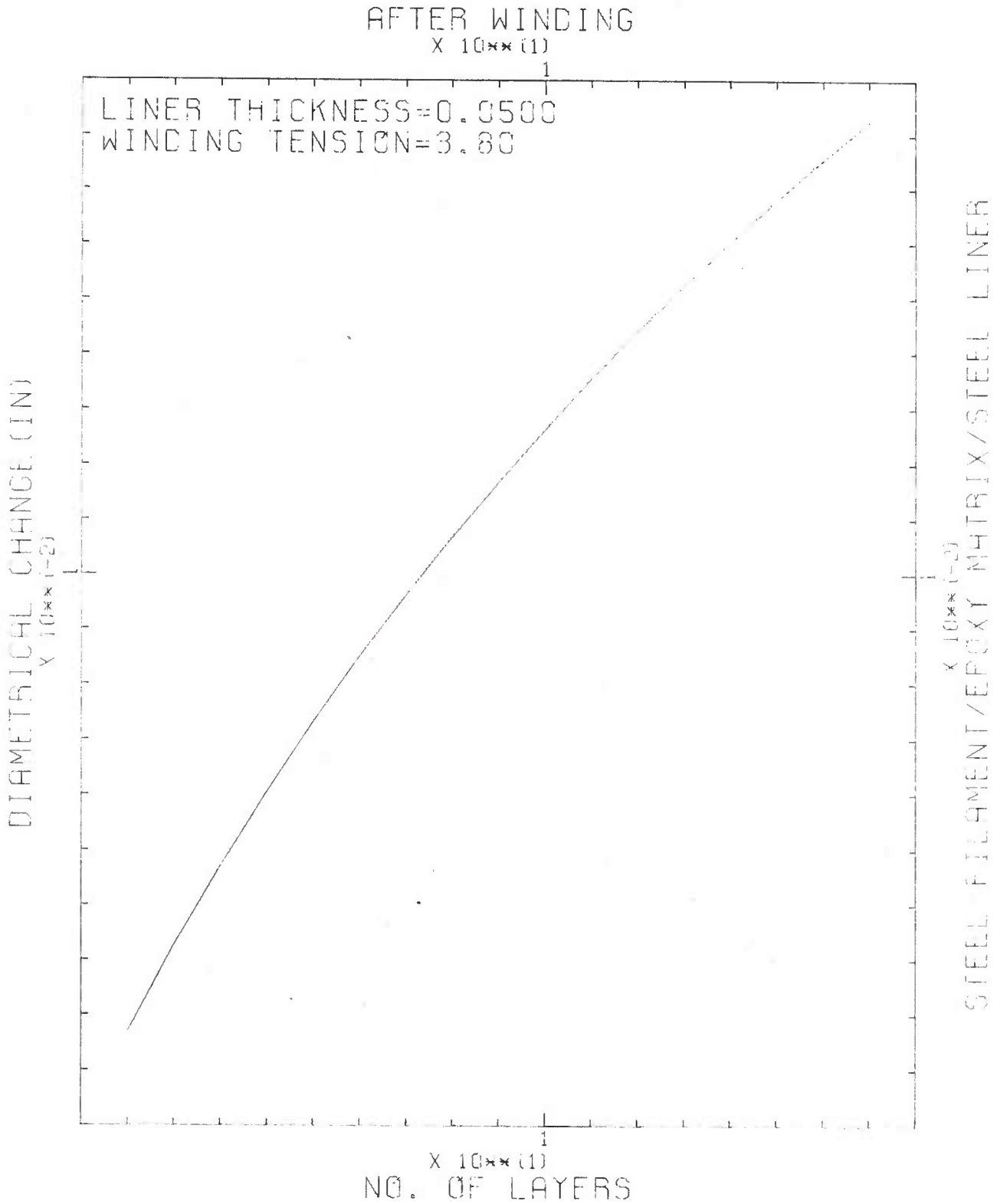

Figure B-3. Plot of the 0.050" liner's diametrical change vs number of layers.

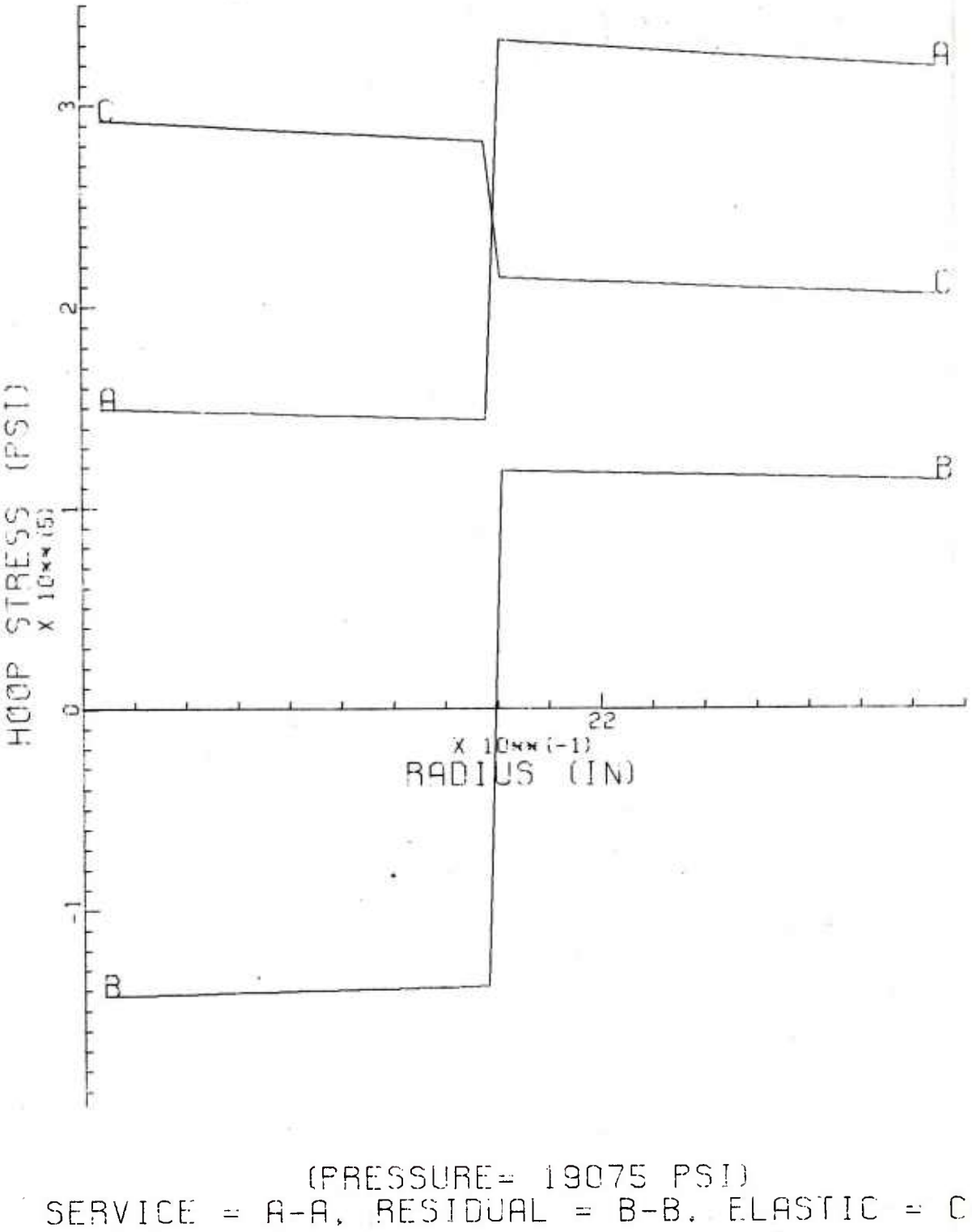

Figure B-4. Plot of ideal stress distribution for a "GUNTUC" designed composite cylinder with an 0.075" steel liner.

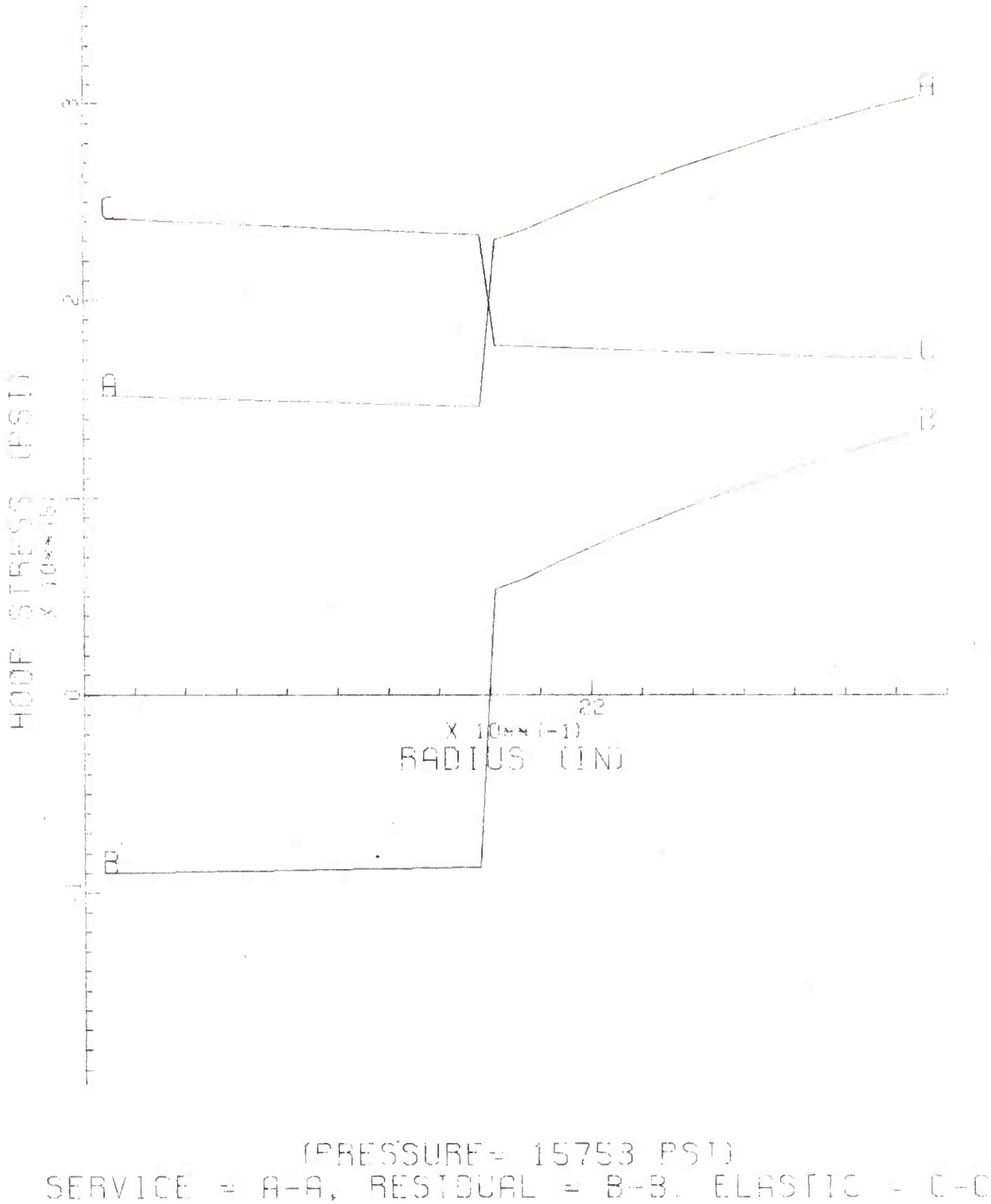

Figure B-5. Plot of stress distribution for an actual fabricated composite (0.075' liner).

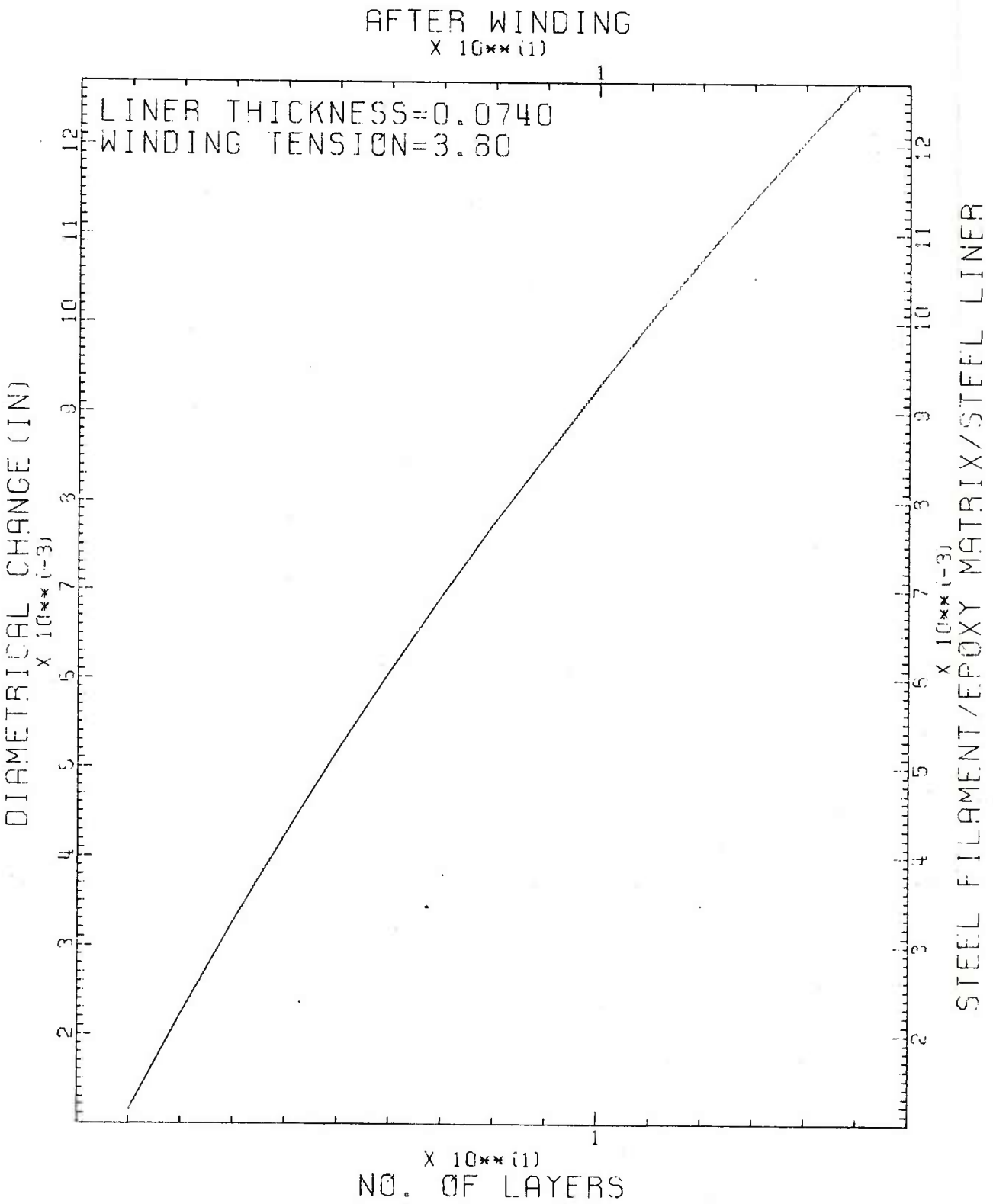

Figure B-6. Plot of the 0.075" liner's diametrical change vs number of layers.

APPENDIX C

SUMMARY OF TESTING ON 106MM CYLINDERS

OCL-2 A. FABRICATION

25" long section of 106mm tube machined to 0.100" wall in gage length.

Wound in gage length with 23 layers of 6 mil NS-355 wire at an avg of 151.6 ends/in/layer and an avg tension of 1.5#/end.

Designed pressure - 28.9 KSI (GUNTUC).

B. BURST TESTED

29 KSI Static loading in 0-20 KSI - 10 min

20-25 KSI - 15 min

25-Burst - 20 min

OCL-3 A. FABRICATION

25" long section of 106mm tube machined to 0.050" wall in gage length.

Wound in gage length with 22 layers of 6 mil NS-355 wire at an avg of 159.9 ends/in/layer and an avg tension of 1.5#/end.

Designed pressure - 24.8 KSI (NETTING ANALYSIS).

B. BURST TESTED

21 KSI Dynamic loading.

Ruptured in recessed shoulder section. Recalculation of expected burst in this reduced wall section was 19.4 KSI.

Only 8 layers on ruptured shoulder area.

OCL-5 A. FABRICATION

25" long, machined to .050" wall in gage length.
17 layers of 6 mil NS-355 wire at an avg of 158.2 ends/in/layer and an avg tension of 3.5#/end.
Design pressure 17.6 KSI (GUNTUC).

B. CYCLIC BURST TEST

18.2 KSI (Cycled at 15 KSI for 10 cycles and checked for bore enlargement. Returned and dynamically ruptured.)

OCL-7 A. FABRICATION

25" long, machined to .100" wall in gage length.
14 layers of 6 mil NS-355 wire at an avg of 158.7 ends/in/layer and an avg tension of 3.8#/end.
Design pressure 20 KSI (GUNTUC).

B. CYCLIC BURST TEST

21.9 KSI (Cycled at 15 KSI for 10 cycles and checked for bore enlargement. Recycled another 12 cycles at 20 KSI. Dynamically burst on 23rd cycle.)

OCL-8 A. FABRICATION

25" long section of 106mm tube machined to 0.100 wall in gage length.

Wound in gage length with 16 layers of 6 mil Hi-carbon (brass plated) wire at an avg of 154 ends/in/layer and an avg tension of 1.5#/end. (T.S. of this wire - 540 KSI)

Designed pressure - 24.7 KSI (NETTING ANALYSIS).

B. BURST TESTED

25.2 KSI Dynamic test.

OCL-9 A. FABRICATION

25" long section of 106mm tube machined to 0.050" wall in gage length.

Wound in gage length with 19 layers of 6 mil Hi-carbon (brass plated) wire at an avg of 156.4 ends/in/layer and an avg tension of 1.5#/end.

Designed pressure - 24.0 KSI (NETTING ANALYSIS).

B. BURST TESTED

21.9 KSI Dynamic test.

Ruptured in recessed shoulder section. Recalculation of burst strength in this reduced wall section was 22.3 KSI.

Only 11 layers on this shoulder area.

OCL-4 A. FABRICATION

25" long section, machined to .050" wall in gage length. 17 layers of 6 mil NS-355 wire at an avg of 161.9 ends/in/layer and an avg tension of 3.8#/end. Designed pressure 17.6 KSI (GUNTUC).

B. FATIGUE TESTED

1398 cycles at 12 KSI (68% burst strength) at a rate of ~8 cycles/min.

OCL-6 A. FABRICATION

25" long section, machined to .750" wall in gage length. 15 layers of 6 mil NS-355 wire at an avg of 161.7 ends/in/layer and an avg tension of 3.8#/end. Designed pressure 19.1 KSI (GUNTUC).

B. FATIGUE TESTED

1884 cycles at 12 KSI (63% burst strength) at a rate of ~ 9.0 cycles/min.

OCL-10 A. FABRICATION

25" long section, machined to .100" wall in gage length. 13 layers of 6 mil NS-355 wire at an avg of 157.5 ends/in/layer and an avg tension of 3.8#/end. Designed pressure 19.1 KSI (GUNTUC).

B. FATIGUE TESTED

4416 cycles at 12 KSI (63% burst strength) at a rate of ~ 7.0 cycles/min.

APPENDIX D

FABRICATION AND INSPECTION SHEETS FOR OCL-4, 5, 6, 7, AND 10

NO:

OCL-5

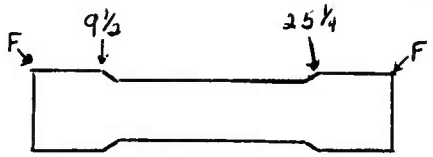

TENSION: 11.5 lb

NO. OF SPOOLS: 3

	LAYERS	ENDS IN	BORE DIAM	RIFLE DIAM	REMARKS
1	F → F	169.8	18.5	18.5	20 = 0 Deflection
2	F ← F	138.6	17.0	17.5	
3	F → 25 1/4	143.0	15.5	17.0	
4	9 1/2 ← 25 1/4	136.5	14.5	16.5	
5	9 1/2 → F	139.1	13.5	14.5	
6	F ← F	172.0	-	-	Winding interrupted after No 6. When continued for No 7, the direction of travel was same as preceding layer.
7	F ← F	172.0	11.5	12.5	
8	F → 25	157.1	10.5	11.0	
9	9 3/4 ← 25	158.0	9.5	10.0	
10	9 3/4 → F	162.8	8.5	9.0	
11	F ← F	160.4	8.0	8.0	
12	F → 24 3/4	156.5	7.0	6.0	
13	10 ← 24 3/4	161.3	5.5	5.0	
14	10 → F	171.0	5.0	4.0	
15	F ← F	158.0	4.0	3.0	
16	F → F	171.0	3.5	2.0	
17	F ← F	161.7	2.5	1.5	
	AVG =	158.2			
	DIAM TOTAL DEFLECTION		.0175	.0185	

NO:

OCL-7

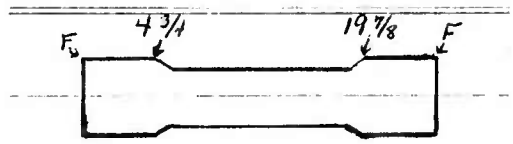

TENSION: 11.5 lb

NO. OF SPOOLS: 3

	LAYERS	ENDS IN	BORE DIAM	RIFLING DIAM	REMARKS
1	F → F	160	15.0	15.5	16 = 0 Deflection
2	" ← "	198	14.0	14.5	
3	" → 19 7/8	103	13.5	14.0	
4	4 3/4 ← "	160	13.0	13.0	
5	" → 19 3/4	153	12.5	12.0	
6	4 7/8 ← "	167	12.0	11.5	
7	" → F	186	11.0	11.0	
8	F ← "	178	10.5	10.5	
9	" → 19 5/8	181	10.0	10.0	
10	5 ← "	133	9.0	9.0	
11	" → 19 1/2	147	8.5	8.5	
12	5 1/8 ← "	136	8.0	8.0	
13	" → F	157	7.5	7.5	
14	F ← "	161	7.0	7.0	
	AVG =	158.7			

NO:

OCL-4

TENSION: 11.5 lb

NO. OF SPOOLS: 3

	LAYERS	ENDS IN	BORE DIAM	RIFLING DIAM	REMARKS
1	F → F	123	19.0	19.0	20 = 0 Deflection
2	F ← F	216	17.0	17.5	
3	" → 19 1/2	147	16.0	16.5	
4	4 7/8 ← "	173	14.5	15.5	
5	" → F	156	13.5	14.5	
6	F ← "	173	12.5	13.0	
7	" → 19 3/8	158	11.5	12.0	
8	5 ← "	173	10.5	11.0	
9	" → F	153	9.5	10.5	
10	F ← "	146	9.0	9.5	
11	" → 19 1/4	136	8.0	9.0	
12	10 1/8 ← "	188	7.0	8.5	
13	" → F	172	6.5	8.0	
14	F ← "	158	6.0	7.5	Infrared lamps turned on for Layers 14 and 15 for better resin flow.
15	" → "	143	4.5	6.5	
16	" ← "	163	3.5	6.0	
17	" → "	175	3.0	5.5	
	AVG =	161.9			

NO:

OCL-6

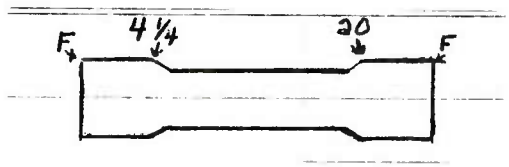

TENSION: 11.5 lb

NO. OF SPOOLS: 3

LAYERS		ENDS IN.	BORE DIAM	RIFLING DIAM	REMARKS
1	F → F	144	19.0	19.0	20 = 0 DEFLECTION
2	" ← "	157	18.0	18.0	
3	" → 20	160	17.0	17.5	
4	4 1/4 ← "	147	16.5	17.0	
5	" → 19 7/8	217	15.5	16.0	
6	4 3/8 ← "	148	14.5	15.5	
7	" → F	139	14.0	15.0	
8	4 1/2 ← "	164	13.5	14.5	
9	" → 19 3/4	171	12.5	14.0	
10	F ← "	177	11.5	13.5	Turn infrared lamps on for Layers 10 and 11 to allow better resin flow.
11	" → F	123	11.0	13.0	
12	4 5/8 ← "	172	10.0	12.5	
13	" → 19 5/8	160	9.5	11.0	
14	F ← "	182	9.0	8.5	
15	" → F	165	8.5	7.5	
		AVG = 161.7			

NO:

OCL-10

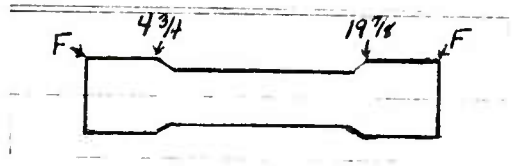

TENSION: 11.5 lb

NO. OF SPOOLS: 3

	LAYERS	ENDS IN.	BORE DIAM	RIFLING DIAM	REMARKS
1	F → 19 7/8	139	19.5	DID	20.0 = 0 Deflection
2	4 3/4 ← "	199	18.5		
3	" → F	152	17.5		
4	4 7/8 ← "	168	17.0		
5	" → 19 3/4	157	16.5		
6	F ← "	181	15.5		
7	" → 19 5/8	137	15.0	NOT	
8	5 ← "	151	14.5		
9	" → F	145	14.0		
10	5 1/8 ← "	154	13.5		
11	" → 19 1/2	141	13.0		
12	F ← "	163	12.5		Last 2 layers wound with infrared lamps on in order to get better resin flow.
13	" → "	160	11.5	RECORD	
	AVG =	157.5			

OCL-4 (0.050" LINER)

Travel (in.)	BEFORE WINDING		AFTER GEL		AFTER CURE	
	Bore	Rifling	Bore	Rifling	Bore	Rifling
2	-	4.2110	-	4.2075	-	4.2075
4	4.1355	4.2110	4.1315	4.2070	4.1315	4.2080
6	4.1350	4.2120	4.1290	4.1990	4.1290	4.2000
8	4.1355	4.2120	4.1215	4.1970	4.1210	4.1980
10	4.1355	4.2115	4.1230	4.1975	4.1225	4.1980
12	4.1350	4.2110	4.1225	4.1960	4.1220	4.1970
14	4.1355	4.2110	4.1220	4.1960	4.1210	4.1965
16	4.1360	4.2110	4.1195	4.1940	4.1185	4.1960
18	4.1360	4.2100	4.1170	4.1965	4.1175	4.1975
20	4.1360	4.2090	4.1280	4.2070	4.1275	4.2080
22	4.1355	4.2110	4.1310	4.2070	4.1305	4.2070
24	-	-	-	-	-	-

OCL-6 (0.075" LINER)

2	-	4.2120	-	4.2100	-	4.2100
4	4.1345	4.2115	4.1330	4.2095	4.1325	4.2100
6	4.1345	4.2110	4.1300	4.2015	4.1305	4.2030
8	4.1365	4.2110	4.1240	4.1995	4.1240	4.2005
10	4.1365	4.2100	4.1240	4.2000	4.1245	4.2010
12	4.1355	4.2105	4.1245	4.2015	4.1240	4.2015
14	4.1360	4.2105	4.1260	4.2020	4.1255	4.2025
16	4.1355	4.2110	4.1260	4.2010	4.1250	4.2020
18	4.1360	4.2100	4.1255	4.2005	4.1250	4.2010
20	4.1360	4.2100	4.1295	4.2065	4.1290	4.2065
22	4.1355	4.2110	4.1335	4.2095	4.1335	4.2095
24	-	-	-	-	-	-

OCL-7 (0.100" LINER)

Travel (in.)	BEFORE WINDING		AFTER GEL		AFTER CURE	
	Bore	Rifling	Bore	Rifling	Bore	Rifling
2	-	4.2115			-	4.2090
4	4.1350	4.2115			4.1325	4.2100
6	4.1350	4.2115	NOT		4.1310	4.2050
8	4.1350	4.2100			4.1260	4.2030
10	4.1355	4.2100			4.1270	4.2020
12	4.1355	4.2100	AVAILABLE		4.1265	4.2020
14	4.1355	4.2100			4.1270	4.2020
16	4.1350	4.2100			4.1270	4.2020
18	4.1355	4.2100			4.1265	4.2020
20	4.1355	4.2100			4.1295	4.2090
22	4.1360	4.2100			4.1330	4.2095
24	-	-			-	-

OCL-10 (0.100" LINER)

2	-	4.2105	-	4.2095	-	4.2085
4	4.1345	4.2100	4.1330	4.2085	4.1335	4.2080
6	4.1345	4.2100	4.1310	4.2025	4.1315	4.2025
8	4.1350	4.2100	4.1280	4.2025	4.1285	4.2025
10	4.1355	4.2100	4.1290	4.2030	4.1295	4.2025
12	4.1355	4.2095	4.1290	4.2025	4.1290	4.2020
14	4.1355	4.2100	4.1285	4.2025	4.1285	4.2025
16	4.1350	4.2100	4.1275	4.2020	4.1275	4.2020
18	4.1355	4.2090	4.1270	4.2025	4.1275	4.2025
20	4.1350	4.2105	4.1300	4.2085	4.1300	4.2085
22	4.1350	4.2105	4.1330	4.2090	4.1335	4.2090
24	-	-	-	-	-	-

OCL-5 (0.050" LINER)

Travel (in.)	BEFORE WINDING Bore	BEFORE WINDING Rifling	AFTER GEL Bore	AFTER GEL Rifling	AFTER CURE Bore	AFTER CURE Rifling
2	-	-			-	-
4	4.1350	4.2110			4.1305	4.2050
6	4.1350	4.2115			4.1230	4.1920
8	4.1345	4.2115			4.1170	4.1940
10	4.1345	4.2115			4.1160	4.1920
12	4.1345	4.2110	NOT		4.1170	4.1930
14	4.1350	4.2110			4.1160	4.1910
16	4.1350	4.2110			4.1150	4.1915
18	4.1350	4.2110			4.1150	4.1965
20	4.1350	4.2110	AVAILABLE		4.1280	4.2060
22	4.1350	4.2110			4.1290	4.2060
24	-	-			-	-

APPENDIX E

TEST PLAN FOR FIRING OF COMPOSITE TUBE AT PICATINNY ARSENAL

SCOPE OF WORK

INTRODUCTION

The objective of this test is to evaluate firing characteristics of a composite (filament wound) 106mm recoilless rifle gun tube made of 0.100" rifled steel liner and a steel filament/epoxy jacket. Data of the following nature is to be ascertained on each firing: (a) projectile velocity, (b) peak pressure, (c) longitudinal and hoop strains and (d) tube temperatures.

INSTRUMENTATION, GAGING AND MOUNTING

Equipment as required to monitor 4 channels of strain gages and two temperature gages per test plan. Equipment is also to be supplied to record projectile velocities. All strain gages and resistance thermometers will be mounted on the tube by Watervliet Arsenal prior to shipment to Picatinny Arsenal. Picatinny Arsenal will supply a tripod stand and mount along with any sand bags needed for additional stabilization of the tripod. Watervliet Arsenal is to supply 20 inert 106mm rounds with T-18 crusher gages (3/16" diam copper balls) pre-loaded with the propellant.

TEST

During all firing, projectile velocity and peak pressure will be recorded.

PHASE I

Fire 4 sets of two rounds each. During these 4 sets of firing, strain gages (see attached sketch) 1 and 2 (longitudinal strain-connected in one bridge) 3 and 4 (hoop strain-connected in another bridge) and

the individual resistance thermometers 5 and 6 (tube temperature) shall be monitored with digital ohmeters. In addition,

Set 1 - Gages 7H and 8L are to be individually monitored on the remaining two channels.

Set 2 - Gages 9L and 10L are to be individually monitored on the remaining two channels.

Set 3 - Gages 11H and 12L are to be individually monitored on the remaining two channels.

Set 4 - Gages 13L and 14H are to be individually monitored on the remaining two channels.

No specific rate of fire is requested during this phase.

PHASE II

Strain gages 1, 2, 3 and 4 are to be individually monitored with the 4 available channels. The resistance thermometers 5&6 will continue to be monitored with the separate ohmeters.

Set 1 - 3 rounds, with no specific rate of fire requested.

Set 2 - 9 rounds fired at the fastest rate that safety on the range will permit.

REPORTS

A brief narrative report of firing with still pictures and recorded data will be required following the completion of the test. A copy of the complete (continuous) strain curves is also desired.

NOTE: THE 106mm R.R. HAS BEEN CLASSIFIED AS A SENSITIVE WEAPON. THIS REQUIRES THAT THE BREECH ASSEMBLED BE STORED IN A SECURE LOCATION (SEPARATE FROM THE TUBE) BEFORE AND AFTER FIRING.

APPENDIX F

FIRING TEST REPORT ON 106MM COMPOSITE GUN TUBE

PICATINNY ARSENAL, DOVER, NEW JERSEY 07801

REPORT NO.

DATE 21 Nov 75

REPORT FROM THE Artillery & Mortar Branch, TSD

SUBJECT: Test firing of Watervliet 106mm Recoilless Rifle Composite Gun Tube No. 2206.

DATE OF TEST: 12 November 1975

OBJECT: To evaluate the firing characteristics of a composite (filament wound) tube made of 0.100" rifled steel liner and a steel filament/epoxy jacket.

REQUESTED BY: Robert Cullinan, Watervliet Arsenal

WEATHER DATA

Temperature	:	50°F
Wind direction & velocity	:	E, 2-6 Mph
Barometer	:	28.96
Relative humidity	:	92%
Sky	:	Rain

PROCEDURE

Twenty (20) each inert loaded M344A1 HEAT Projectiles were fired from the tube mounted on a standard M79 mount. The following data was recorded: peak chamber pressures, projectile velocity, change of tube temperature in °F, longitudinal and hoop strains in u in/in. Motion pictures and video tape were provided on each round fired for any malfunction that might occur. All gages were mounted by Watervliet personnel. Gage locations are shown on attached sketch.

INSTRUMENTATION

Velocity: Magnetic screens were positioned 10ft apart with the first screen 20ft forward of the muzzle. The time interval for the projectile to pass through both screens was measured by a chronograph.

Pressure: Taken by two copper crusher type T-18 gages inserted into each cartridge case.

Temperature Change: Sensors 5 and 6 (shown in sketch of gage locations) were resistance monitored by a digital ohmmeter to give temperature readings before and after each test firing.

Strain Measurements: The remaining sensors on the gage location sketch sheet are strain gages. Their location and orientation are as shown. These strain sensors are manufactured by BLH Electronics, Inc. SR4 type FAE-25-12S6 with a gage factor of 2.05± 1% and a resistance of 120± .2 ohms.

CEC 814 strain gage conditioning amplifiers in conjunction with a Honeywell 1858 optic oscillograph and an Ampex 1300 tape recorder were used for strain gage data recovery and playback.

RESULTS

NOTE: Where strain gage numbers are indicated as additive - such as gages 1 and 2 - the readings were taken with both gages as active bridge arms to obtain a cumulative strain reading. Single gage numbers indicate one active arm per bridge to obtain individual gage readings. Both the double and single active arm bridges were calibrated for a full scale readout of 3000 u in/in of strain.

Strains much greater than the full scale setting (gages 3 and 4) saturated the readout and as such are not presented in the data. Also, gage 2 was damaged during test #9 and disconnected from the system.

Data Accuracy: The system has an instrumentation error potential of 150 u in/in strain based on the full scale reading of 3000 u in/in. This error potential is constant, regardless of the magnitude of the reading; thus, for a full scale deflection the instrumentation error is relatively low and a data resolution of up to 95% accuracy is obtained. However, for very low readings, the error potential becomes highly significant, For example, a strain reading of 300 u in/in with this gage amplification has an error of ± 50%. This can be corrected only when the strain is predictable by adjusting the full scale reading accordingly. Hence, low scale strain measurements presented in this memo report are potentially in error.

PICATINNY ARSENAL, DOVER, NEW JERSEY 07801

REPORT NO.

DATE

REPORT FROM THE Artillery & Mortar Branch, TSD

21 Nov 75 page 3

Submitted by: A. T. Kocur
A. T. Kocur

Approved by: L. D. Bercow
L. D. Bercow, Ch, Arty & Mortar Br TSD

Reviewed by: R. Geany
R. Geany, Ch, Ammo Eval Div, TSD

SMUPA FORM 1243A MAR 67 REPLACES SMUPA 45A WHICH MAY BE USED

Test No.	Time Fired	Ft/Sec Velocity	Pres Avg Psi x 1000	TEMPERATURE F° (GAGES 5/6) Before	After	Increase	Gage No/μ in per in		
1	0900	1600	9.5	66.5 65.0	114.7 112.5	48.2 47.5	1&2/1656	7/2650	10/2730
2	1016	1629	9.6	78.9 76.7	121.6 119.5	42.7 42.8	1&2/1520	7/2721	10/2823
3	1040	1642	9.5	81.5 81.2	122.8 121.6	41.3 40.4	1&2/1480	8/690	9/730
4	1055	1631	9.7	82.4 82.8	121.6 120.7	39.2 37.9	1&2/1607	8/627	9/663
5	1115	1607	9.7	79.9 77.3	119.5 117.4	39.6 40.1	1&2/1590	11/1779	12/488
6	1121	1639	9.6	97.5 95.3	137.9 133.1	40.4 37.8	1&2/1650	11/1758	12/464
7	1140	1631	9.9	94.7 89.7	135.8 131.3	41.6 41.6	1&2/1520	13/576	14/1526
8	1145	1610	9.5	113.1 108.4	150.0 148.5	36.9 40.1	1&4/1637	13/541	14/1493
9	1315	1620	9.9	66.2 65.5	106.2 105.6	40.0 40.1	1/878	3/3108	4/3191
10	1320	1616	9.7	91.5 92.2	129.8 129.8	38.3 37.6	1/796	3/2963	4/3006

SMUPA FORM 1243A MAR 67 REPLACES SMUPA 45A WHICH MAY BE USED

PICATINNY ARSENAL, DOVER, NEW JERSEY 07801

REPORT NO.

REPORT FROM THE Artillery & Mortar Branch, TSD

DATE 21 Nov 75 page 5

Test No.	Time Fired	Ft/Sec Velocity	Pres Avg Psi x 1000	TEMPERATURE F° (GAGES 5/6) Before	After	Increase	Gage No/μ in per in		
11	1325	1597	9.4	108.7 108.7	146.1 147.9	37.4 39.2	1/757	3/2985	4/3063
12	1353	1618	9.5	89.0 86.6	125.3 126.8	36.3 40.2	1/759	3/3036	4/3106
13	1356	1618	9.6	111.8 112.8	142.6 148.5	30.8 35.7	1/723	3/2855	4/2960
14	1400	1629	9.5	131.3 130.7	156.7 168.9	25.4 38.2	1/806	3/2819	4/2963
15	1402	1618	9.5	143.8 150.5	173.2 182.8	29.4 31.7	1/798	3/2702	4/2808
16	1404	1595	9.2	154.4 160.7	185.5 191.9	31.1 30.4	1/791	3/2666	4/2763
17	1410	1613	9.5	143.2 157.2	176.3 192.2	33.1 35.0	1/723	3/2657	4/2719
18	1412	1616	9.5	159.2 168.9	193.3 201.2	34.1 32.3	1/736	3/2610	4/2721
19	1414	1603	9.5	171.2 177.2	205.0 209.1	33.8 31.9	1/718	3/2580	4/2728
20	1416	1642	9.3	176.6 177.7	209.1 208.8	32.5 36.7	1/670	3/2650	4/2763

SMUPA FORM 1243A MAR 67 REPLACES SMUPA 45A WHICH MAY BE USED

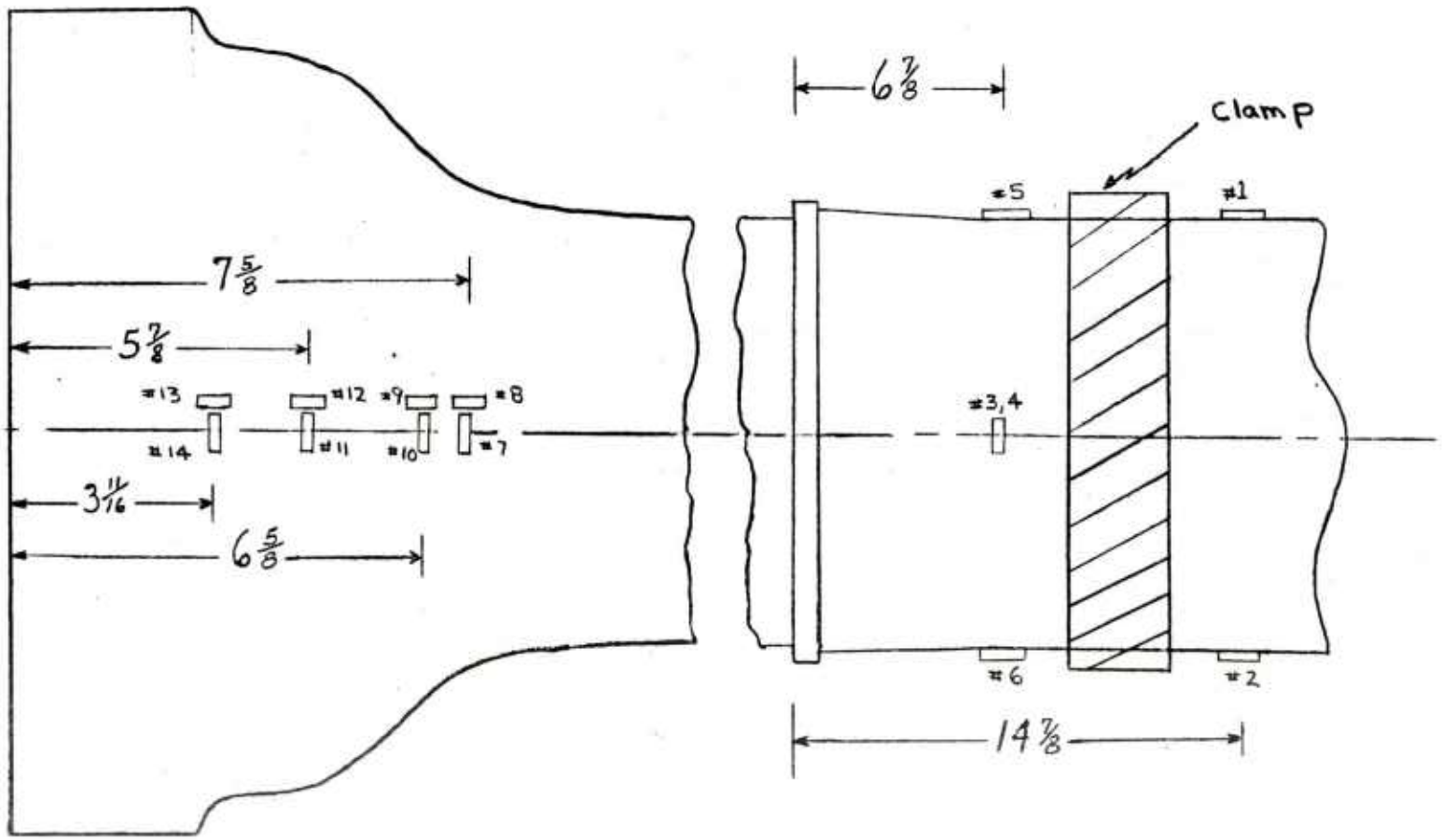

Sketch of Gage Locations
(Not to Scale)

WATERVLIET ARSENAL INTERNAL DISTRIBUTION LIST

May 1976

	No. of Copies
COMMANDER	1
DIRECTOR, BENET WEAPONS LABORATORY	1
DIRECTOR, DEVELOPMENT ENGINEERING DIRECTORATE	1
ATTN: RD-AT	1
RD-MR	1
RD-PE	1
RD-RM	1
RD-SE	1
RD-SP	1
DIRECTOR, ENGINEERING SUPPORT DIRECTORATE	1
DIRECTOR, RESEARCH DIRECTORATE	2
ATTN: RR-AM	1
RR-C	1
RR-ME	1
RR-PS	1
TECHNICAL LIBRARY	5
TECHNICAL PUBLICATIONS & EDITING BRANCH	2
DIRECTOR, OPERATIONS DIRECTORATE	1
DIRECTOR, PROCUREMENT DIRECTORATE	1
DIRECTOR, PRODUCT ASSURANCE DIRECTORATE	1
PATENT ADVISORS	1

EXTERNAL DISTRIBUTION LIST

December 1976

1 copy to each

OFC OF THE DIR. OF DEFENSE R&E
ATTN: ASST DIRECTOR MATERIALS
THE PENTAGON
WASHINGTON, D.C. 20315

CDR
US ARMY TANK-AUTMV COMD
ATTN: AMDTA-UL
AMSTA-RKM MAT LAB
WARREN, MICHIGAN 48090

CDR
PICATINNY ARSENAL
ATTN: SARPA-TS-S
SARPA-VP3 (PLASTICS
TECH EVAL CEN)
DOVER, NJ 07801

CDR
FRANKFORD ARSENAL
ATTN: SARFA
PHILADELPHIA, PA 19137

DIRECTOR
US ARMY BALLISTIC RSCH LABS
ATTN: AMXBR-LB
ABERDEEN PROVING GROUND
MARYLAND 21005

CDR
US ARMY RSCH OFC (DURHAM)
BOX CM, DUKE STATION
ATTN: RDRD-IPL
DURHAM, NC 27706

CDR
WEST POINT MIL ACADEMY
ATTN: CHMN, MECH ENGR DEPT
WEST POINT, NY 10996

CDR
HQ, US ARMY AVN SCH
ATTN: OFC OF THE LIBRARIAN
FT RUCKER, ALABAMA 36362

CDR
US ARMY ARMT COMD
ATTN: AMSAR-PPW-IR
AMSAR-RD
AMSAR-RDG
ROCK ISLAND, IL 61201

CDR
US ARMY ARMT COMD
FLD SVC DIV
ARMCOM ARMT SYS OFC
ATTN: AMSAR-ASF
ROCK ISLAND, IL 61201

CDR
US ARMY ELCT COMD
FT MONMOUTH, NJ 07703

CDR
REDSTONE ARSENAL
ATTN: AMSMI-RRS
AMSMI-RSM
ALABAMA 35809

CDR
ROCK ISLAND ARSENAL
ATTN: SARRI-RDD
ROCK ISLAND, IL 61202

CDR
US ARMY FGN SCIENCE & TECH CEN
ATTN: AMXST-SD
220 7TH STREET N.E.
CHARLOTTESVILLE, VA 22901

DIRECTOR
US ARMY PDN EQ. AGENCY
ATTN: AMXPE-MT
ROCK ISLAND, IL 61201

EXTERNAL DISTRIBUTION LIST (Cont)

1 copy to each

CDR
US NAVAL WPNS LAB
CHIEF, MAT SCIENCE DIV
ATTN: MR. D. MALYEVAC
DAHLGREN, VA 22448

DIRECTOR
NAVAL RSCH LAB
ATTN: DIR. MECH DIV
WASHINGTON, D.C. 20375

DIRECTOR
NAVAL RSCH LAB
CODE 26-27 (DOCU LIB.)
WASHINGTON, D.C. 20375

NASA SCIENTIFIC & TECH INFO FAC
PO BOX 8757, ATTN: ACQ BR
BALTIMORE/WASHINGTON INTL AIRPORT
MARYLAND 21240

DEFENSE METALS INFO CEN
BATTELLE INSTITUTE
505 KING AVE
COLUMBUS, OHIO 43201

MANUEL E. PRADO / G. STISSER
LAWRENCE LIVERMORE LAB
PO BOX 808
LIVERMORE, CA 94550

DR. ROBERT QUATTRONE
CHIEF, MAT BR
US ARMY R&S GROUP, EUR
BOX 65, FPO N.Y. 09510

2 copies to each

CDR
US ARMY MOB EQUIP RSCH & DEV COMD
ATTN: TECH DOCU CEN
FT BELVOIR, VA 22060

CDR
US ARMY MAT RSCH AGCY
ATTN: AMXMR - TECH INFO CEN
WATERTOWN, MASS 02172

CDR
WRIGHT-PATTERSON AFB
ATTN: AFML/MXA
OHIO 45433

CDR
REDSTONE ARSENAL
ATTN: DOCU & TECH INFO BR
ALABAMA 35809

12 copies

CDR
DEFENSE DOCU CEN
ATTN: DDC-TCA
CAMERON STATION
ALEXANDRIA, VA 22314

NOTE: PLEASE NOTIFY CDR, WATERVLIET ARSENAL, ATTN: SARWV-RT-TP, WATERVLIET, N.Y. 12189, IF ANY CHANGE IS REQUIRED TO THE ABOVE.